CONTRACT NO. NAS5-3173

ATTITUDE HANDBOOK

FOR THE

TIROS IX
METEOROLOGICAL
SATELLITE SYSTEM

Prepared for the

GODDARD SPACE FLIGHT CENTER

NATIONAL AERONAUTICS
AND SPACE ADMINISTRATION

WASHINGTON, D.C.

Prepared by

ASTRO-ELECTRONICS DIVISION
DEFENSE ELECTRONIC PRODUCTS

RADIO CORPORATION OF AMERICA

PRINCETON, NEW JERSEY

AED M-2036

OCTOBER 7, 1964

CONTRACT NO. NAS5-3173

ATTITUDE HANDBOOK

FOR THE

TIROS IX
METEOROLOGICAL
SATELLITE SYSTEM

Prepared for the

GODDARD SPACE FLIGHT CENTER

NATIONAL AERONAUTICS
AND SPACE ADMINISTRATION

WASHINGTON, D.C.

Prepared by

ASTRO-ELECTRONICS DIVISION
DEFENSE ELECTRONIC PRODUCTS
RCA / RADIO CORPORATION OF AMERICA
PRINCETON, NEW JERSEY

AED M-2036

OCTOBER 7, 1964

RADOS

PREFACE

This document is prepared for the Goddard Space Flight Center of the National Aeronautics and Space Administration by the Astro-Electronics Division of RCA, under Contract No. NAS5-3173.

The procedures set forth herein are to be used for routine maintenance of the operational attitude of the TIROS IX Meteorological Satellite.

V - IX replaces V-VII

TABLE OF CONTENTS

TABLE OF CONTENTS (Continued)

TABLE OF CONTENTS (Continued)

Appendix

LIST OF ILLUSTRATIONS

LIST OF ILLUSTRATIONS (Continued)

LIST OF TABLES

SECTION I. INTRODUCTION

1-1. SCOPE

1-2. The purpose of this manual is to define and detail the data-processing operations required to support the attitude and spin-rate control function for the TIROS IX Wheel-satellite. It contains procedures specifically designed for the data-processing technicians who are to establish attitude and spin-rate command information which is directly suitable for delivery to the programming personnel. This manual includes only that background material considered to be specifically required to establish the relationship between the data-processing operations and the overall attitude and spin-rate control function. Descriptions of the circuits and devices that implement these functions are included in the TIROS IX Operating and Instruction Handbook.

1-3. FUNDAMENTALS OF ATTITUDE CONTROL

1-4. GENERAL

1-5. The operational concept for TIROS IX requires that the satellite's spin axis be maintained nearly perpendicular to the orbit plane. This requirement is implemented, basically, by a two-channel, V-headed, attitude sensor, a Quarter-Orbit Magnetic Attitude Control (QOMAC) System, and a Magnetic Bias Control (MBC). The attitude sensor includes two bolometers which provide outputs when exposed to the earth's irradiation, and the resulting signals are telemetered to earth and recorded by the Command and Data Acquisition (CDA) stations. These recordings are then analyzed to determine whether or not the two channels of data exhibit measurable time differences. If no measurable time difference exists, no attitude error exists; if a time difference does exist, an attitude error exists and must be corrected. Normally, an attitude error will be corrected by use of QOMAC. However, if long term observation indicates that the satellite attitude tends to drift continually in one direction, the MBC can be used to reduce the drift rate and, thus, to reduce the number of QOMAC cycles required to maintain the desired attitude.

1-6. When the satellite is in a spin-synchronized camera triggering mode, the spin rate must be maintained between 9.62 and 9.93 rpm. This spin rate is maintained by programming the Magnetic Spin Control (MASC) whenever the spin rate drifts from the specified range. Although the spin rate can be determined from the recording of attitude-sensor data, the rate is normally computed by NASA and transmitted to the attitude reduction and programming personnel.

1-7. ATTITUDE MEASUREMENT

1-8. Figure 1-1 depicts the TIROS IX satellite in the correct orbital attitude. The spin axis is normal to the orbital plane and the two channels of the attitude sensor sweep equal arcs on the earth's surface. As can be seen from the waveforms accompanying this figure, the condition of no-attitude error is indicated by equal earth-scan periods and, consequently, equal T_E/T_{SPIN} ratios for both sensor channels.

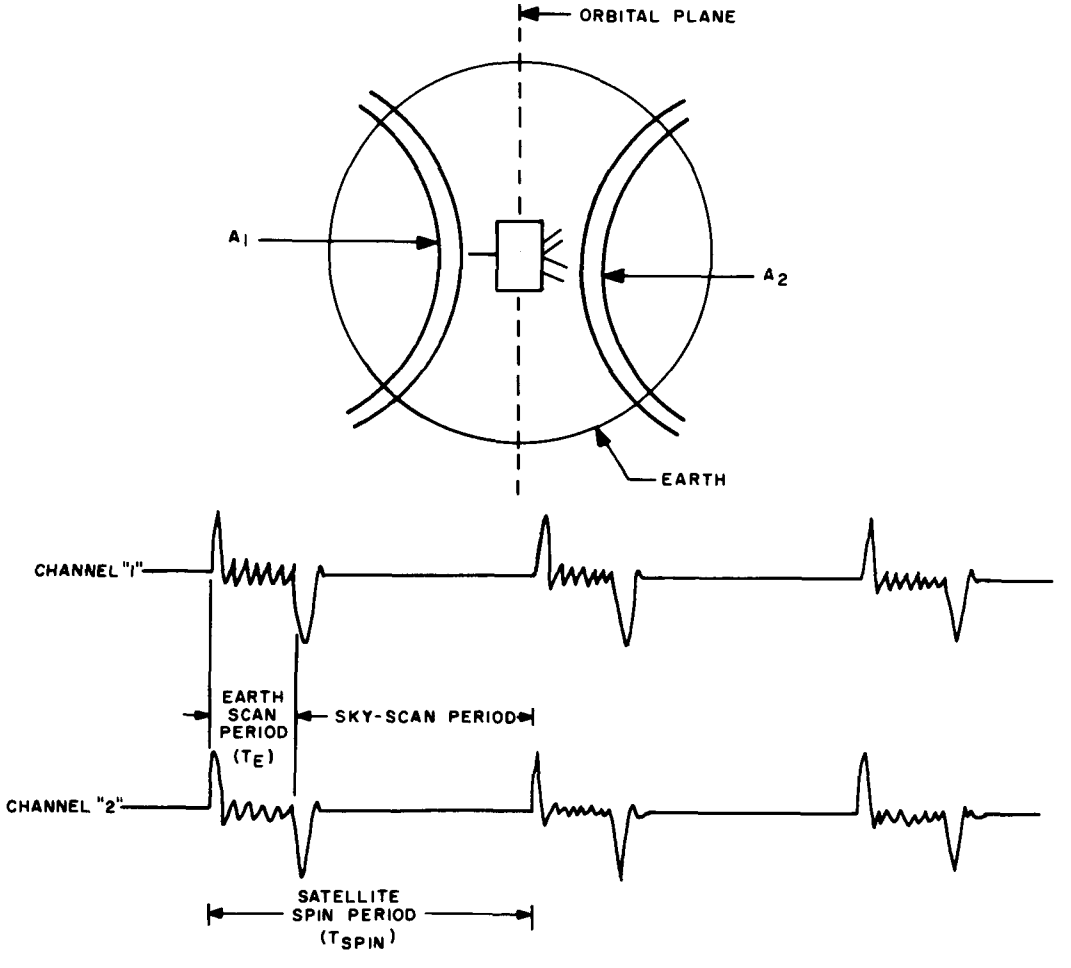

Figure 1-1. Attitude-Sensor Data With No Attitude Error

1-9. When an attitude error does exist, its measured magnitude will vary sinusoidally as the spacecraft orbits the earth. This apparent variation is the result of two factors: first, two components, yaw and roll, comprise an attitude error, but only the roll component can be detected by the attitude sensor; second, the position of the satellite spin

axis tends to remain fixed in space. Because of this apparent variation in attitude error, a series of T_E/T_{SPIN} ratios must be checked and plotted to permit determination of the actual attitude error.

1-10. Figure 1-2 shows the effect of the two factors described in the preceeding paragraph on an attitude error of constant magnitude. In Figure 1-2a, the satellite is assumed to be at a point in its orbit where the yaw component of attitude error is zero and the roll angle, i.e., the tipping of the spin axis toward the earth's surface, comprises the entire error. With the satellite in this position, the difference in the earth-scan period of the two sensor channels is at a maximum and the roll angle-indicated by the attitude data is the actual attitude error.

1-11. As shown in Figure 1-2c, the roll angle becomes zero after the satellite orbits to a position 90 degrees from its position in Figure 1-2a. Thus, although the same magnitude of attitude error exists, the error is composed solely of its yaw component and cannot be detected by the attitude sensor.

1-12. Figure 1-2b shows the spacecraft halfway between conditions a and c. With the spacecraft in this orbital position, both components of attitude error are present. Although analysis of the channel 1 and 2 waveforms would indicate the existance of an attitude error (due to its roll-angle component), the indicated error would be significantly less than the actual error.

1-13. If a series of orbital positions is assumed and the measured magnitude of the attitude error (i.e., the roll angle) for each position is plotted against time, the resulting curve will be a sinewave with a period equal to the orbital period.

1-14. Because of the sinusoidal variation of roll-angle, it is apparent that no single roll-angle datum point will, by itself, define the attitude error of the spacecraft. Rather, a long series of datum points must be obtained and plotted. Then, a sinecurve overlay is selected to provide the best fit, matching the slope of the plotted data points to the slope of the sinecurve. After a sinecurve has been fitted to the data points, the maximum value of the sinewave curve is equal to the magnitude of the attitude error. The orbital position of the satellite at the time the roll-angle sinecurve becomes positive must be determined from the resulting graph. When these two parameters are known, a program can be formulated for correcting the attitude error.

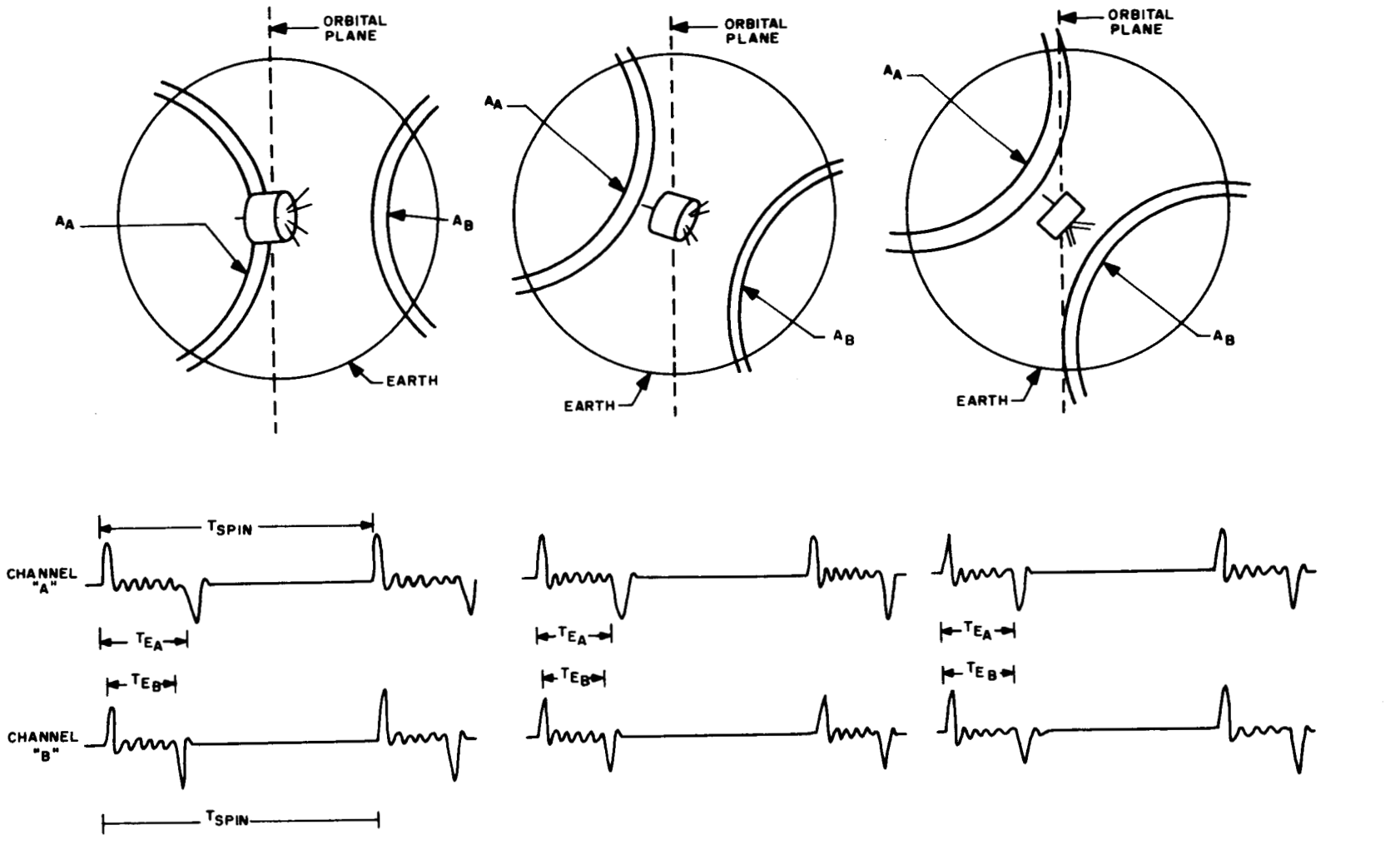

a. SPACECRAFT ORBIT POSITION FOR WHICH ROLL ANGLE = ATTITUDE ERROR

b. ORBIT POSITION ADVANCED 45° FROM a. (ROLL ANGLE = 0.7 ATTITUDE ERROR)

c. ORBIT POSITION ADVANCED 90° FROM a. (ROLL ANGLE = 0)

Figure 1-2. Phasing of Attitude-Sensor Data For Different Orbital Positions of Spacecraft

1-15. ATTITUDE CORRECTION

1-16. Attitude correction is effected by use of the QOMAC system. In establishing a QOMAC sequence, the magnitude of the attitude error is used to determine the number of QOMAC cycles required and the orbital position at which the roll angle becomes positive is used to determine the start time of the sequence.

1-17. When the spin axis continually drifts from the desired attitude in one direction, and the rate of drift is excessive, the MBC can be programmed to reduce the drift rate by altering the magnetic moment of the satellite. The amount of change in magnetic moment required to reduce the drift rate to an acceptable level is determined from a history of attitude data; this history is maintained by personnel assigned to the TIROS Technical Control Center (TTCC).

1-18. PERSONNEL RESPONSIBILITIES

1-19. GENERAL

1-20. As outlined in this handbook, three groups of personnel have the responsibility for data reduction and analysis. They are (1) CDA station operators, (2) CDA station data analysts, and (3) TTCC operators. The responsibilities of these personnel are outlined in the following paragraphs.

1-21. CDA STATION OPERATORS

1-22. The CDA station operators are responsible for the performance of the procedures outlined in Section II, paragraphs 2-1 through 2-10. Briefly, the responsibilities of these personnel are as follows:

(1) Ensuring that the recording devices are in proper operation;

(2) Marking the recorded data with the CDA station designation, date, etc.;

(3) Delivering the data recordings to the CDA station data analyst; and

(4) Transmission of raw data to TTCC upon request and as directed.

1-23. CDA STATION DATA ANALYSTS

1-24. The CDA station data analysts are responsible for the performance of the procedures in Section II, paragraphs 2-11 through 2-17. Briefly, the responsibility of these personnel are as follows:

(1) Selection of data suitable for reduction and evaluation;

(2) Marking of data with rotation number and determination of event time;

(3) Measurement of the T_E/T_{SPIN} ratios for the selected data;

(4) Transmission of the reduced data to the TTCC operator; and

(5) Maintenance of an orbit-by-orbit history of roll-angle data, when requested by TTCC.

1-25. TTCC OPERATORS

1-26. The TTCC operators are responsible for performance of all of the procedures in Section II and Section III. Briefly, the responsibilities of the TTCC operators are as follows:

(1) Reduction and marking of the raw data as outlined under paragraphs 1-21 and 1-23;

(2) Determination of the instantaneous roll angle for each value of T_E/T_{SPIN};

(3) Determination of the maximum roll angle (i.e., actual attitude error);

(4) Determination of the required attitude-correction sequences;

(5) Maintenance of an orbit-by-orbit system history;

(6) Determination of any required spin-rate correction sequences; and

(7) Delivery of the attitude and spin-rate correction information to the TTCC Programmer Personnel to allow formulation of the required program.

SECTION II. PRIMARY METHOD OF DATA REDUCTION

2-1. PURPOSE

2-2. The purpose of this section is to detail the procedures for reducing raw attitude-sensor data to obtain the two parameters (roll angle and orbit phasing angle) that are required to define the attitude of the satellite. In the event that either or both channels of the attitude sensor are inoperative the procedures in Appendix A and/or Appendix G should be used for determining these two parameters.

2-3. DESCRIPTION OF RAW ATTITUDE-SENSOR DATA

2-4. The raw data used to determine the attitude are obtained from the satellite's attitude sensor. These data are transmitted to a Command and Data Acquisition (CDA) station via the beacon transmitters (No. 1 and No. 2). Hence, data can only be obtained when the satellite is within beacon-transmitter range of a CDA station. Figure 2-1 shows a sample of attitude data as recorded on an attitude recorder at a CDA station. Peculiar data interference patterns, such as sun interference and earth noise, are illustrated. Figure 2-2 shows the same data as they appear when recorded on a telemetry recorder at a CDA station. On the telemetry recorder, the channel assignments for attitude-sensor channels are reversed and the time-code markers appear on the edge of the paper rather than in the center of the paper.

2-5. The following information shall be extracted from the recorded attitude data:

a. Values of earth-time to spin-period ratios (T_E/T_{SPIN}), for approximately every fifth spin of the satellite from acquisition through beacon fade.

b. The real time (GMT) of occurrence of the first and last ratios measured.

c. An estimate of data quality for each ratio measured.

2-6. PREPARATION FOR REDUCTION

2-7. IDENTIFICATION OF RAW DATA

2-8. Immediately following the end of contact with the satellite, all of the chart recordings obtained shall be identified at the beginning and at the end of each chart by the CDA, and TTCC personnel with the following information (in the order listed):

a. Date,

b. Ground Station Name,

c. Satellite Name, and

d. Orbit No.

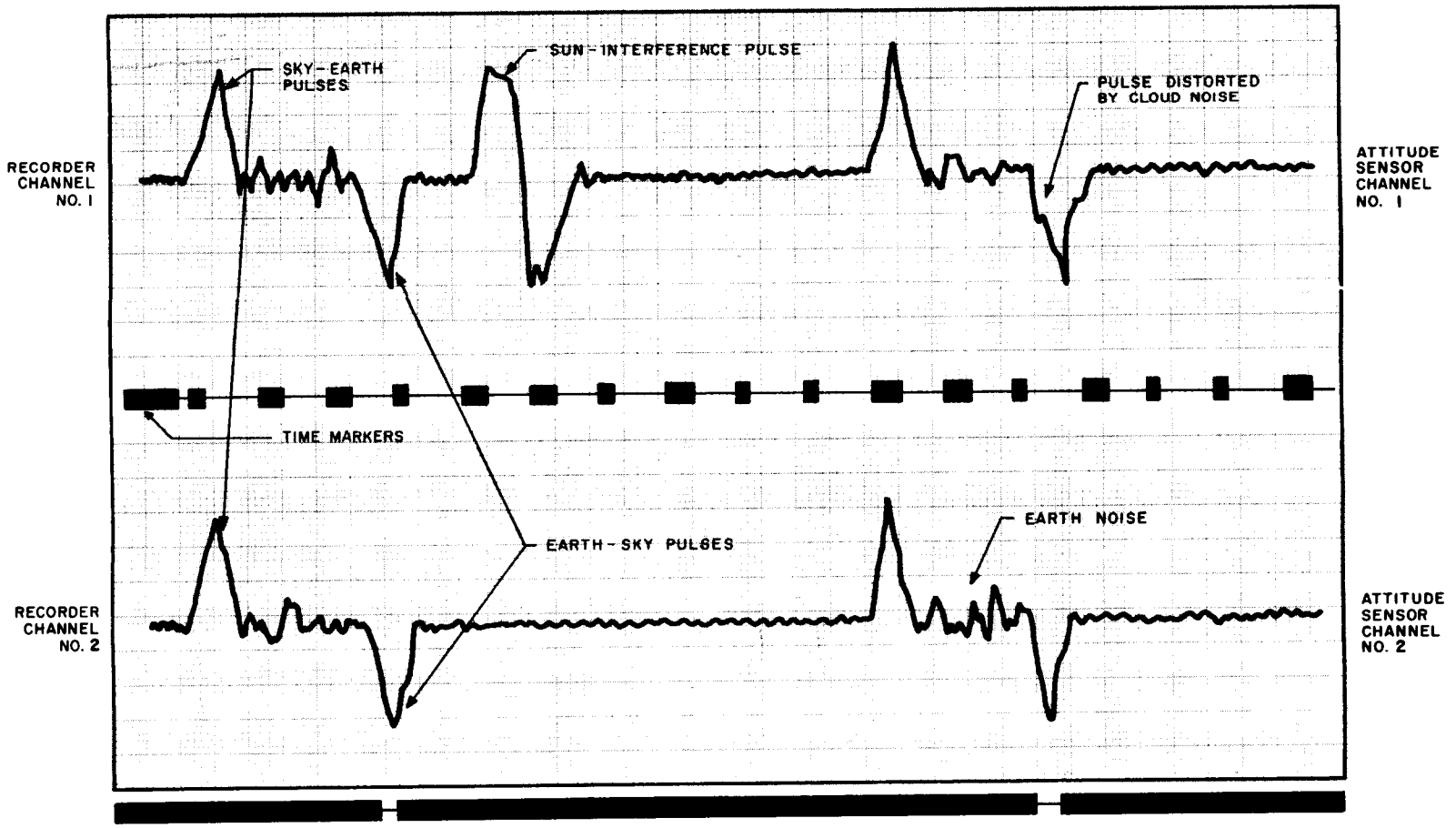

Figure 2-1. Attitude Sensor Data as Recorded on Attitude Recorder

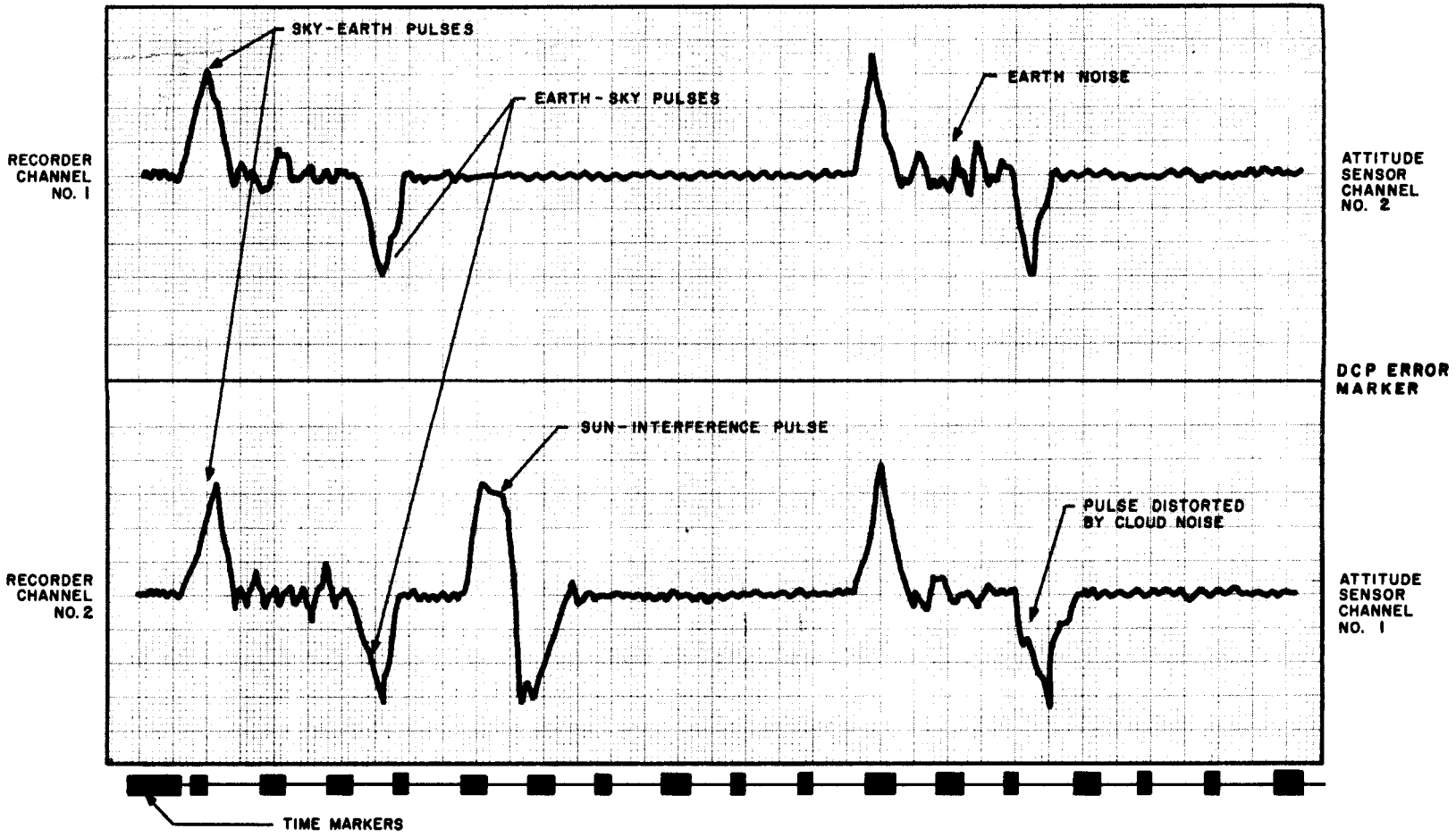

Figure 2-2. Attitude Sensor Data as Recorded on Telemetry Recorder

A sample of proper identification is as follows:

1 JUNE 1965

WALACQ

TIROS IX

ORBIT NO. 1342

2-9. DATA HANDLING INSTRUCTIONS

2-10. Within the five minutes after the pass, the copy of Sanborn paper from the Attitude Recorder shall be delivered to the Attitude Data Reduction Analyst at both the WALACQ and ULASKA Stations. Reduction of the Attitude data will not be performed at NICOLA. However, a GO-NO-GO evaluation will be performed as per the procedures specified in the telemetry calibration handbook at all stations.

NOTE

Transmission of the raw beacon receiver data to TTCC during the pass, and/or playback of the data recorded on the magnetic tape recorders, will be performed upon request and as directed.

2-11. DATA REDUCTION PROCEDURES FOR ATTITUDE-SENSOR DATA

2-12. REDUCED-DATA RECORDS

2-13. The reduced data shall be recorded on an Attitude Data Sheet (Figure 2-3), as indicated in the steps of the data-reduction procedures. All sheets shall be filled out in duplicate. Figures 2-4 and 2-5 illustrate the teletype message formats and provide data which will be used in later examples.

2-14. MARKING OF RAW DATA

2-15. The markup procedure which follows is to be applied to the Sanborn Recordings of both channels of attitude data prior to making attitude measurements. To mark the raw data, proceed as follows:

a. Mount the recording chart on the Gerber Scanner, and advance to the beginning of the chart.

ATTITUDE DATA SHEET

SATELLITE NAME_____ ORBIT NO. _____

GROUND STATION NAME_____ DATE _____

DATA SPAN: INITIAL ROTATION NO._____ FINAL ROTATION NO. _____

TIME_____ Z TIME _____ Z

Rotation No.	Earth-to-Spin Time Ratio (T_E/T_{SPIN})		Roll Angle* (φ_i)	Normalized* Time (t_N)
	Chan. 1	Chan. 2		

*These columns to be filled in at TTCC only.

Figure 2-3. Format of Attitude Data Sheet

GHN001A
PP GOSI GULA GWEA GHNJ GOLA
DE GACQ 000A
28/0001Z

TIROS IX
ATTITUDE DATA SHEET
WALACQ ORBIT 0022 03 NOV 64

DATA SPAN: INITIAL ROTATION NO. 000 FINAL ROTATION NO. 105
TIME: 192406Z 193509Z

ROTATION NO.	T E/T SPIN	
	CHAN 1	CHAN 2
000	2321	2801
005	2321	2781
010	2321	2801
015	2341	2781
020	2322	2761
025	2342	2741
030	2342	2721
035	2392	2711
040	2362	2731
045	2372	2721
050	2412	2701
055	2412	2681
060	2401	2670
068	2401	2670
070	2451	2670
076	2441	2640
080	2481	2630
090	2501	2650
094	2531	2640
100	2540	2610
105	2550	2600

28/0002Z NOV GACQ

Figure 2-4. Format of Teletype Message from WALACQ

```
GHNØØØA
PP GOSI GACQ GWEA GHNJ GOLA
DE GULA ØØØA
28/ØØØØA

TIROS IX
ATTITUDE DATA SHEET
ULASKA ORBIT ØØ22  Ø3 NOV 64

DATA SPAN:  INITIAL ROTATION NO. ØØØ  FINAL ROTATION NO. Ø4Ø
TIME:                    193706Z                    1941197

ROTATION NO.                    T E/T SPIN
                          CHAN 1          CHAN 2
ØØØ                       2571            2561
ØØ5                       2581            2541
Ø1Ø                       26ØØ            2531
Ø15                       262Ø            2491
Ø2Ø                       265Ø            247Ø
Ø25                       266Ø            25ØØ
Ø31                       266Ø            248Ø
Ø35                       248Ø            246Ø
Ø4Ø                       267Ø            245Ø

28/ØØØ1Z NOV GULA
```

Figure 2-5. Format of Teletype Message from ULASKA

b. Select the first clearly usable set of horizon-crossing pulses and draw in the slope and zero-reference lines (as shown in Figure 2-6). For the dual-channel case, a set of usable pulses consists of three consecutive, well-defined crossing pulses on each of both channels.

c. Identify the sky-earth crossing of the first set of horizon-crossing pulses as rotation No. 000.

d. Determine the real time of the first sky-earth-crossing pulse of rotation No. 000 of channel No. 2 in GMT as follows:

(1) Draw a line on the chart parallel to a chart grid-line, through the point of intersection of the slope and zero-reference lines of the first sky-earth-crossing pulse and across the line of time marks.

(2) Note the point of intersection of the line on the coded time scale. Convert the coded time value into GMT in accordance with the system described in Appendix A, and record this value of time on the Attitude Data Sheet.

e. Advance the chart, and add slope lines and zero-reference lines to the set of horizon-crossing pulses associated with rotation No. 005. If judgment indicates that this is not a usable set, advance or back up one or, if necessary, two sets of pulses to make a selection. Label the choice with its correct rotation number. If no usable set of pulses exists within two rotations of rotation No. 005, advance to rotation No. 010.

f. Repeat the selection and marking process at every fifth set of horizon-crossing pulses (i.e., at rotation No. 000, 005, 010, 015, etc.) until all the available sets are marked.

g. Using the procedure of Step d, determine the GMT of the last sky-earth-crossing pulse in the last set of pulses of Channel No. 2. Record this time value and the corresponding rotation number on the Attitude Data Sheet.

2-16. DETERMINATION OF EARTH-TO-SPIN TIME (T_E/T_{SPIN}) RATIOS

2-17. Proceed as follows:

a. Adjust the Gerber Variable Scale so that the length represented by its scale reading of 0 to 10 is equal to the linear distance (L) between two consecutive sky-earth crossings.

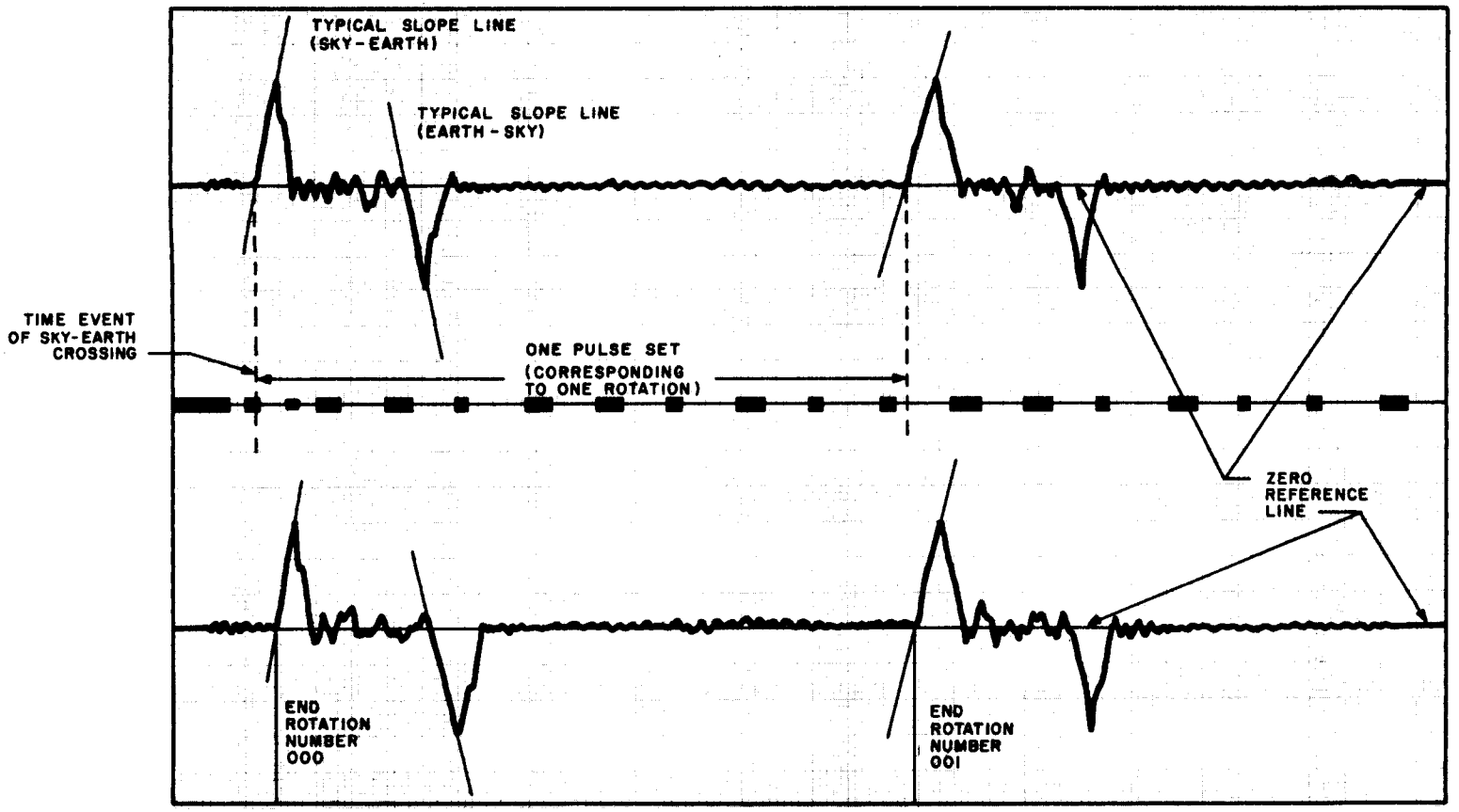

Figure 2-6. Marking of Raw Attitude-Sensor Data

b. Place the Gerber Variable Scale on the chart recording so that its left index is at the point of intersection of the slope line and zero-reference line for the sky-earth-crossing pulse of rotation No. 000 on channel No. 2. Align the edge of the Gerber Variable scale with the zero-reference line, and read the T_E/T_{SPIN} ratio off the variable scale marker which is directly opposite the intersection of the slope line and zero-reference line of the earth-sky-crossing pulse. Record the measured value of T_E/T_{SPIN}, in three digits, in the appropriate place in the Attitude Data Sheet.

c. Select from the following list the digit whose corresponding description most nearly meets the description of the data used in the determination of the T_E/T_{SPIN} ratio of Step b. If the character of the data is such that a choice of more than one data-description digit is possible, the one that should be chosen is the one which appears to be the most damaging to the accuracy of the measurement.

0 Clean

1 Noisy

2 Probable cloud interference at earth-sky transition

3 Probable sun interference at earth-sky transition

4 Probable cloud interference at sky-earth transition

5 Probable sun interference at sky-earth transition

6 Low-amplitude signal

7 Jamming by another transmitter (crosstalk, beats, etc.)

Record on the Attitude Data Sheet the selected data-description digit with the three-digit number representing the T_E/T_{SPIN} ratio of Step b. This digit should be placed in the position of a least significant digit (in the far-right position).

d. Repeat the procedures of Steps b and c for each set of data for both channels of all marked rotation No. Record all the T_E/T_{SPIN} ratios and the corresponding data-description digits in the Attitude Data Sheet.

2-18. DETERMINATION OF INSTANTANEOUS ROLL ANGLES

2-19. The TTCC has responsibility for the determination of instantaneous roll angles from the ratios reported on the Attitude Message. The instantaneous roll angle for each rotation number marked in the data span is determined through the use of the proper roll-angle nomogram. Once the T_E/T_{SPIN} ratios have been determined, the nomograms illustrated in Figures 2-7 and 2-8 may be entered using these ratios to obtain instantenous roll angles.

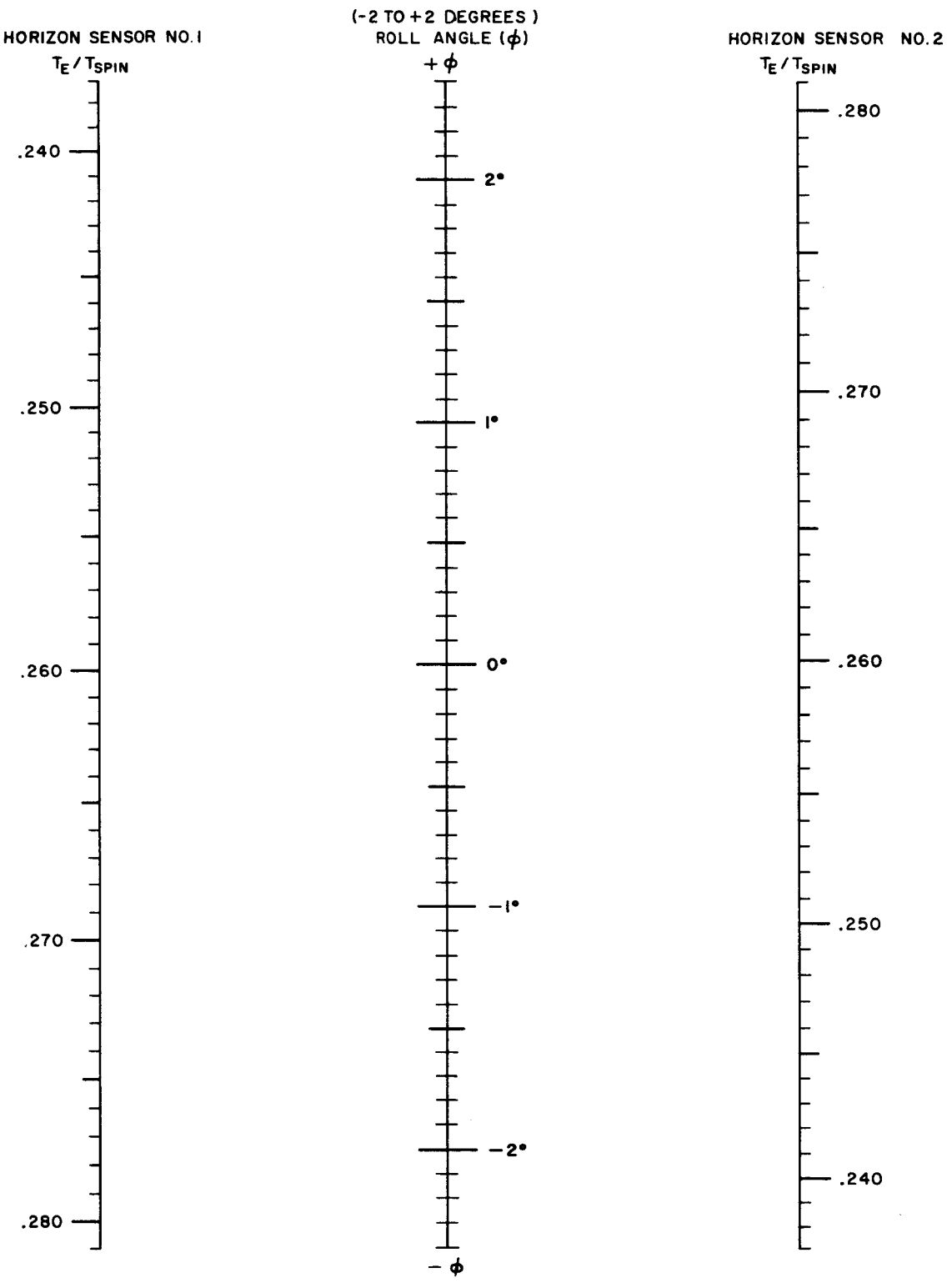

Figure 2-7. Two-Degree Roll-Angle Nomogram

TIROS WHEEL

ROLL ANGLE NOMOGRAM FOR DUAL HORIZON SENSORS
(-14 TO +14 DEGREES)

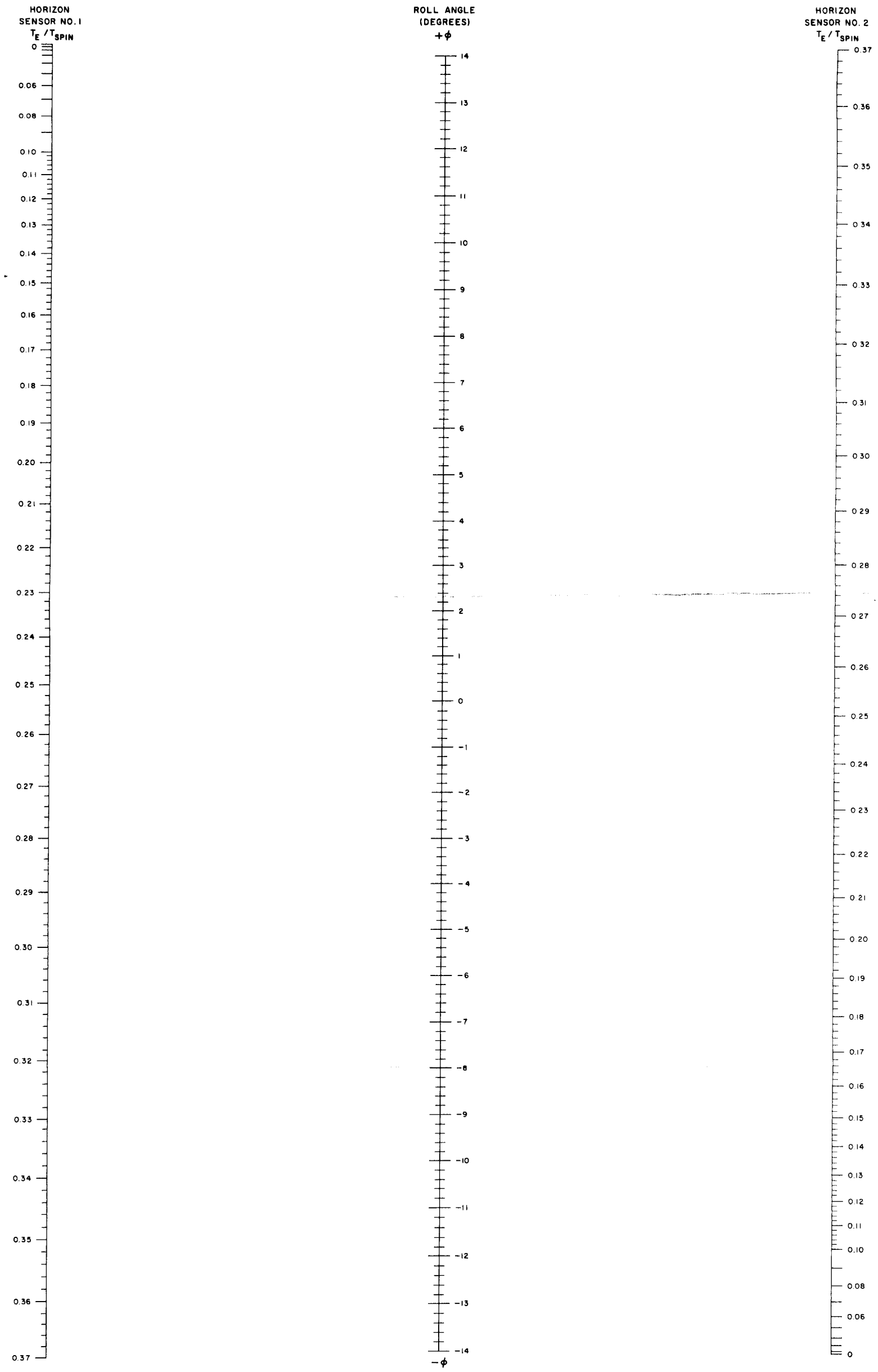

NOTES:
1. T_E / T_{SPIN} IS THE RATIO OF EARTH TIME TO SPIN TIME
2. SENSOR MOUNTING ANGLES ARE 40 AND 140 DEGREES WITH RESPECT TO SPIN AXIS

Figure 2-8. Fourteen-Degree Roll-Angle Nomogram

2-20. The procedure for using a roll-angle nomogram is as follows:

a. Line up the values of the two entering parameters using a transparent straight edge. (Be careful to note the direction of scaling on the parameter axes of the nomogram.)

b. Read the value of the instantaneous roll angle in degrees at the point where the transparent straight edge crosses the roll-angle axis. Record the value of instantaneous roll angle obtained on the Attitude Data Sheet. (Be careful to indicate the polarity of the roll angle.)

2-21. NORMALIZATION OF TIME

2-22. The time elapsed between the ascending node crossing and the moment of occurrence of each instantaneous roll angle must be divided by the orbital period, τ, in order to permit the use of a common overlay of roll curves in ascertaining the roll history. The quantities thus obtained are referred to as normalized time. The "zero" of normalized time will be taken as the time of the ascending node crossing. To calculate the value of normalized time associated with the moment of occurrence of the instantaneous roll angle of rotation No. 000 at any of the CDA stations, use the relationship

$$(t_N)_{000} = \frac{GMT_{000} - GMT_{AN}}{\tau} ,$$

where:

GMT_{000} is the GMT of rotation No. 000, and

GMT_{AN} is the GMT of the ascending node crossing.

To calculate the normalized time associated with succeeding rotation numbers, an incremental time value, Δt_N, is calculated which is added to the normalized time of rotation number 000. The incremental time (Δt_N) associated with rotation number n is given by

$$(\Delta t_N)_n = \frac{n P}{\tau} ,$$

where:

n is the rotation number,

P is the spacecraft spin period in minutes, and

τ is the anomalistic period in minutes.

Finally, to obtain the normalized time $(t_N)_n$ associated with a particular rotation number, n, use the relationship

$$(t_N)_n = (t_N)000 + (\Delta t_N)_n$$

Record all values of normalized time on the Attitude Data Sheet.

2-23. PLOTTING OF INSTANTANEOUS ROLL ANGLE AGAINST NORMALIZED TIME

2-24. For the character of the data and the accuracy of the results contemplated for the TIROS-Wheel satellite, a sheet of 11-by 17- inch (or larger) graph paper with 10 x 10 grid lines to the 1/2-inch is required for plotting of a single-orbit, roll-angle history, from the ascending node to the next ascending node.

2-25. The roll angle history is plotted as follows:

a. Set up a normalized-time scale on the abscissa so that the normalized time for one orbit is represented by a length of 10 inches.

b. Set up an instantaneous roll-angle scale on the ordinate to the same scale as the appropriate sine-curve overlay used to aid in the curve-fitting procedure. Judgment and experience will dictate which sine-curve is to be used.

c. Plot all data points listed on the Attitude Data Sheets associated with the CDA stations that obtained data during the orbit under consideration.

d. Draw the locus using either of the following methods.

(1) Sketch the curve of best fit, using personal judgment and experience as a guide, or

(2) Use one of the three available sine-curve overlays to obtain a curve which closely fits the data points, and trace in the curve. (Figures 2-9, 2-10, and 2-11 illustrate the three overlays available to cover maximum instantaneous roll angles of 2-, 10-, and 90-degrees, respectively.)

2-26. DETERMINATION OF MAXIMUM ROLL ANGLE (φ_{MAX})

2-27. The maximum roll angle is the amplitude, in degrees, of the curve plotted in step d-2 of paragraph 2-25. The amplitude is marked on the sine-curve overlays used in construction of the data curve.

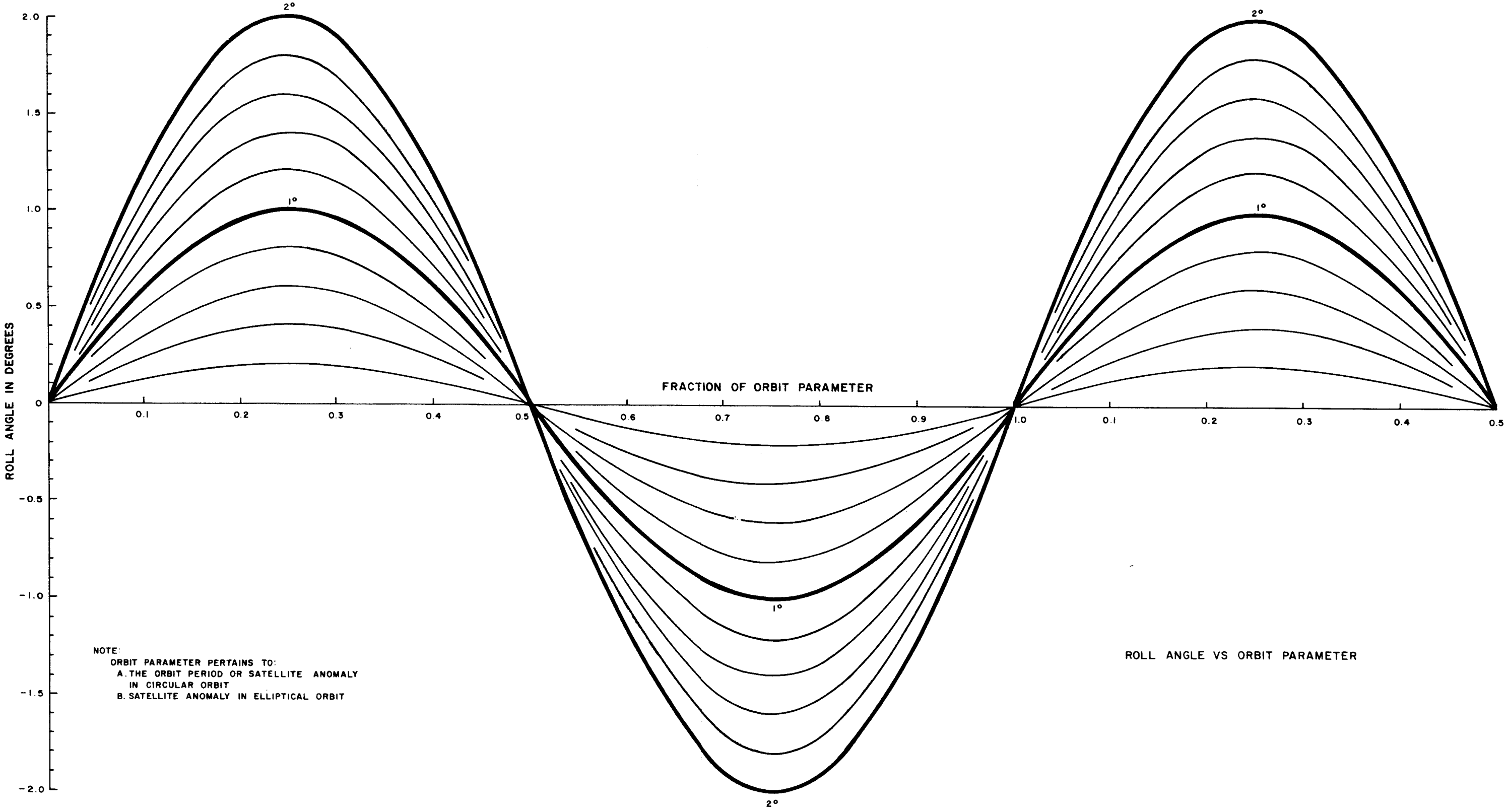

Figure 2-9. Example of 2-Degree Sine-Wave Template

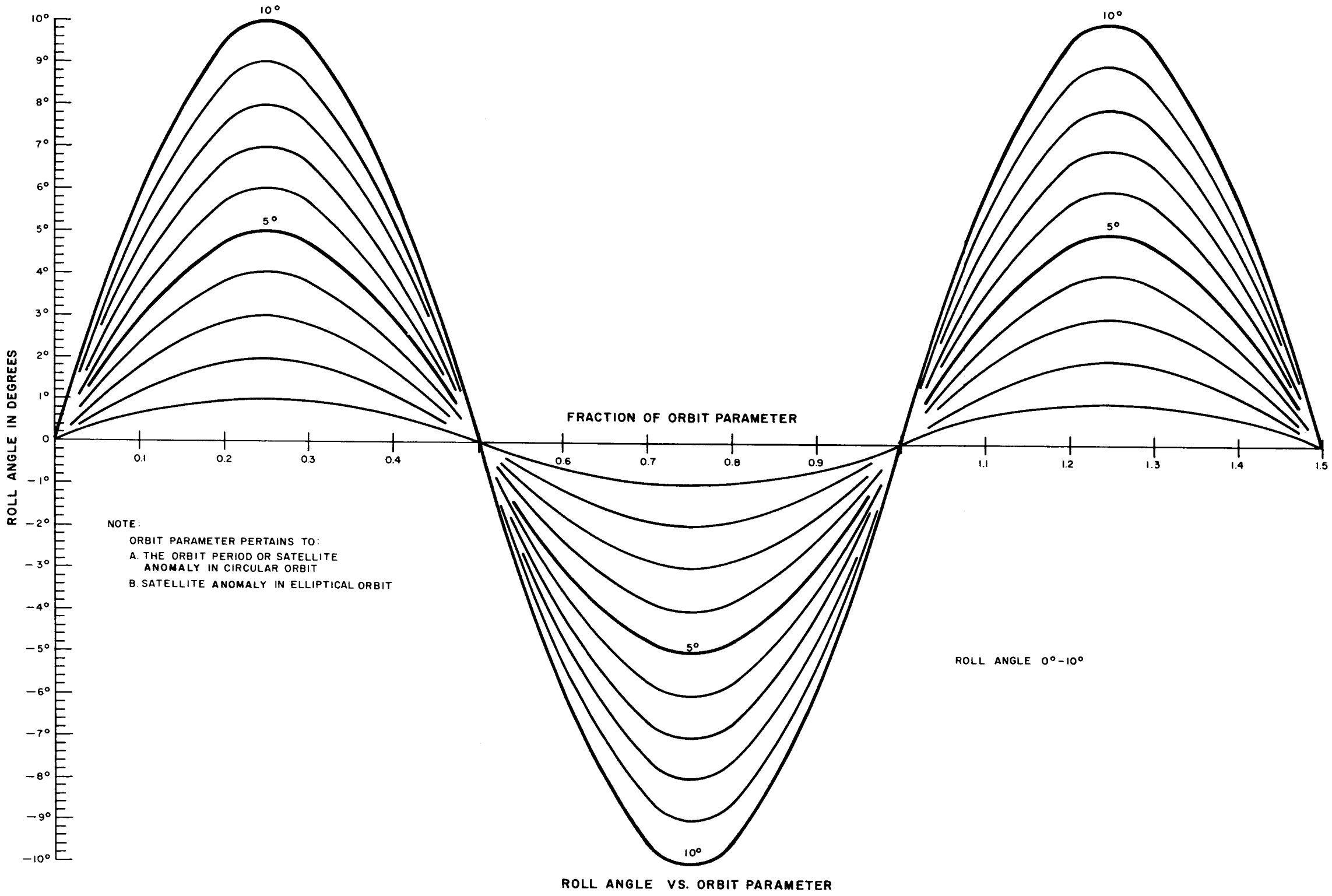

Figure 2-10. Example of 10-Degree Sine-Wave Template

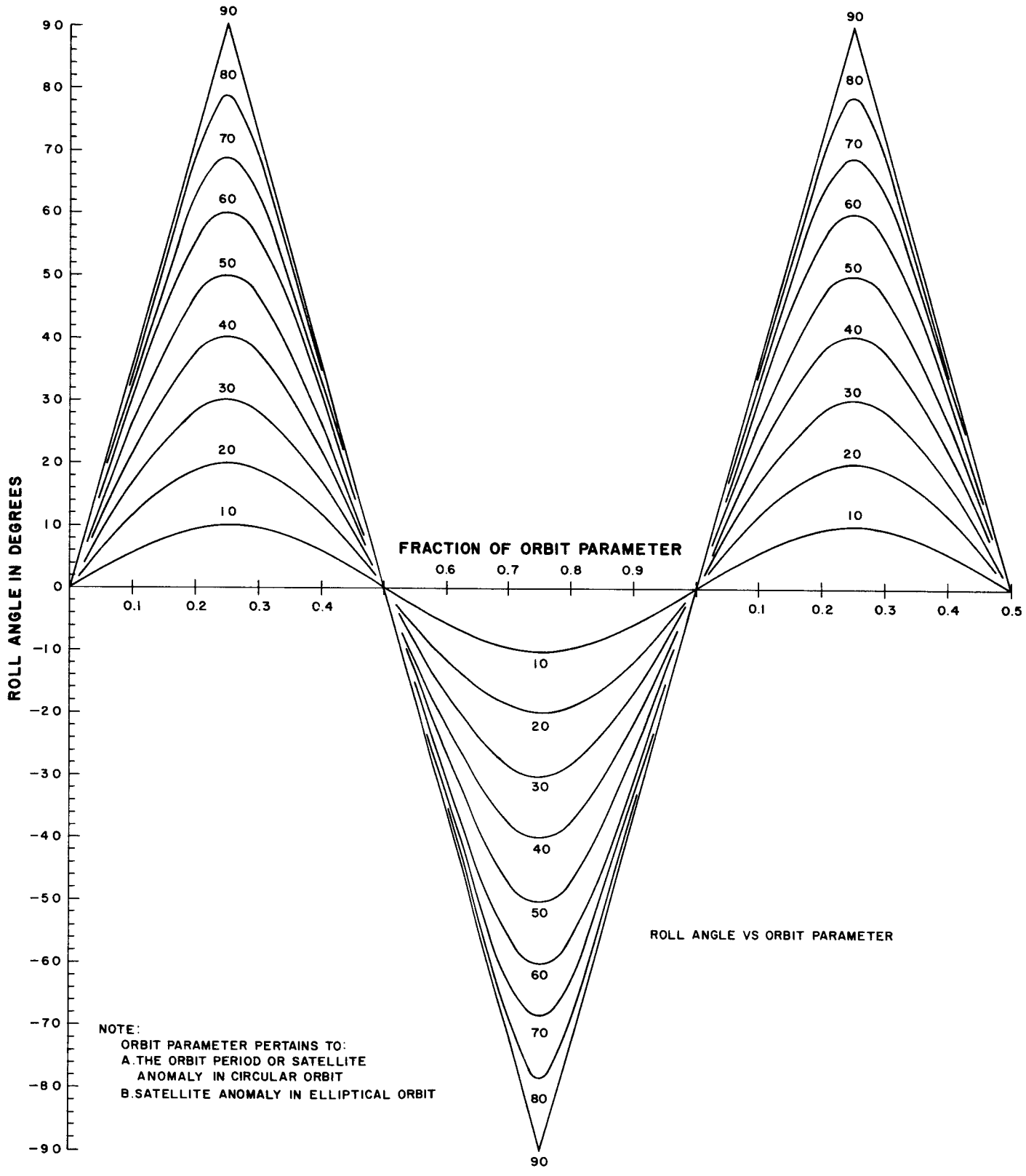

Figure 2-11. Example of 90-Degree Sine-Wave Template

2-26. DETERMINATION OF ORBITAL-PHASING PARAMETER (λ)

2-27. To obtain the orbital-phasing parameter (λ), in degrees, use the relationship

$$\lambda = 360\,(t_N)_\lambda \ ,$$

in which $(t_N)_\lambda$ is read from the plot of normalized roll-angle history and is the normalized time from the ascending node to a zero value of roll angle at an upward crossing of the time axis (i.e., for zero roll angle with a positive slope).

2-28. EXAMPLE OF THE DETERMINATION OF φ_{MAX} AND λ

2-29. The attitude data given in the teletype messages of Figure 2-4 and 2-5 will be used for this example.

2-30. Three items of information not given in the teletype message are needed to carry out the determination. The first two, the GMT of the ascending node crossing and the satellite anomalistic period, are obtained from the Orbital Elements and Equator Crossings published by NASA. The third item of information, the satellite spin period, can be obtained either from the Telemetry Pass Summary Message or from the summary plot of Spin Period versus orbit number. For the example, the following values are assumed.

GMT_{AN} = 191903Z,

Orbital Period, τ, = 99.72 minutes, and

Satellite spin period, P, = 6.3158 seconds.

2-31. The data from WALACQ will be treated first since its real-time of occurrence is earlier than that from ULASKA. The procedure is as follows:

a. Determine the value of normalized time, $(t_N)_{000}$, associated with rotation number 000 at WALACQ. To do this, use

$$(t_N)_{000} = \frac{(19\text{h } 24\text{ m } 06\text{s} - 19\text{h } 19\text{m } 03\text{s})}{99.72}$$

$$= \frac{5.05 \text{ min.}}{99.72 \text{ min.}}$$

WALACQ, $(t_N)_{000} = 0.0506 \approx 0.051$

e. Determine, by use of the appropriate nomogram, the instantaneous roll angles corresponding to the time ratios, T_E/T_{SPIN}. The instantaneous roll angles corresponding to several of the sample T_E/T_{SPIN} ratios are shown in Table 2-3.

TABLE 2-3. SAMPLE TABULATION OF INSTANTANEOUS ROLL ANGLE

Rotation No.	T_E/T_{SPIN}		Instantaneous Roll Angle
	Chan. 1	Chan. 2	
000	2321	2801	2.6
005	2321	2781	2.5
010	2321	2801	2.6
↓	↓	↓	↓
105	2550	2600	0.2

f. Record the reduced data in the Format shown in Figure 2-12.

g. Repeat steps a through e using the data from the other CDA stations for the pass under consideration. (In the illustrative example, these procedures should be repeated using the data in the Attitude Message from ULASKA, and the data tabulated as shown in Figure 2-13.)

h. The reduced attitude data, instantaneous roll angle and its associated normalized time, is then plotted. Normalized time is plotted as the abscicca to a scale of 0.1 unit of time to 1 inch of graph. The instantaneous roll angle is plotted as the ordinate. The ordinate scale is made to agree with that of the selected sine-curve overlay (i.e., the 2-degree, 10-degree, or 90-degree overlay). For the case at hand, the 10-degree overlay is used and 2 degrees of roll angle are taken equal to 1 inch. A completed data plot is shown in Figure 2-14.

i. Place the selected sine-wave overlay on the data plot and, by sliding the overlay to the left or right along the zero line, determine which sine-curve, either by a direct fit or by interpolation between the available sine-curves, most nearly fits the data points. Once this fit is achieved, φ_{MAX}, is read directly from the graph. As shown in Figure 2-14, the φ_{MAX} for the example is 4 degrees.

j. Obtain the orbit phasing parameter, λ, by multiplying the normalized time of the positive-going zero crossing of the roll angle by 360 degrees. For the case of the illustration this is:

$$\lambda = 3600\ (0.665) = 239.40 \text{ or } 239°.$$

TIROS IX ORBIT 0022 3 NOV. 1964 WALACQ

Rotation No.	$(\Delta t_N)_n$	Normalized Time $\left[(t_N)_n = (t_N)_{000} + (\Delta t_N)_n\right]$	Instantaneous Roll Angle (φ_i)
000	0	0.051	2.6
005	0.005	0.056	2.5
010	0.011	0.062	2.6
015	0.016	0.067	2.4
020	0.021	0.072	2.4
025	0.026	0.077	2.2
030	0.032	0.083	2.1
035	0.037	0.088	1.8
040	0.042	0.093	2.0
045	0.048	0.099	1.9
050	0.053	0.104	1.6
055	0.058	0.109	1.5
060	0.063	0.114	1.5
068	0.072	0.123	1.5
070	0.074	0.125	1.2
076	0.080	0.131	1.1
080	0.085	0.136	0.8
090	0.095	0.146	0.8
094	0.099	0.150	0.6
100	0.106	0.157	0.4
105	0.111	0.162	0.2

Figure 2-12. Example of Reduced Attitude Data Derived from WALACQ Attitude Message

TIROS IX ORBIT 0022 3 NOV. 1964 ULASKA

Rotation No.	$(\Delta t_N)_n$	Normalized Time $\left[(t_N)_n = (t_N)_{000} + (\Delta t_N)_n\right]$	Instantaneous Roll Angle (φ_i)
000	0	0.181	-0.1
005	0.005	0.186	-0.2
010	0.011	0.192	-0.4
015	0.016	0.197	-0.7
020	0.021	0.202	-1.0
025	0.026	0.207	-0.9
031	0.032	0.214	-1.0
035	0.037	0.218	-1.2
040	0.042	0.223	-1.2

Figure 2-13. Example of Reduced Attitude Data Derived from ULASKA Attitude Message

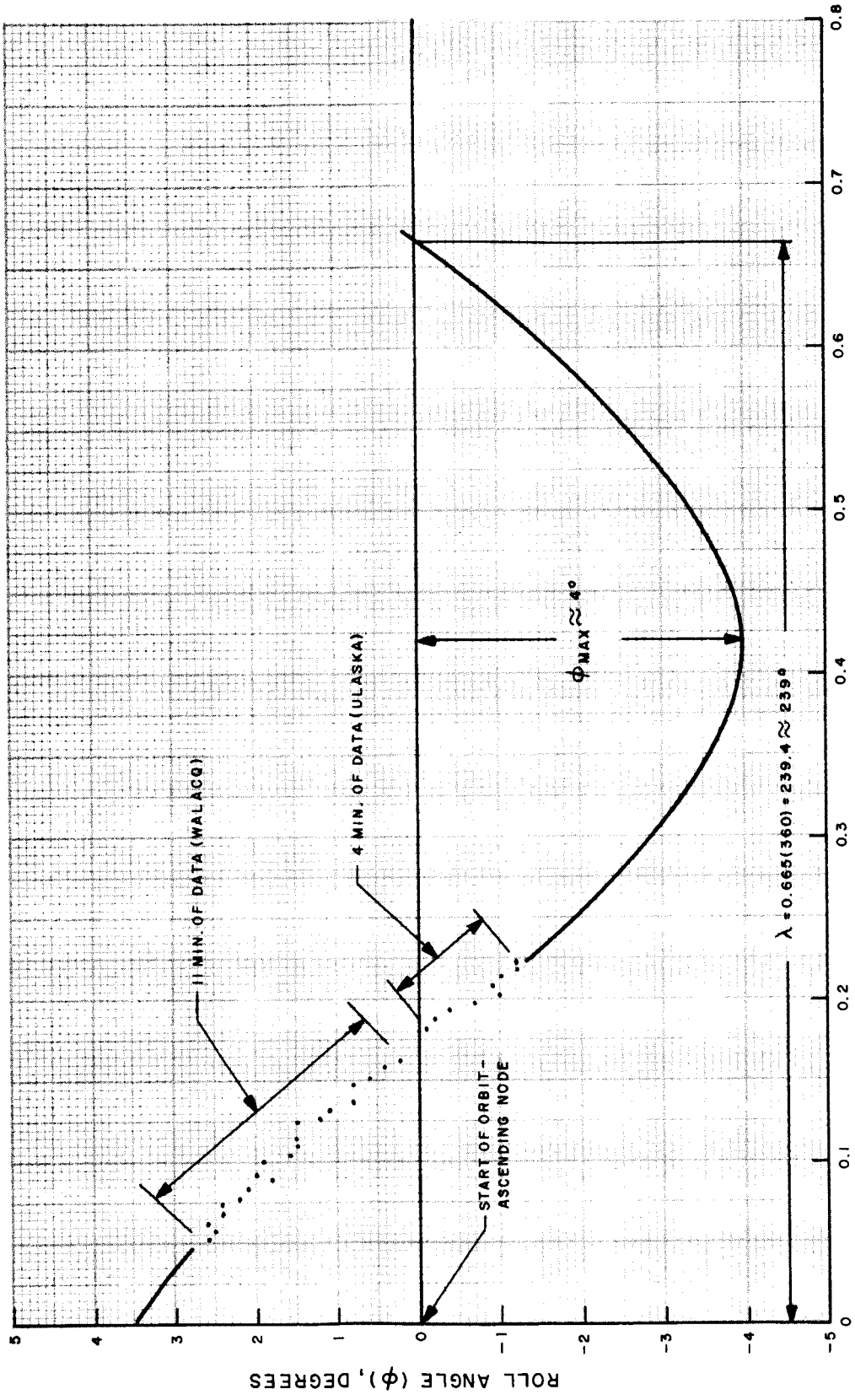

Figure 2-14. Example of Graphical Determination of φ_{max} and λ

SECTION III. CONTROL DECISIONS

3-1. PURPOSE

3-2. The purpose of this section is to define criteria for evaluation of the attitude error and the spin-rate error of the satellite, and to detail the procedures for preparing the commands which are available for implementing corrections.

3-3. REQUIREMENTS

3-4. Control commands are required for directing the operation of the QOMAC, MBC, and MASC coils of the satellite. The QOMAC and MBC coils are used to maintain proper satellite attitude. The MASC coil is used to maintain the proper satellite spin rate.

3-5. GENERAL PROCEDURE

3-6. The general method for arriving at each of the control decisions covered in this section is as follows:

a. Compare the present condition of the satellite with the allowable-error criteria.

b. Determine the amount of correction required to eliminate (or reduce) the error.

c. Determine, if applicable, the required time-of-application of the correcting control.

3-7. To implement a control command, it must always be submitted to the TTCC personnel responsible for actually programming commands to the satellite as far in advance of the desired time of implementation as possible.

3-8. REDUCED-DATA GRAPHS SUITABLE FOR EVALUATION

3-9. Four graphs should be maintained to provide historical records for evaluation of satellite spin rate and attitude. These graphs are as follows:

a. Spin rate (ordinate) in revolutions per minute against orbit number.

b. Maximum roll angle (ordinate) in degrees against orbit number.

c. Orbital-phasing parameter (ordinate) in degrees against orbit number.

d. Polar plot of the maximum roll angle φ_{max} (magnitude) in degrees against a λ' parameter (angle) in degrees as shown in Figure 3-1.

3-10. The data for the required graphs are conveniently available from the following sources:

a. Spin rate is listed on the latest Telemetry Pass Summary,

b. Maximum roll angle and orbital-phasing parameter (λ) are obtained from the plot of the latest roll-angle history, and

c. The λ' parameter in degrees is determined from the relationship

$$\lambda' = \lambda + 90$$

3-11. Set up the graphs to any convenient scale. Add data points to each plot as reduced data from each orbit becomes available.

3-12. QOMAC DECISIONS

3-13. EVALUATION CRITERIA

3-14. Whenever the maximum roll angle, φ_{max}, of the satellite spin axis becomes equal to or greater than 1 degree, a QOMAC command should be prepared. The value of the existing maximum roll angle can be determined from the graph of maximum roll angle versus orbit number, described in Paragraph 3-9.

3-15. SELECTION OF OPERATING MODE

3-16. Two modes of QOMAC operation are available: high-torque (5 degrees per cycle) and low-torque (2 degrees per cycle). Select the mode of operation in accordance with the following criteria:

a. If the maximum roll angle is less than 15 degrees, select the low-torque mode of operation.

b. If the maximum roll angle is equal to or greater than 15 degrees, select the high-torque mode of operation.

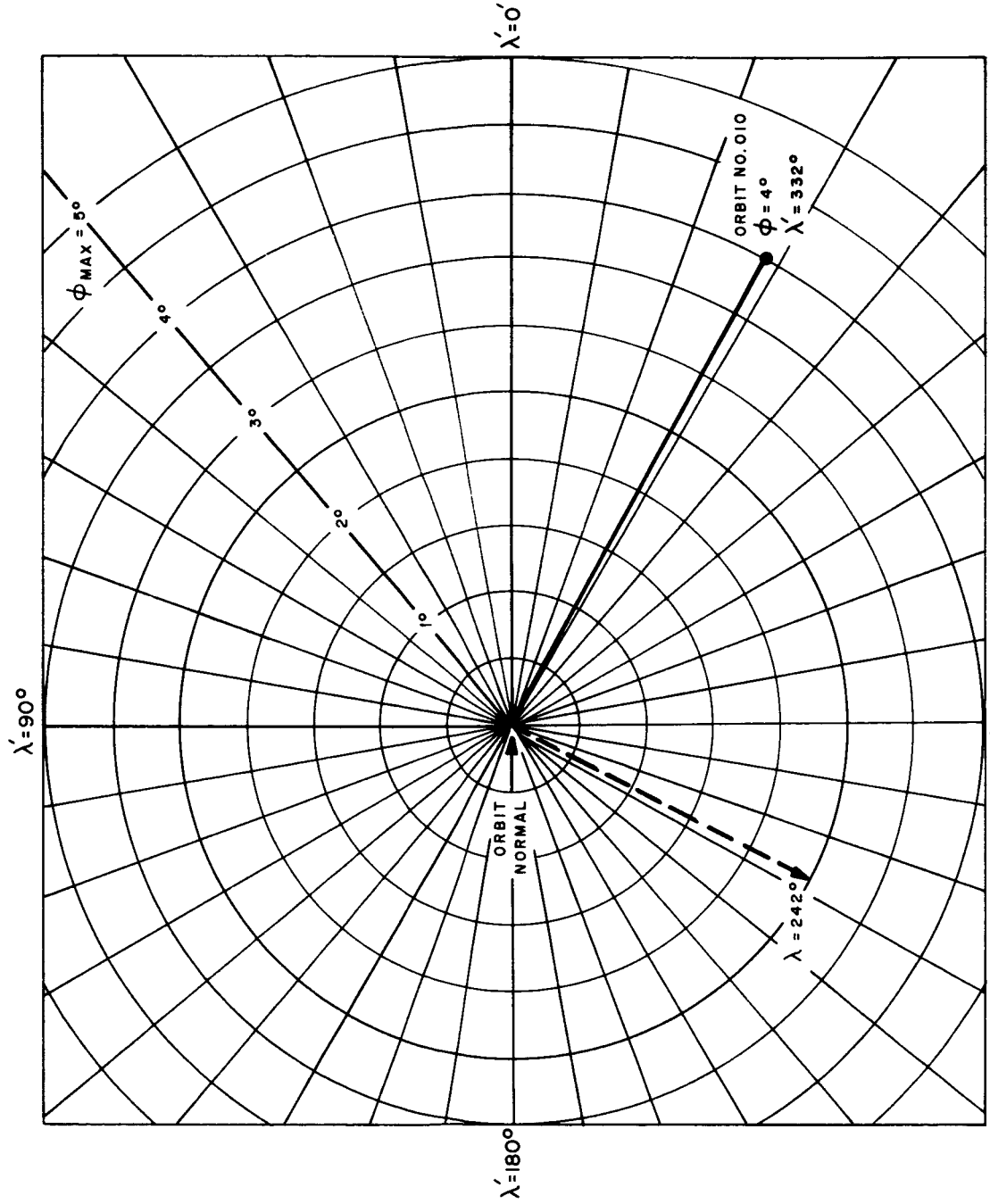

Figure 3-1. Sample Polar Graph of φ_{max} Versus λ'

NOTE

The High Torque Mode normally will be used only once during spacecraft life, i.e., during the orientation maneuver on Julian days 000 and 001.. The Low-Torque Mode should be used for routine torquing.

3-17. DETERMINATION OF NUMBER OF CORRECTION CYCLES REQUIRED

3-18. If the low-torque mode of operation has been selected, use one of the two following alternative relationships to determine the required number of QOMAC cycles (N_Q)*:

a. If the orbital-phasing parameter (λ) is equal to or greater than 180 degrees (as determined from the graph of λ versus orbit number) use the relationship

$$N_Q = \frac{\varphi_{MAX}}{2} ,$$

where

φ_{MAX} is the maximum roll angle (degrees).

b. If the orbital-phasing parameter (λ) is less than 180 degrees, use the relationship

$$N_Q = \frac{\varphi_{MAX}+1}{2} ,$$

3-19. If the high-torque mode of operation has been selected, use the following relationship to determine the required number of QOMAC cycles*:

$$N_Q = \frac{\varphi_{MAX}}{5} ,$$

where

φ_{MAX} is the maximum roll angle (degrees).

---

*A maximum of eight cycles can be programmed. Roundoff the N_Q as computed above to the lower whole number.

3-20. DETERMINATION OF THE REQUIRED ALARM TIME

3-21. Calculate the time after ascending node T_{AAN} in minutes, for the start of a QOMAC sequence using the equation

$$T_{AAN} = \frac{\tau}{720} (\lambda - K) - (100 - \tau) \frac{N_Q}{4},$$

where

τ is the anomalistic period (minutes),

λ is the orbital-phasing parameter (degrees), and

K is a correction angle (degrees) obtained from the graph of K versus the east longitude of the ascending node (E_{LAN}) on the west longitude of the ascending node (W_{LAN}) (see Figure 3-2).

NOTE

The longitude of the ascending node is obtained from ephemeral data.

NOTE

When T_{AAN} as computed above is a negative number, add 50 minutes to the computed value to obtain the desired T_{AAN}.

3-22. Calculate the GMT of the QOMAC alarm time using the equation

QOMAC Alarm Time = $GMT_{AN} + T_{ANN}$ =_____h____M____s GMT,

where

GMT_{AN} is the time of the ascending node.

NOTE

If the QOMAC alarm time (in GMT) computed in paragraphs 3-22 occurs prior to the CDA station contact time, or so early in the contact period that sufficient time for QOMAC command transmission is not available, 50 minutes should be added to the computed QOMAC alarm time.

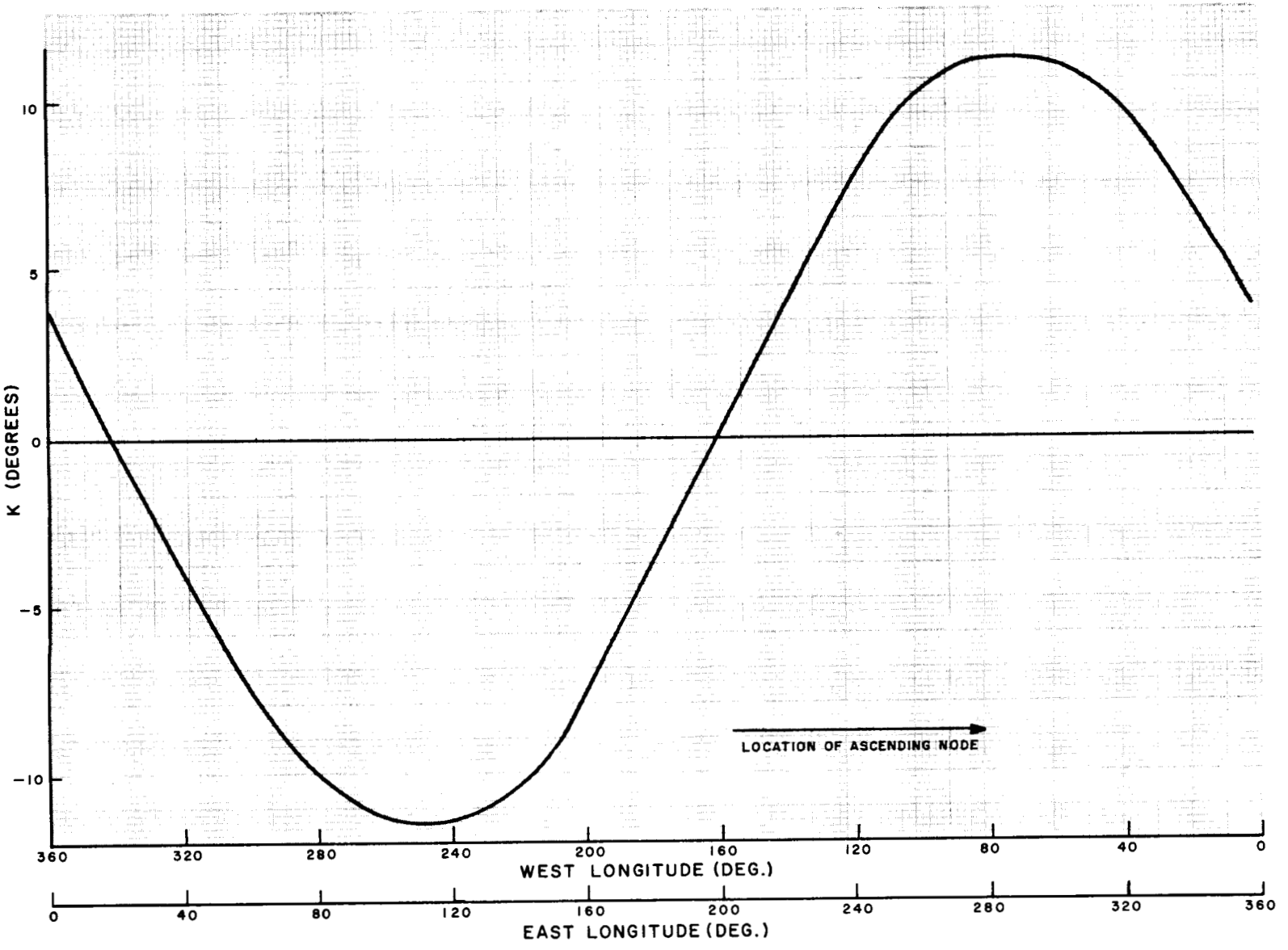

Figure 3-2. Correction Required to Compensate λ for Effect of Inclined Earth Dipole (K vs E_{LAN} and W_{LAN})

3-23. COMPOSITION OF A QOMAC COMMAND

3-24. Submit all of the following QOMAC information to the TTCC personnel responsible for programming the satellite:

a. The number of the orbit during which the command is to be implemented.

b. The mode of operation (selected in Paragraph 3-16).

c. The number of cycles N_Q (calculated in Paragraph 3-17).

d. The alarm time of the QOMAC Sequence (calculated in Paragraph 3-21).

NOTE

Because some orbits are more available for contact than others, final determination of the alarm time and orbit number should be coordinated with the programming personnel.

3-25. MBC DECISIONS

3-26. EVALUATION CRITERIA

3-27. Whenever the maximum roll angle of the satellite's spin axis is observed to increase at an average rate greater than 0.5 degrees per day, a suitable MBC command must be derived.

3-28. MONITORING SPIN-AXIS DRIFT

3-29. The rate of change of the φ_{MAX} is to be monitored through use of the polar graph of φ_{MAX} versus λ' described in Paragraph 3-9. To determine the rate and polarity of maximum roll-angle drift, proceed as follows:

a. Mark the φ_{MAX} and λ' of the satellite on the graph at the beginning of the day.

b. Mark the final φ_{MAX} and λ' of the satellite on the graph at the end of the day.

c. Lay off the distance between the initial and final maximum roll angles of the satellite spin axis. Start at the origin and mark off this distance along any radial line.

d. Read the value of the marked-off change in maximum roll angle. This is the absolute value (approximate) of the maximum roll angle drift per day, ω_D in degrees.

e. Determine the polarity of ω_D as follows:

(1) Draw a drift line on the polar graph to connect the points which correspond to the initial and final values of maximum roll angle.

(2) Mark the direction of this drift line.

(3) Project the drift line and its corresponding direction onto the 0- to 180-degree axis.

(4) Establish the polarity of ω_D in accordance with the following criteria:

(a) If the direction of the drift line as projected onto the 0- to 180-degree axis is toward the left, the polarity of ω_D is negative.

(b) If the projection is toward the right, ω_D is positive.

3-30. DETERMINATION OF THE REQUIRED MAGNITUDE OF CORRECTION MOMENT

3-31. Calculate the magnitude of magnetic moment (amp-turns-meters^2) which is to be programmed into the MBC coil of the satellite, using the relationship

$$M_{MB} = 0.344 - M_R$$

where

M_R is the approximate residual magnetic moment (ampere-turns-meters^2) of the satellite, M_R can be determined from the graph in Figure 3.3 which was plotted using the relationship

$$M_R \simeq 3.43 \times 10^{-2} \omega_S [1 + 1.01 \omega_D]$$

where

ω_D is the maximum roll-angle drift in degrees per day (as calculated in Step d and with the polarity as determined in Step e of Paragraph 3-29), and

ω_S is the present spin rate (revolutions-per-second) of the satellite.

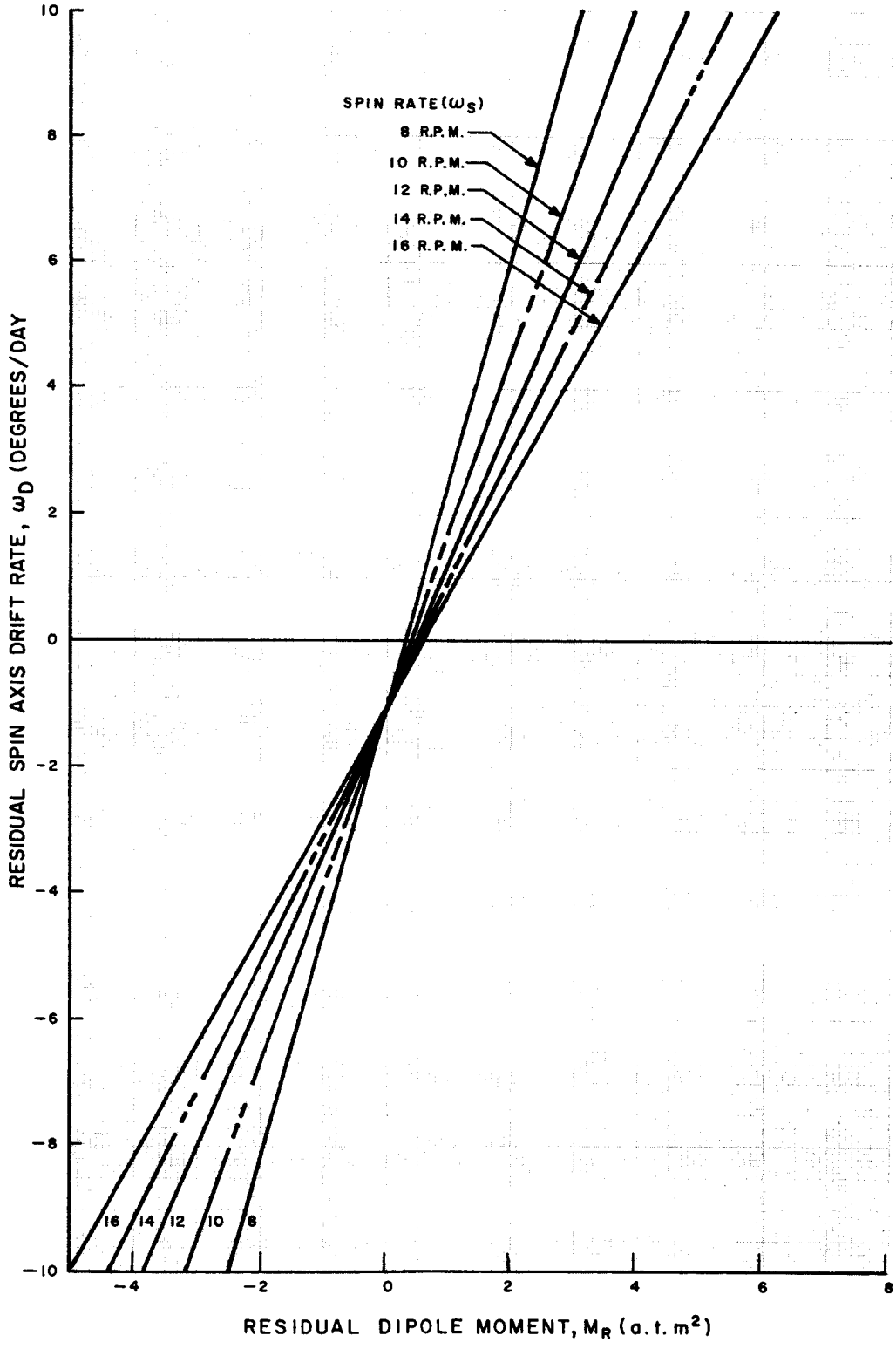

Figure 3-3. Residual Dipole Moment Versus Drift Rate

3-32. COMPOSITION OF A MBC COMMAND

3-33. Table 3-1 lists the M_{MB} for each position of the MBC switch. The satellite-borne MBC switch is to be set to the position providing the magnetic moment that most closely matches the calculated M_{MB}. The polarity of the programmed magnetic moment required to overcome the spin-axis drift is identical to the algebraic sign of M_{MB} computed above. After determining the required switch position and polarity, give this information to the programmer to allow preparation of the necessary commands.

TABLE 3-1. MBC SWITCH-POSITION DATA

MBC Switch Position	Magnetic Moment For The MBC Coil (M_{MB}) (Ampere-Turns-Meter^2)		Notes
	Positive	Negative	
1	+1.92	-1.86	
2	+1.85	-1.73	
3	+1.62	-1.49	
4	+1.43	-1.32	
5	+1.18	-1.07	
6	+1.09	-0.96	
7	+0.89	-0.77	
8	+0.68	-0.56	
9	+0.47	-0.38	
10	+0.25	-0.15	
11	--	--	High QOMAC Torque Enable
12	0	0	"Home" position

3-34. MASC DECISIONS

3-35. EVALUATION CRITERIA

3-36. If desired, the MASC system can be used to control the spin rate within the limits of 8 to 12 rpm. If the spin-synchronized camera triggering mode is used, the spin rate must be maintained within the range of 9.62 to 9.93 rpm. The optimum spin rate for this operation is 9.78 rpm.

3-37. DETERMINATION OF THE REQUIRED AMOUNT OF SPIN-RATE CORRECTION

3-38. If the satellite spin rate is too slow, a spin-up command is formulated. If the satellite spin rate is too fast, a spin-down command is formulated; however, spin-down commands are not normally required since the satellite spin rate decays naturally.

3-39. Determine the desired spin rate increment, (i.e., the difference between the desired spin rate and the present spin rate) to within 0.05 rpm accuracy.

3-40. DETAILED PROCEDURE

3-41. For simplicity of operation, only WALACQ (or RCAHNJ) shall be used to command MASC sequences. Any station could be used; however, an east cost station provides many advantages and simplifications which will not be discussed in detail here. Table 3-2 lists various spin rate increments which can be obtained for particular West Longitude of Ascending Node and the MASC Start Time after the Ascending Node (AAN).

TABLE 3-2. MASC PERFORMANCE (WALACQ CONTACTS ONLY)

Start Time After Ascending Node, T_S	Spin Rate Increment (RPM) Versus Longitude of Ascending Node			
	10°W	40°W	70°W	100°W
8 min 20 sec	0.13	0.13	0.13	0.13
16 min 40 sec	0.12	0.12	0.12	0.12
25 min	0.09	0.08	0.07	0.07
33 min 20 sec	0.03	0.02	0.01	0.01

3-42. The procedure for formulation a MASC command is as follows:

a. Determine the magnitude of the required change in spin-rate and whether a spin up or spin down is required.

b. Determine the longitude of the ascending node for the next orbit providing WALACQ contact.

c. Choose a start time after ascending node, T_S, from Table 3-2 which most closely approximates spin rate increment, or the closest value.

NOTE

If the desired spin rate increment is greater than all values in the table, several cycles of the MASC Sequence will be required. Select the number of cycles which will give the closest value to the desired spin rate increment; a maximum of eight cycles are available.

d. Determine the MASC alarm time, using the relationship

$$\text{MASC Alarm Time} = GMT_{AN} + T_S = \_\_\_\_\ h \_\_\_\ m \_\_\_\ S^{GMT}.$$

3-43. COMPOSITION OF A MASC COMMAND

3-44. Submit all of the following MASC information to the programmer personnel:

a. The number of the orbit selected.

b. The number of cycles required.

c. The alarm time of the MASC sequence.

d. Whether spin up or spin down is required.

ADDENDUM I

TO THE TIROS IX ATTITUDE HANDBOOK

ADDENDUM I

1. SCOPE

2. This addendum to the Attitude Handbook contains an elaboration of the material presented in the initial publication. Additional details on the nature of the attitude control system philosophy and the alternate methods for reducing the attitude data, which were omitted in the initial publication for the sake of clarity, are included herein. Wherever information contained in this section has a direct bearing on the previous material, reference is made to the appropriate paragraph of the initial publication. It is anticipated that as experience with TIROS IX operations increases, the various procedures that have been recommended in this document will be modified to create a more efficient system of attitude control.

3. FUNDAMENTALS OF ATTITUDE CONTROL

4. GENERAL

5. Two aspects of a spinning satellite may be controlled by means of magnetic fields generated within the satellite, namely, the orientation of the spin axis in space and the rate of spin. The desired control is achieved by utilizing the torque developed by interaction of the earth's magnetic field and the field resulting from current flow in specially designed coils. Two principles are involved: one, the generation of the torque and two, the effect produced by the torque on spacecraft attitude and spin rate. A heuristic explanation of the phenomena of magnetic attitude control is presented below; the mathematical bases is contained in Appendices C and D.

6. When current flows through a coil (see Figure I), a magnetic field is set up about the coil in such a way that the coil exhibits a magnetic axis through its center. The coil is said to have a dipole moment along this axis. When the coil is energized, its dipole moment reacts with the earth's magnetic field to produce a torque which tends to move the dipole moment into coincidence with the earth's field lines. This implies that the torque vector is normal to the plane determined by the vectors representing the coil's dipole moment and the earth's magnetic field in the vicinity of the coil. Depending upon the orientation of the coil, the direction of the torque may be made to lie along, or at right angles to, the spin axis of the satellite. For spin rate control, a torque co-linear with the satellite spin axis is needed. To obtain this, the plane of the magnetic spin control coil (MASC) is put parallel to the spin axis. On the other hand, to effect a change in direction of the momentum vector (pitch axis), a torque which is normal to the spin axis is required. Therefore, the coil for this application is installed with its magnetic axis parallel to the momentum vector.

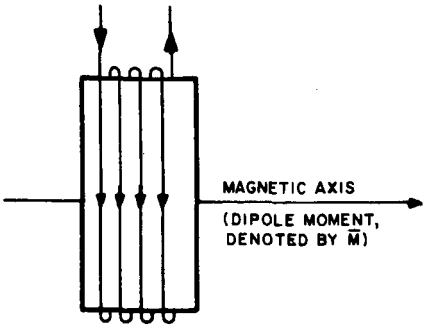

a. Dipole Moment of Current-Carrying Coil. Direction of Current and Magnetic Dipole Moment are Related by the Right-Hand-Rule.

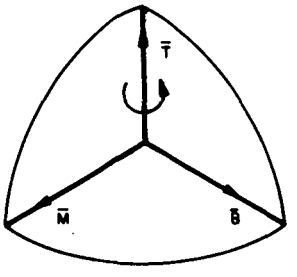

b. Torque $\bar{T}$ Developed by Interaction of Coil's Dipole Moment, $\bar{M}$, and Earth's Magnetic Field, $\bar{B}$. (Directionally, $\bar{M}$, $\bar{B}$, and $\bar{T}$ are related by RIGHT-HAND-RULE, Mathematically their Relationship is Expressed as $\bar{T} = \bar{M} \times \bar{B}$)

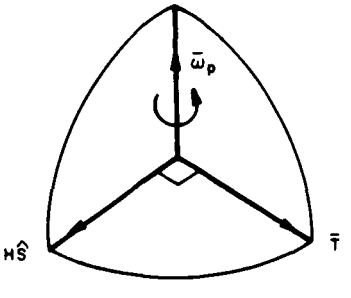

c. Precession Motion $\bar{\omega}_p$ of Spin Axis $\hat{S}$ Caused by Torque $\bar{T}$.
($\bar{T} = \bar{\omega}_p \times \bar{H}$)

Figure I. Elements of Magnetic Attitude Control

7. However, because the satellite is a spinning body, it will undergo gyroscopic motion when subjected to torque which is transverse to the direction of spin. The basic law of the gyroscopic indicates that, when a gyroscope is torqued at right angles, its spin vector will move into coincidence with the torque vector. The resulting motion, which gives rise to a change of direction of the spin axis, is referred to as precession. To utilize this precession motion to move the momentum axis in essentially any desired direction, the current in the coil used for attitude maneuvering is programmed according to a technique referred to as Quarter Orbit Magnetic Attitude Control (QOMAC). The programming scheme is characterized by two parameters: satellite orbit angle, or time from ascending node at which the torquing is initiated, and cyclic variation of coil current from plus to minus every quarter of an orbit. The physical reasons for this scheme, together with some of its limitations, are presented in the following mathematical description. In addition to QOMAC, continuous torquing of the satellite by means of a Magnetic Bias Coil (MBC) is provided for the purpose of offsetting the residual magnetism of the satellite and to correct for orbital regression.

8. QOMAC AND MBC

9. As the satellite orbits about the earth, the direction of the earth's magnetic field (B-field) lines change with respect to the orbit coordinate system described in Appendix C. As shown in equations (C-10), the field component along the ascending node varies at twice orbital rate; the component along the orbit normal is independent of orbit angle; and the component along an axis normal to the plane defined by the ascending node and the orbit normal, varies at twice orbital rate plus a constant term. Therefore, if a positive dipole moment exists along the spin axis of the satellite, a precession vector will be generated in a direction opposite to the instantaneous field lines. If this dipole moment is maintained over a segment of the orbit, the change in the direction of the earth field lines will cause a change in the direction of the precession vector. The average direction and magnitude may be computed by integrating the B-field components over that segment of the orbit. By utilizing the averaging procedure it may be shown that for a positive dipole polarity, over a complete orbit, the average precession vector will be perpendicular to the line of nodes, lie almost in the orbit plane, and be directed northward. It may also be shown that reversing the dipole polarity over a complete orbit will have an effect identical to that of reversing the earth's B-field and, as a result, the average precession vector will be opposite to the one just described. Further, if the dipole polarity is reversed every quarter of an orbit, for an integral number of cycles (1 cycle = 1/2 orbit), it may be shown that the effective average B-field, which is anti-parallel with the average precession vector, will lie completely in the orbit plane, and that its location with respect to the ascending node will be linearly related to the start time for the ascending node of a cycle. It should also be noted that cycles which start 180^{o} apart yield the same average precession vector. This latter technique with the associated properties form the basis of the QOMAC technique. The Mag Bias (or standard TIROS) mode of operation is associated with orbit averaging of a specific dipole polarity over a complete orbit.

10. The flexibility of being able to select a precession vector anywhere in the orbit plane as a function of the start time is ideal for attaining and maintaining a wheel mode of operation. For example, assume that the spin axis is displaced from the orbit normal by some angle, ϕ_{max}, as shown in Figure II. Due to the inertial rigidity of a spinning body the relationship between the spin axis and orbit normal can be depicted as shown, and the attitude determined uniquely by the two parameters ϕ_{max} and λ'. If the precession axis can be selected so that the spin axis moves in a plane (i.e., a precession 1/2-cone angle of 90 degrees) toward the orbit normal, a control technique exists which will bring the satellite into wheel orientation. To visualize this technique, note that a vector lying in the orbital plane normal to the projection of the spin axis on the orbital plane must also be normal to the spin vector itself. As a result, the desired precession axis (i.e., for the 1/2-cone angle of 90 degrees) is given by a vector lying in the orbit plane at an angle $\lambda = \lambda' - 90$ from the ascending node. QOMAC provides the flexibility required to achieve and maintain the desired precession axis throughout the orbit. The problem of determining the values of ϕ_{max} and λ has been discussed at some length in the initial publication of the Attitude Manual.

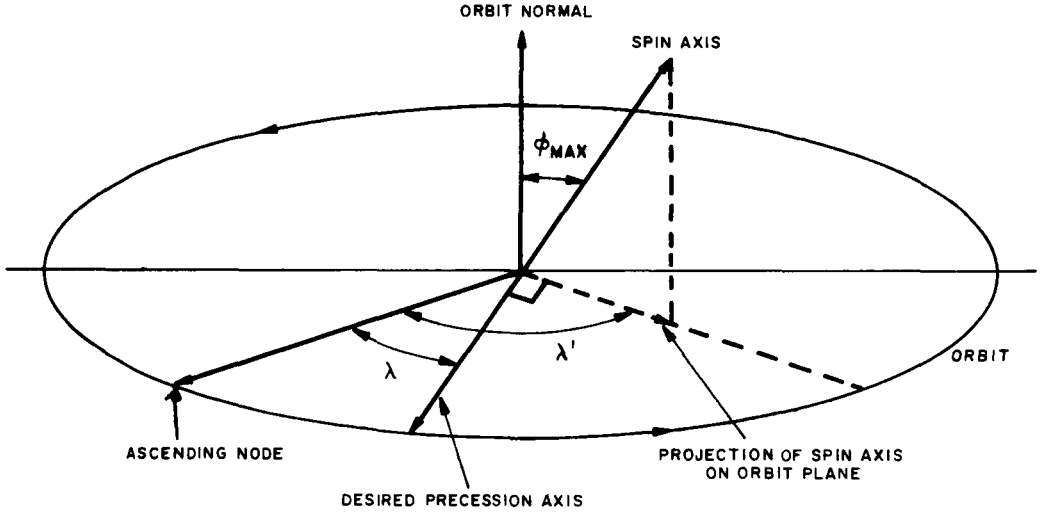

Figure II. Attitude and Orbit Geometry

11. Attitude control through use of MBC consists of selecting a particular resistor, one of ten on a 12-position switch that may be set by ground command, to be connected in series with the magnetic-bias coil and the -13 volt power source. This effectively determines the magnitude of the d-c magnetic moment of the satellite. The polarity may also be selected by driving the current through different halves of the center tapped coil. After evaluating the residual dipole of the satellite by observing the rate at which the spin axis drifts from the desired attitude, a particular switch position is selected to yield a resultant dipole that generates a precession rate of approximately one degree per day, the anticipated orbital regression rate (see Appendix C). The location of the average precession vector using this technique is such that its combined effects are similar to that of orbital regression. That is, MBC in this orbit generates, for the most part, changes in the right ascension of the spin vector, while orbital regression causes the right ascension of the orbit normal to vary.

12. MASC

13. Since TIROS is a spin-stabilized satellite, it is necessary to maintain a nominal rotational velocity about the axis of maximum moment of inertia. On previous TIROS satellites, the decay in spin rate (due primarily to eddy currents) was cancelled by occasional firing of spin-up rockets. In order to provide a spin control capability which is not limited by stored rocket impulse and which can be utilized bi-directionally (i.e., spin up or spin down) in fine rate-increments, Magnetic Spin Control (MASC) has been installed in the TIROS-Wheel satellite. The basic concept of the MASC system is presented in the following paragraphs; the mathematical analysis for MASC are included in Appendix C. For those who are familiar with the operation of an electric d-c motor, the close analogy to the MASC concept will be obvious.

14. As stated previously, to change the spin rate of the satellite a torque is necessary along the spin axis and hence a coil whose axis is perpendicular to the spin axis is required. For the sake of discussion, it is assumed that the TIROS-Wheel satellite is in a polar orbit and that the earth's magnetic field may be represented as an uncanted dipole, as shown in Figure III. As the satellite travels along the orbit path, the instantaneous $\bar{B}$ field is always in the orbit plane, although changing direction and magnitude with satellite position. (At the poles the field lines, which are almost vertical and point South, are twice as dense as those at the equator where the lines are horizontal and point North.) Since the magnetic moment is along the coil axis, it also must lie in the orbit plane because of the wheel orientation. Therefore the torque will be along spin axis and either positive or negative, depending on the relative positions of $\bar{M}$ and $\bar{B}$ ($\bar{T} = \bar{M} \times \bar{B}$).

15. However, because the coil is rigidly attached to a spinning body, the magnetic moment will rotate through 2π radians on every spin as shown in Figure IVa. As a result, without commutation, the net dipole moment per spin would be zero. However, the MASC system provides the required commutation every half spin and the net average dipole moment for each spin is $2\bar{M}/\pi$.

16. The MASC system uses the two orthogonal IR sensors, which are located 180 degrees apart and are used primarily for camera triggering, to achieve this commutation function. As each sensor sweeps from sky to earth, the dipole moment is reversed by the satellite-born Dycon unit. As a result the geometry between the sensor line and the plane of the coil fixes the average magnetic moment per spin with respect to the local vertical. The local vertical, on the other hand, also rotates with respect to the satellite due to the satellite's orbital motion as shown in Figure V. Therefore, if the current through the coil is maintained through the entire orbit, the average magnetic moment per spin will rotate through 2π radians during the orbit, and will average to zero. Thus the MASC system on TIROS IX can only be operated over segments of the orbit, without further rectification of the average magnetic moment per spin. Because of this, the Dycon unit is designed to energize the spin coil over quarter orbit intervals, i.e., a quarter ON followed by a quarter OFF (one MASC cycle). Switching the initial orientation of $\bar{M}$ with respect to the local vertical every half orbit permits consecutive MASC cycles.

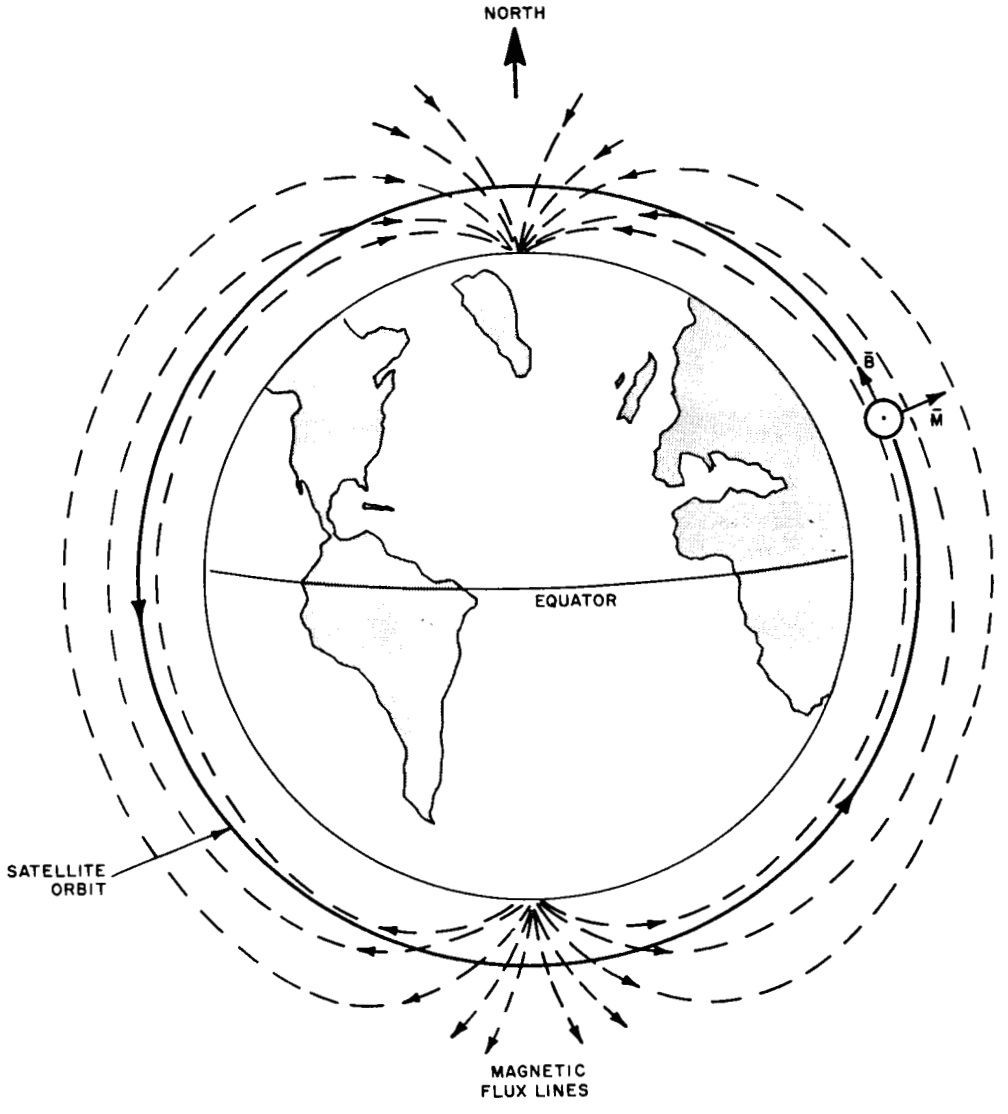

Figure III. Simplified Orbit and Earth's Magnetic Field Geometry

17. Since the magnetic field at the poles is twice as strong as that at the equator, the orientation of the coils with respect to the orthogonal sensors was selected to provide the most efficient commutation at the poles. That is, $\bar{T} = \bar{M} \times \bar{B}$ is maximized for given magnitudes of $\bar{M}$ and $\bar{B}$ by arranging $\bar{M}$ to be perpendicular to $\bar{B}$, and operating in a quarter orbit interval over the poles yields an average $\bar{B}$ field pointing south. Hence the average magnetic moment (already averaged over one spin) over the quarter orbit should be perpendicular to the north-south line. This condition is depicted in Figure V which shows that $\bar{M}$ should be perpendicular to the local vertical (L. V.). This is achieved using the geometry of Figures IV and VI. The actual performance of the MASC system is analyzed in Appendix D. In this appendix the effects

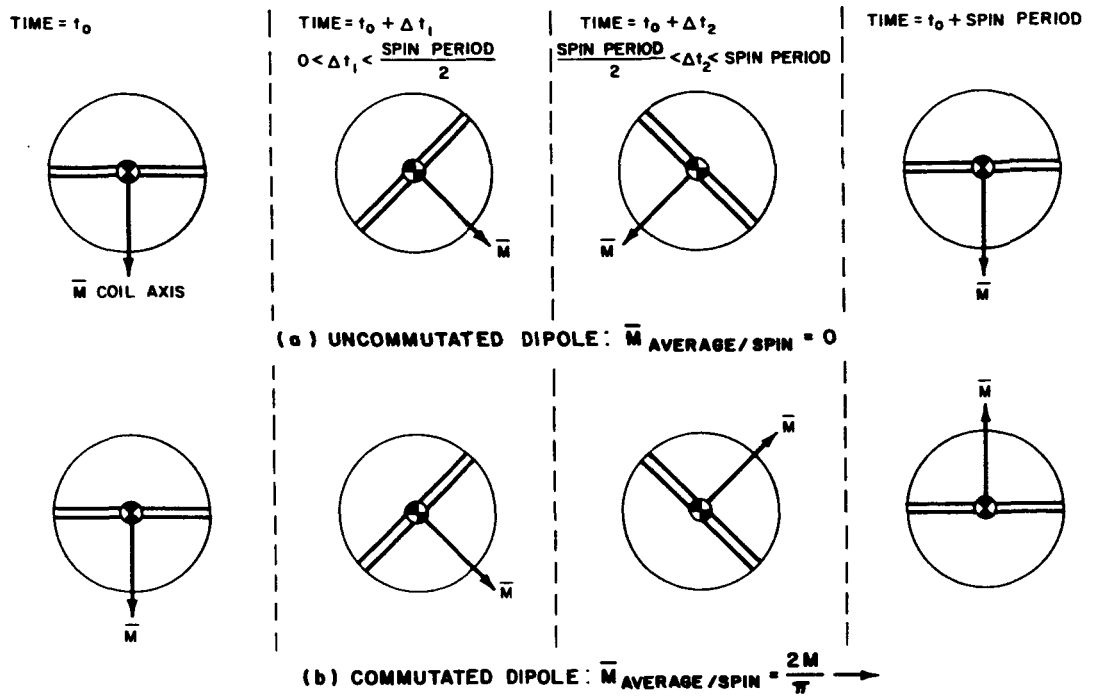

Figure IV. Dipole Motion per Spin

of the canted dipole, the near-polar (as opposed to exactly polar) orbit, orbital altitude not equal to 400 nautical miles, and the start time of a MASC cycle have been included in the performance analysis.

18. STATION KEEPING

19. GENERAL

20. The TIROS IX satellite will be launched south-eastward from Cape Kennedy into a sun-synchronous orbit. The payload will reach orbit altitude at or near the equator, at which time it will be spinning at a nominal rate of 125 rpm. Shortly after separation of the satellite from the third-stage of the rocket, the Yo-Yo despin device will spin down the satellite to a nominal rate of 10 rpm. During the remaining portion of the first orbit, the satellite is expected to remain in the initial injection attitude, with the spin axis lying approximately in the orbital plane, perpendicular to the line of nodes. Throughout this period, pertinent raw data will be accumulated, reduced, and evaluated to verify that the initial attitude and reduced spin rate are as expected.

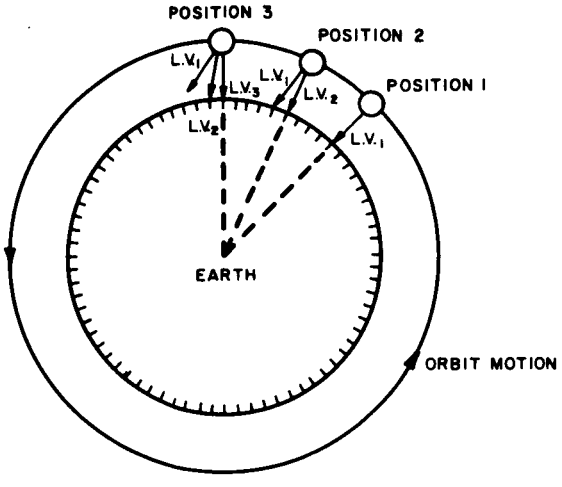

A. LOCAL VERTICAL MOTION

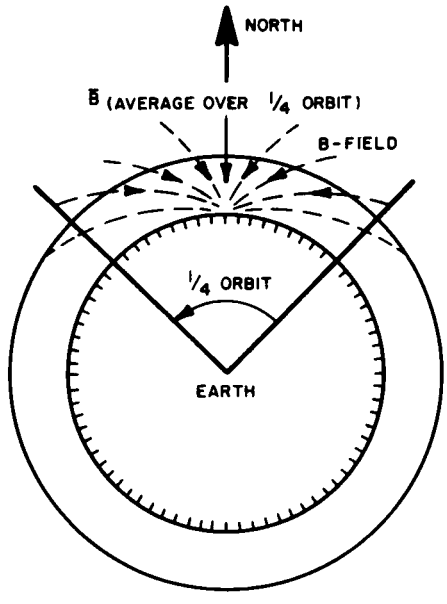

B. AVERAGE B-FIELD OVER POLAR 1/4 ORBIT

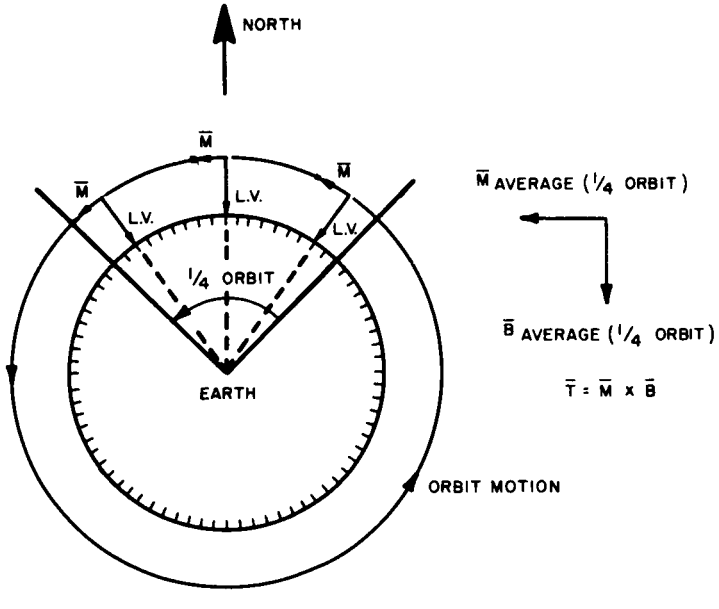

C. AVERAGE DIPOLE MOMENT PER SPIN WITH RESPECT TO LOCAL VERTICAL

Figure V. MASC Operation over Poles

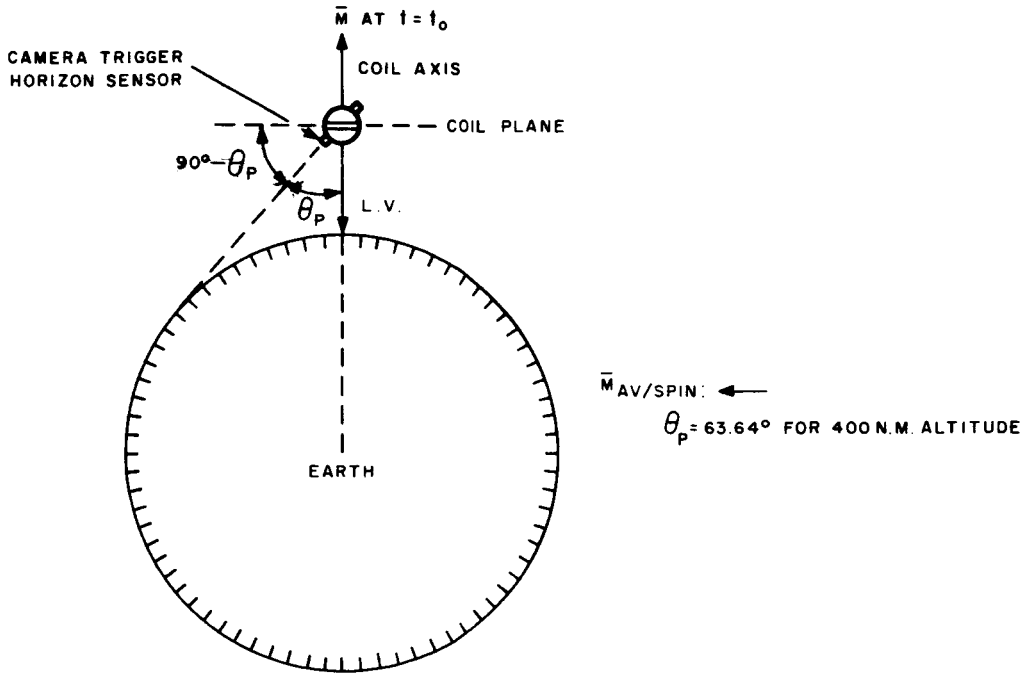

Figure VI. Geometry of MASC Coil With Respect to Trigger Sensors

21. At some time during the second orbit, if all conditions are satisfactory, an attitude-control program will be transmitted to the satellite. This program will command the attitude-control subsystem to precess the spin axis of the satellite toward a position very nearly normal to the orbit plane. Ten to fourteen orbits later, the spin axis will have reached the approximate normal position. Throughout the wheel-orientation maneuver (which is depicted in Figure VII), pertinent raw data will be accumulated, reduced, and evaluated in order to monitor and verify proper operation. (The control commands may be updated, if necessary, to achieve the desired maneuver.)

22. After the wheel-orientation maneuver is completed, the attitude and spin rate will be monitored and evaluated on a routine basis. When necessary, control commands will be prepared and implemented to keep the attitude and spin rate within the acceptable limits. This operation is known as station keeping.

23. The basic procedures for station keeping have been described in Section III of the initial publication. The purpose of this presentation is to describe the expected spin axis behavior in the wheel mode and also to indicate the overall flexibility of the QOMAC system using the polar plot representation of the spin axis.

24. In Section III, paragraphs 3-12 to 3-20, the calculations for torquing the spin axis directly toward the orbit normal are described by relating the start time of a QOMAC cycle to the orbit phasing parameter, λ, obtained from the attitude data.

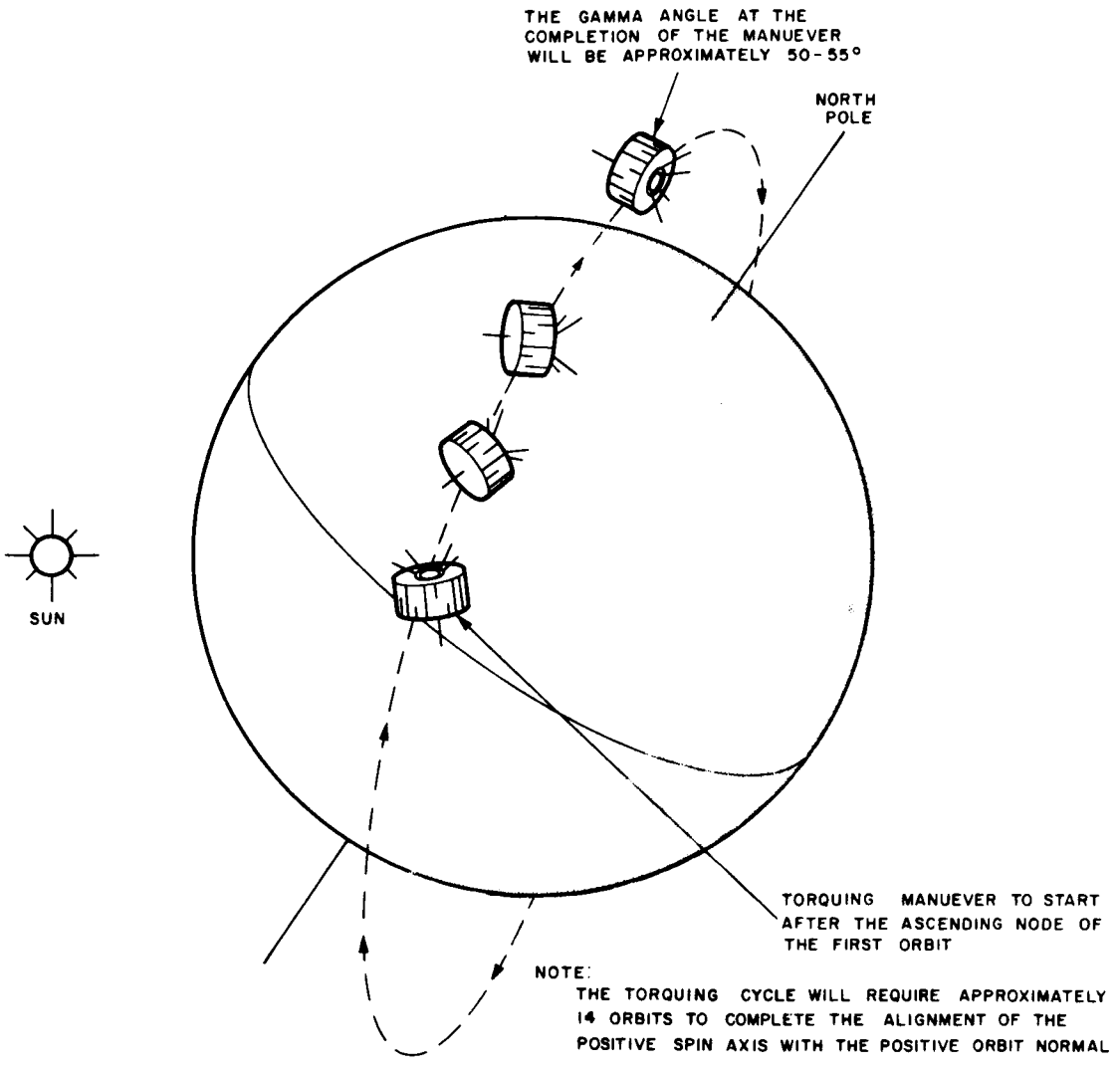

Figure VII. TIROS Wheel-Orientation Maneuver

This essentially generates a precession vector ($\tilde{\omega}\rho$) which lies in the orbit plane in a direction given by λ. However, as described in appendix A, the location of the precession vector, given by Λ, can be made to lie anywhere within the orbit plane as a function of β_s (start angle which is essentially equivalent to start time). By using the polar plot, provided $\phi_{max} \leq 15^o$, it is possible to evaluate Λ and thus T_{AAN} in such a way as to move the spin axis to any position.

25. POLAR PLOT OF SPIN AXIS ATTITUDE

26. The polar plot of spin axis attitude of ϕ_{max} versus λ', shown in Section III, Figure 3-1, is a representation of the actual unit spin vector position as viewed from the orbit normal. The origin (0, 0) corresponds to the orbit normal, the radial line $\lambda' = 0$

corresponds to the line of nodes ($\hat{\ell}$, pointing toward the ascending node) and $\lambda' = 90$ corresponds to the $\hat{b}$ axis described in Appendix C. To make the projection precise, sin ϕ_{max} rather than ϕ_{max} should be plotted on the radial scale. However for $\phi_{max} \leq 15^{o}$, sin ϕ_{max} is within 1% of ϕ_{max}, so that a linear radial scale in ϕ_{max} may be used with sufficient accuracy.

27. Under this projection, motion in a plane toward the orbit normal from an initial position off the normal is represented by a radial line at λ'. Requiring the spin axis to move in this manner suggests the the precession axis must be normal to this line, in fact, 90^{o} clockwise (i.e., $\Lambda = \lambda' - 90^{o}$). Since, by definition, $\lambda' = \lambda + 90^{o}$ it follows that $\Lambda = \lambda' - 90^{o}$ or $\Lambda = \lambda$. This agrees with the previous analysis for the required $\tilde{\omega}_{\rho}$ direction. Referring again to Figure 3-1, the desired precession axis direction for orbit normal acquisition from the point ($\phi_{max} = 4^{o}$, $\lambda' = 332^{o}$) is given by the dotted arrow.

28. SPIN AXIS DRIFT

29. The polar plot is particularly useful for describing the characteristics of spin-axis drift. The only two significant factors in spin axis drift with respect to the orbit normal are orbit plane regression (toward the east for the orbit of TIROS IX) and d-c dipole effects (caused by residual dipole plus MBC dipole). The orbit plane regresses about the north geographic pole of the earth at the rate of very nearly 0.988^{o} per day, provided the design orbit is attained. Since the spin axis is fixed in space, the orbit normal will rotate away from the spin axis as the orbit plane regresses. In orbit coordinates, i.e., in the polar plot, the effect will be an apparent drift of the spin axis away from the orbit normal. Since the rotation of the orbit plane is about geographic north and since the $\hat{b}$ axis is very nearly colinear with the north axis (approximately 8^{o} apart), the drift will appear on the plot as nearly perpendicular to the $\hat{b}$ axis and toward negative $\hat{\ell}$. Looking at the polar plot with $\lambda' = 0$ directed toward the right, the spin axis point, identified by ϕ_{max} and λ', will move approximately parallel to the radial line $\lambda' = 0$ and from right to left. (See Figure VIII.) Similarly, as pointed out in Appendix C, the precession vector due to d-c torquing is very nearly parallel to $\hat{b}$ and hence the motion of the spin axis due to this effect is also parallel to the $\hat{\ell}$ axis. If the d-c dipole is greater than 0.344 atm^2, the motion is from left to right on Figure VIII; if less than 0.344 atm^2, it is from right to left. If the d-c dipole is exactly 0.344 and the spin axis has acquired the orbit normal, it should maintain this position for extended periods of time. The analysis to explain this behavior in detail is contained in Appendix C.

30. The linearity of motion in the neighborhood of the orbit normal and the character of the two factors which cause spin axis drift permit the application of the technique described in Section III, paragraph 3-25 for graphically determining the residual dipole. Use of the procedure given in Section III, paragraph 3-30 should induce a d-c dipole moment in the satellite very nearly equal to 0.344 atm^2 (within ± 0.125 atm^2). In addition, the MBC setting should be established in such a way as to make it likely that the drift will be from right to left in Figure VIII.

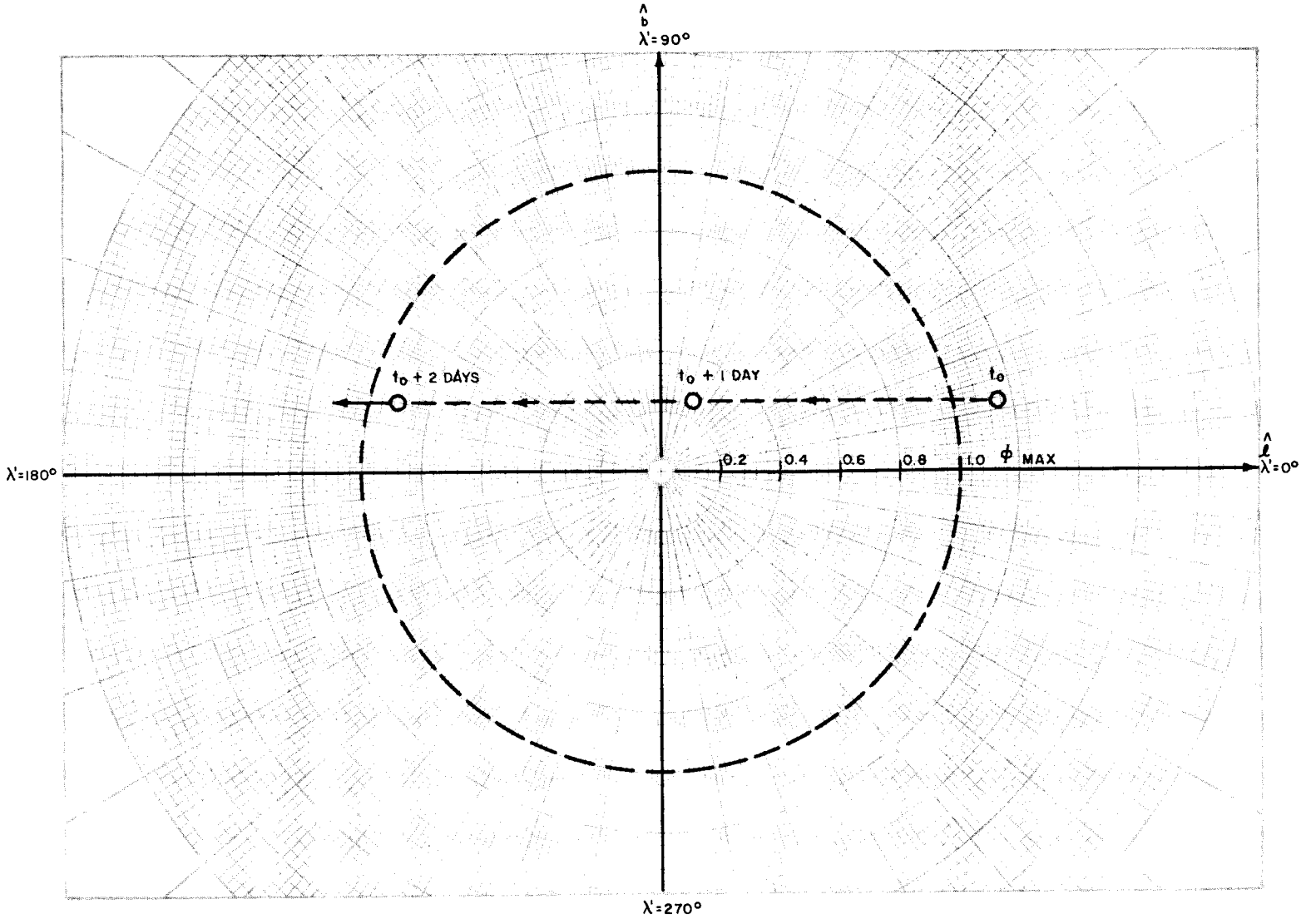

Figure VIII. Orbit Precession Effect on Spin Axis Orientation with Zero D-C Dipole

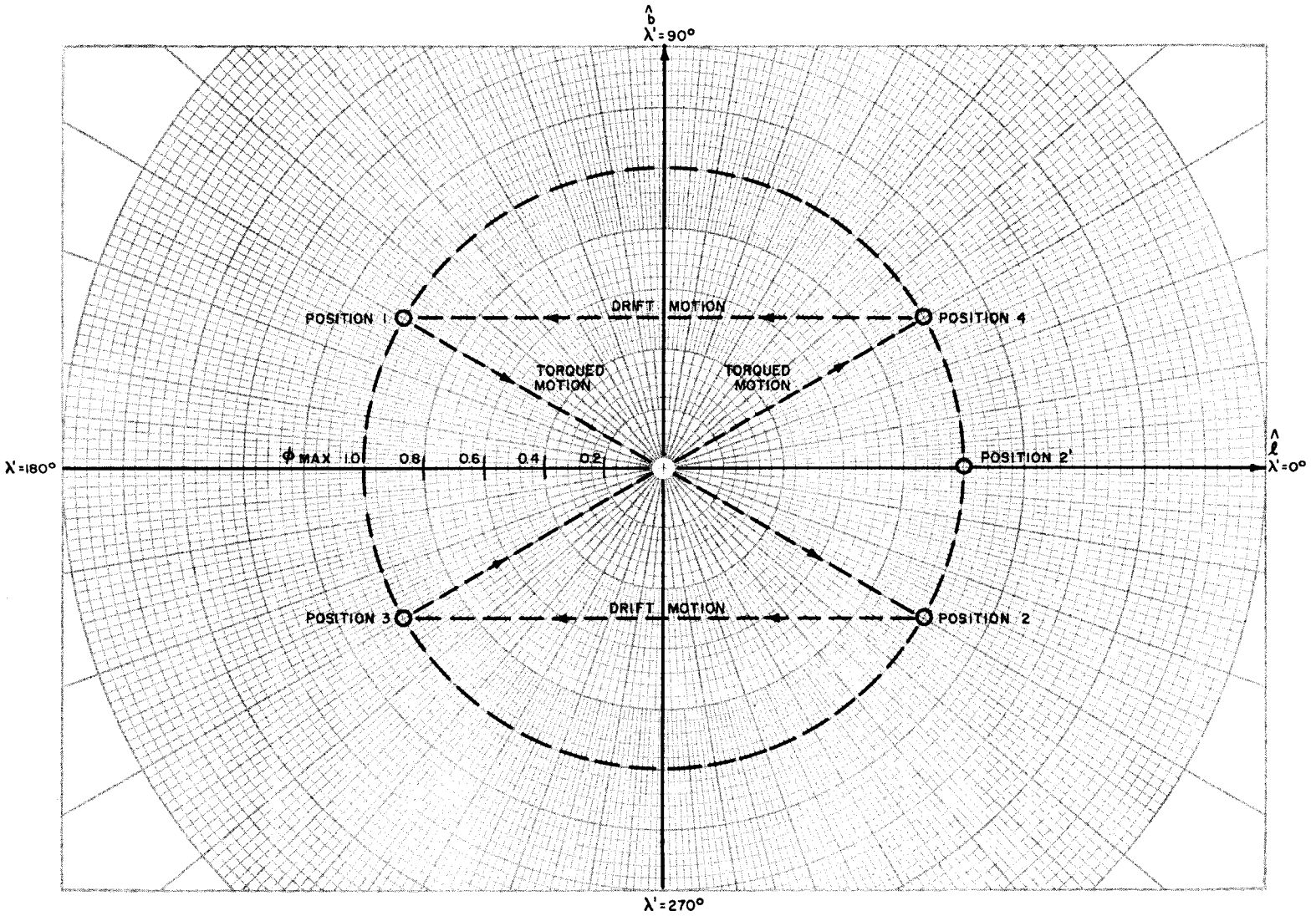

Figure IX. Limit-Cycle QOMAC Operation

31. OPTIMUM ATTITUDE TORQUING

32. The operational QOMAC procedure used for maintaining the wheel-mode attitude is a limit-cycle type; that is, when spin-axis drift is such that a ϕ_{max} of 1^{o} is exceeded, the low-torque QOMAC mode is used to torque the spin axis across the orbit normal for a distance corresponding to 2^{o}. Then the spin axis is permitted to drift back. Unless the spin axis lies on the line $\lambda' = 0^{o}$ or 180^{o}, a situation such as depicted in Figure IX will occur since spin-axis drift is nearly parallel to the $\hat{\ell}$ axis. Hence, it would be advantageous to have a scheme whereby motion other than toward the orbit normal is achieved. From Figure IX, it can be seen that it would be better to move the spin axis to the position 2' instead of position 2 on the first torque cycle, in order to take advantage of the normal direction of drift.

33. The following procedure, which provides this flexibility, is valid for changes in attitude of 10^{o} or less in the neighborhood of the orbit normal. Assume that a change in spin-axis orientation from position 1 to position 2 (as shown in Figure X) is required. As in any other QOMAC torquing, it is necessary to determine the number of torque cycles, N_Q, to effect the change and the QOMAC phasing parameter, λ, which determines the time of start.

34. The required incremental change in attitude, denoted previously as $\Delta\phi_{max}$, to be achieved can be ascertained with sufficient accuracy by use of the polar graph of ϕ_{max} versus λ', and the following procedure (refer to Figure X):

a. Draw a line on the polar graph connecting the plot of the initial attitude and that of the attitude desired (Line AB of Figure X).

b. Using a divider, lay the distance AB off along a radial line, starting at the origin.

c. Read the value of $\Delta\phi_{max}$ which corresponds to the distance (AB) layed off. The value obtained will be a close approximation to value of attitude change desired.

d. To determine the number of torque cycles required to effect the orientation desired, apply the value of $\Delta\phi_{max}$ thus determined to the appropriate relationship given in Section III, paragraph 3-18 (according to whether high-torque or low-torque mode is to be used).

35. To determine the value of the proper phasing parameter, Λ, proceed as follows:

a. From the origin draw a line, NP, which is perpendicular to the line AB connecting the attitude coordinates.

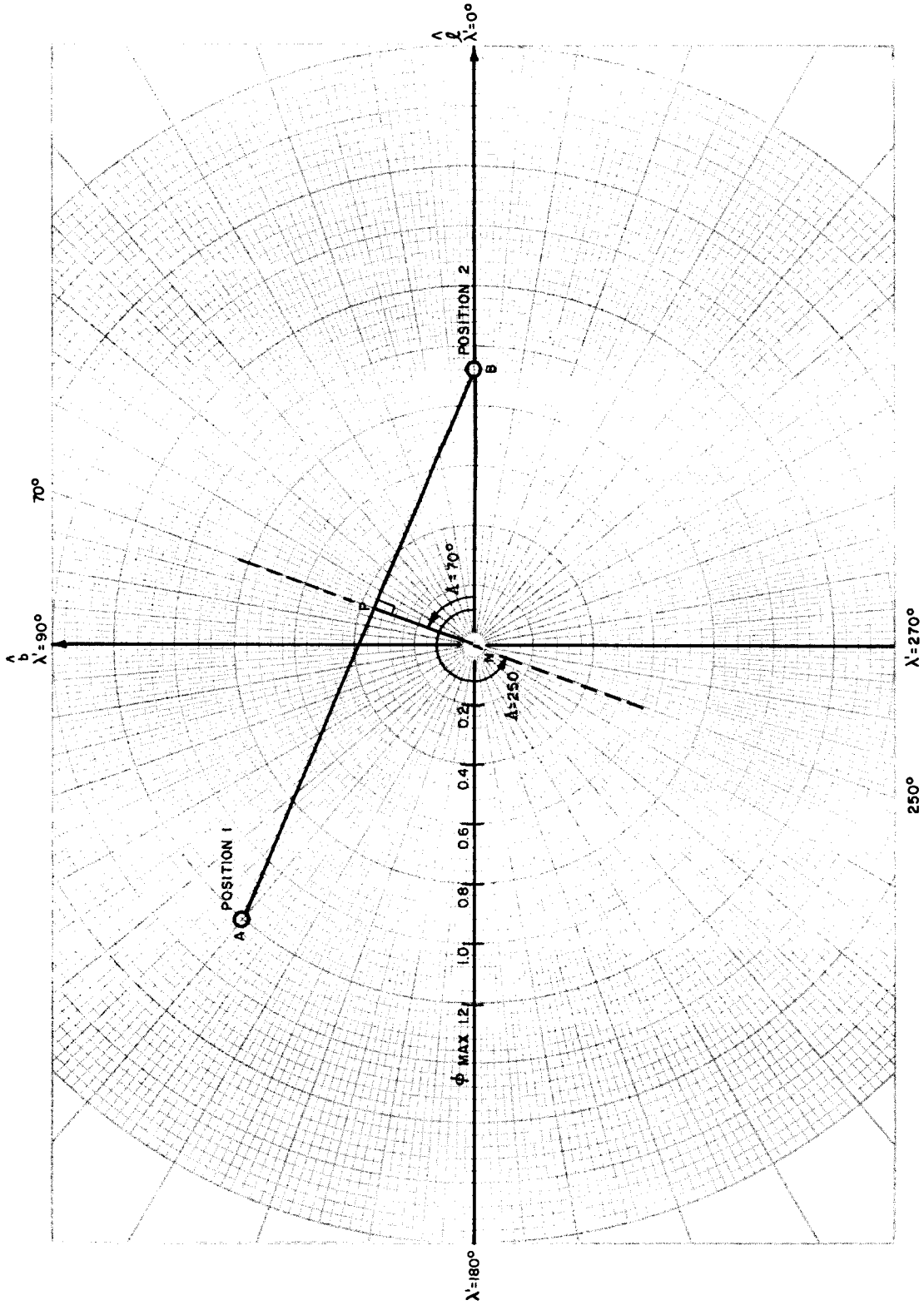

Figure X. Arbitrary Attitude Maneuver Near the Orbit Normal

b. The argument (angle) of the line NP measured from the zero axis of the λ' parameter, is the desired value of Λ.*

36. In the example depicted in Figure 2-3-4, $\Delta\phi_{max}$ has a value of 2 degrees and Λ a value of 70^{o}. The time in minutes after the ascending node, T_{AAN}, for the start of the QUOMAC sequence by using a relationship similar to that given in Section III, paragraph 3-21, or

$$T_{AAN} = \frac{\tau}{720}(\Lambda - K) - (100 - \tau)\frac{N_Q}{4}.$$

37. ATTITUDE HISTORY GRAPHS

38. Two types of graphs of attitude history, which will become part of the official record of the spacecraft, are to be maintained by the analyst at TTCC. The first of these graphs shall be referred to as preliminary and the second as definitive.

39. The preliminary graphs shall consist of the following plots:

(a) Spin Rate in RPM versus Orbit Number

(b) Roll Angle, ϕ_{max}, in degrees versus Orbit Number

(c) Orbital Phasing Parameter, λ, versus Orbit Number

Monitored attitude data shall be plotted on these graphs as soon as the data has been reduced. Faired curves shall be drawn through the points plotted at the completion of the posting of data associated with the decade numbered orbits: that is, orbits numbered 10, 20, 30, etc.

40. The definitive graph will be one showing the attitude history and shall consist of a polar graph of ϕ_{max} versus λ'. This graph shall be compiled by cross plotting the best value of the attitude coordinates of the decade numbered orbits obtained from preliminary graphs. Entries should be identified by orbit number, and a faired curve should be drawn through the points plotted. This final curve shall constitute the official attitude record of the spacecraft.

---

*Note that the argument of the line NP is double valued when extended. (See the dashed extension shown in Figure X.) The appropriate value is determined by the argument of that section of the line that is 90 degrees clockwise from AB measured from position 1.

APPENDIX A

OTHER ASPECTS OF DETERMINING Φ_{max} AND λ FROM HORIZON SENSORS

APPENDIX A

OTHER ASPECTS OF DETERMINING ϕ_{max} AND λ FROM HORIZON SENSORS

A-1. USE OF SINGLE CHANNEL OF ATTITUDE SENSOR OR ORTHOGONAL (TRIGGER) SENSOR

A-2. When both channels of the V-head attitude sensor are functioning correctly, the value for instantaneous roll angle for each set of data is determined using the nomograms contained in the main body of this report. In the event of interference* or failure of one or both channels of the V-head sensor, additional procedures exist for determining the instantaneous roll angle, and therefore, ϕ_{max} and λ.

A-3. If the attitude sensor is not operating properly, the appropriate one of the following two procedures may be followed.

(1) When one channel of the attitude sensor is inoperative, mark the data from the useful channel and determine the T_E/T_{SPIN} ratios as outlined in the main body of the report. Then, using these values along with the spacecraft altitude listed in the WMSAD for the corresponding measurement times, determine the corresponding values of instantaneous roll angle from the nomogram of Figure A-1. Finally, plot these values of roll angle according to the procedures outlined in the main body of the report and determine ϕ_{max} and λ.

(2) When both channels of the attitude sensor are inoperative use the orthogonal (trigger) sensor data recorded on the telemetry recorder for determining spacecraft attitude. Mark and measure the T_E/T_{SPIN} ratios of the orthogonal sensor data according to the procedures outlined in the main body of the report for V-head sensor data. Then, using these ratios and the spacecraft altitude listed in the WMSAD for the corresponding measurement times, determine the corresponding values of instantaneous roll angles using the nomogram shown in Figure A-2.** Finally plot these values of roll angle and determine ϕ_{max} and λ using the procedures in the main body of this report.

---

*It is likely that, during the lifetime of TIROS IX, the sun angle, γ, will be such that while the spacecraft is in sunlight, sun interference on channel No. 1 of the V-head attitude sensor will obliterate the useful data on that channel. However, during those passes over ground stations that occur when the spacecraft is in the earth's shadow, this sensor should return to normal operation.

**Notice, in Figure A-2, that when the instantaneous roll angle, ϕ, is close to zero degrees, the value of ϕ can be determined only to a very poor accuracy. It is for this reason that the V-head attitude sensor is required for wheel-mode operation.

A-4. ATTITUDE DETERMINATION IN THE PRESENCE OF NUTATION

A-5. A nutation, or wobbling motion, of the spin axis will introduce a modulation into successive readings of instantaneous roll angle. If this effect is permitted to remain uncompensated, it may lead to errors in attitude determination. Should the plot of instantaneous roll angle versus normalized time exhibit a scatter in roll angle greater than ±0.75 degree, indicating the possible presence of nutation, the following procedure may be used to compensate for the nutation scattering effect.

A-6. Whenever roll angle scatter is ±0.75 degrees or greater, the procedure for determining instantaneous roll angle from the T_E/T_{SPIN} ratio described in the main body of the report (i.e., using every fifth satellite rotation, or Nos. 0, 5, 10. . . .) should be augmented by the marking and measurement of two additional ratios for each original reading. These ratios should be measured from the rotation that is numbered two less than the originally selected rotation, and from the rotation numbered two greater than the originally selected rotation. For example, if the T_E/T_{SPIN} ratio from rotation No. 15 had originally been selected for use in attitude reduction, then the ratios from rotations 13 and 17 will also be included in the reduction treatment.

A-7. For each such group of three rotations (13, 15 and 17 shown in the example) the arithmetical average of the three T_E/T_{SPIN} ratios should be calculated. The resulting average is to be reported as the T_E/T_{SPIN} ratio associated with the original datum point (rotation 15 in the example given). The balance of the attitude-determination process is performed as described in the main body of this report.

TIROS WHEEL

ROLL ANGLE NOMOGRAM FOR USE WHEN
ONLY ONE HORIZON SENSOR INTERCEPTS EARTH

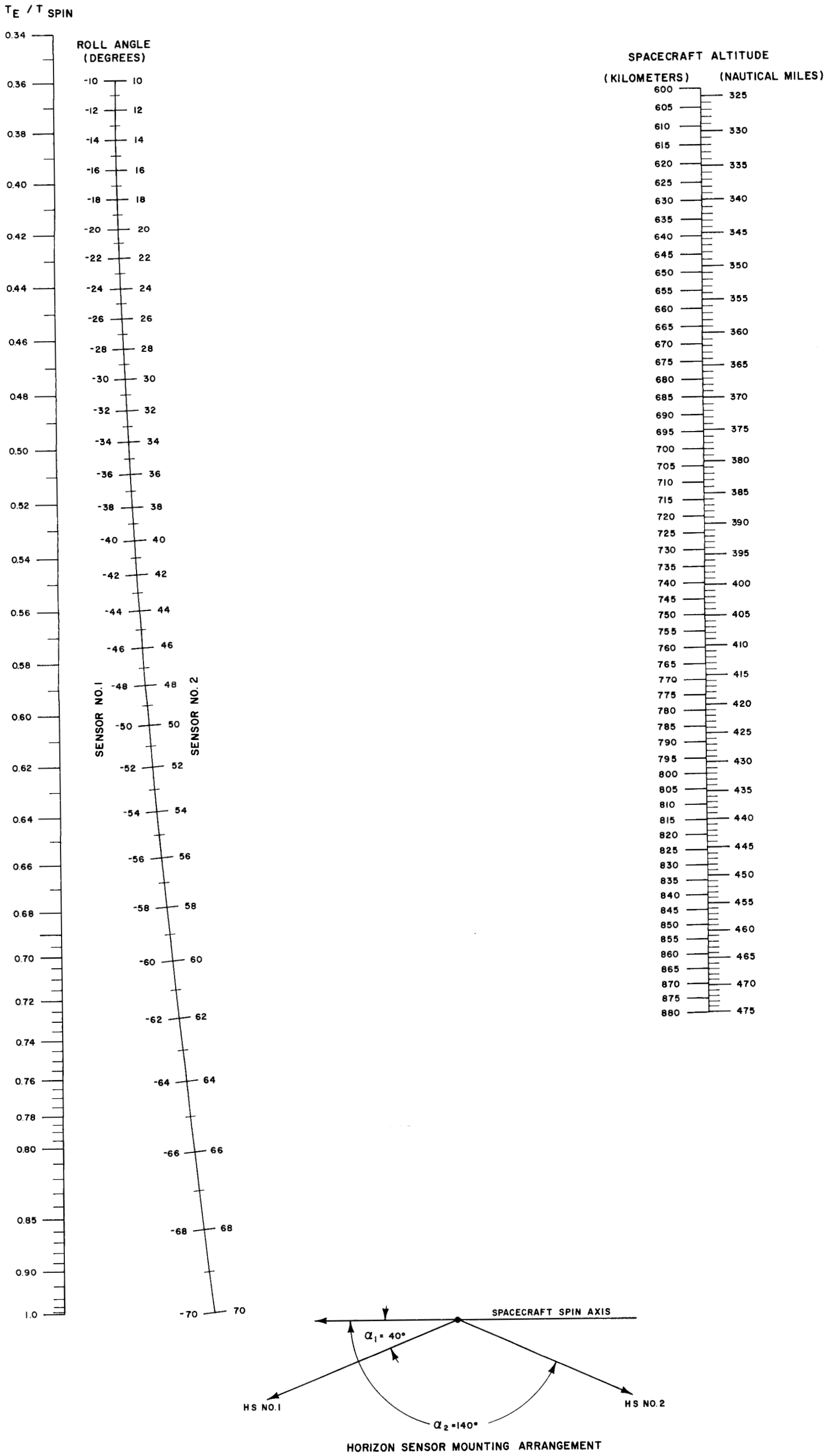

HORIZON SENSOR MOUNTING ARRANGEMENT

NOTES:
1. T_E / T_{SPIN} IS THE RATIO OF EARTH TIME TO SPIN TIME
2. SENSOR MOUNTING ANGLES ARE 40 AND 140 DEGREES WITH RESPECT TO SPIN AXIS

Figure A-1. Roll-Angle Nomogram for Use With One Channel of V-Head Attitude-Sensor Data

TIROS WHEEL

ROLL ANGLE NOMONOGRAM FOR ORTHOGONAL HORIZON SENSOR

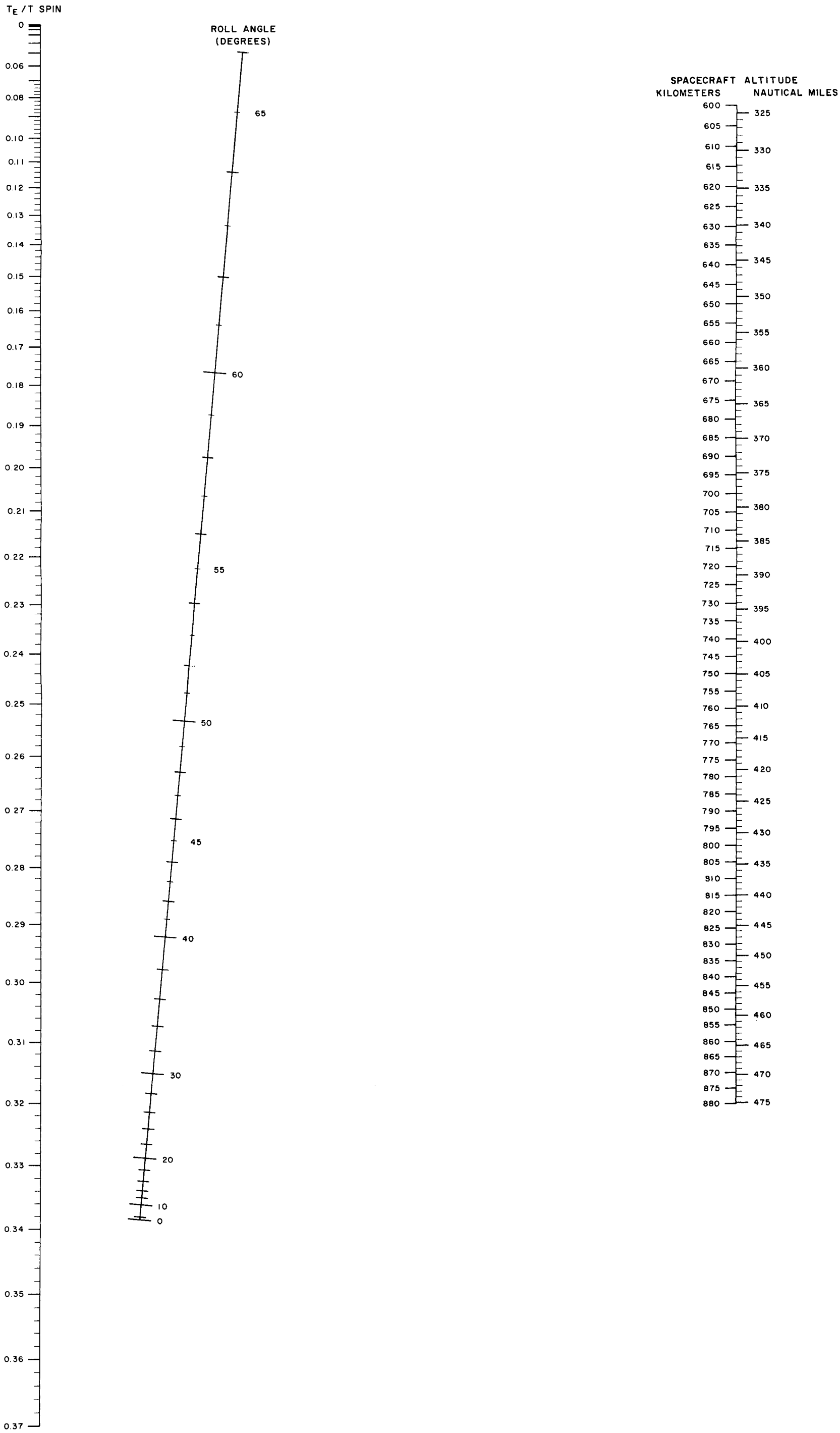

Figure A-2. Roll-Angle Nomogram for Use With Orthogonal (Trigger) Sensor Data

APPENDIX B

TIME-MARKING SYSTEM ON SANBORN CHART RECORDING

APPENDIX B. TIME-MARKING SYSTEM ON SANBORN CHART RECORDING

B-1. At the discretion of the operator at the CDA station, a time code can be recorded on the Sanborn charts concurrent with the recording of horizon-sensor data. The time code consists of width-modulated pulses which indicate the Greenwich Mean Time (GMT) of a reference pulse in hours, minutes, and seconds. The reference pulse is triggered by the station clock to occur at the beginnng of a second of real time. The time-marker pen records the time code in the lower margin of the chart on the telemetry recorder and in the center channel on the attitude recorder.

B-2. This pulse train, which has a repetition rate of 30 seconds, consists of 60 pulses that are spaced at half-second intervals. The pulses are of three different widths. The reference pulse has a duration of 400 milliseconds; the binary "zero" pulse a duration of 100 milliseconds; and the binary "one" pulse a duration of 200 milliseconds. The information carried by a pulse is a function of its position number in the frame, counting consecutively from the reference mark as listed in Table B-1.

B-3. To read out the GMT indicated by a particular frame, sum the equivalent time values of the binary "one" pulses only. For the illustrative example shown in Figure B-1, the GMT indicated is 36 seconds. $[2(1) + 4(1) + 1(10) + 2(10)]$, 59 minutes $[1(1) + 8(1) + 1(10) + 4(10)]$ and 14 hours $[4(1) + 1(10)]$, which is written 14:59:36 GMT.

B-4. The GMT of a particular event, such as an earth-sky-crossing pulse, is found by increasing the time associated with the proper reference pulse by the time increment to the event. To evaluate this time, measure the distance (in millimeters and tenths of millimeters) from the leading edge of the reference pulse at the beginning of the frame in which the event occurred to the datum point of interest. Divide this distance by the chart speed in millimeters per second, and add the result to the time associated with the reference pulse. For the event shown in Figure B-1, the time increment is 6.906 or 6.91 seconds (140.2 millimeters per second divided by 20.3 millimeters per second*). Hence the time of the event is 14:59:42.91 GMT (14:59:36 + 6.91).

TABLE B-1. ASSIGNMENTS OF TIME-CODE BITS

Pulse Position No.	Time Unit	Time Value
1,2,3, and 4	Unit Seconds	1,2,4 and 8, respectively
5,6, and 7	Tens of Seconds	1,2, and 4, respectively
8,9,10, and 11	Unit Minutes	1,2,4 and 8, respectively
12,13, and 14	Tens of Minutes	1,2 and 4, respectively
15,16,17, and 18	Unit Hours	1,2,4 and 8, respectively
19 and 20	Tens of Hours	1 and 2, respectively
21 through 59	None	Zero

*The value selected for this example is not necessarily typical for these recorders.

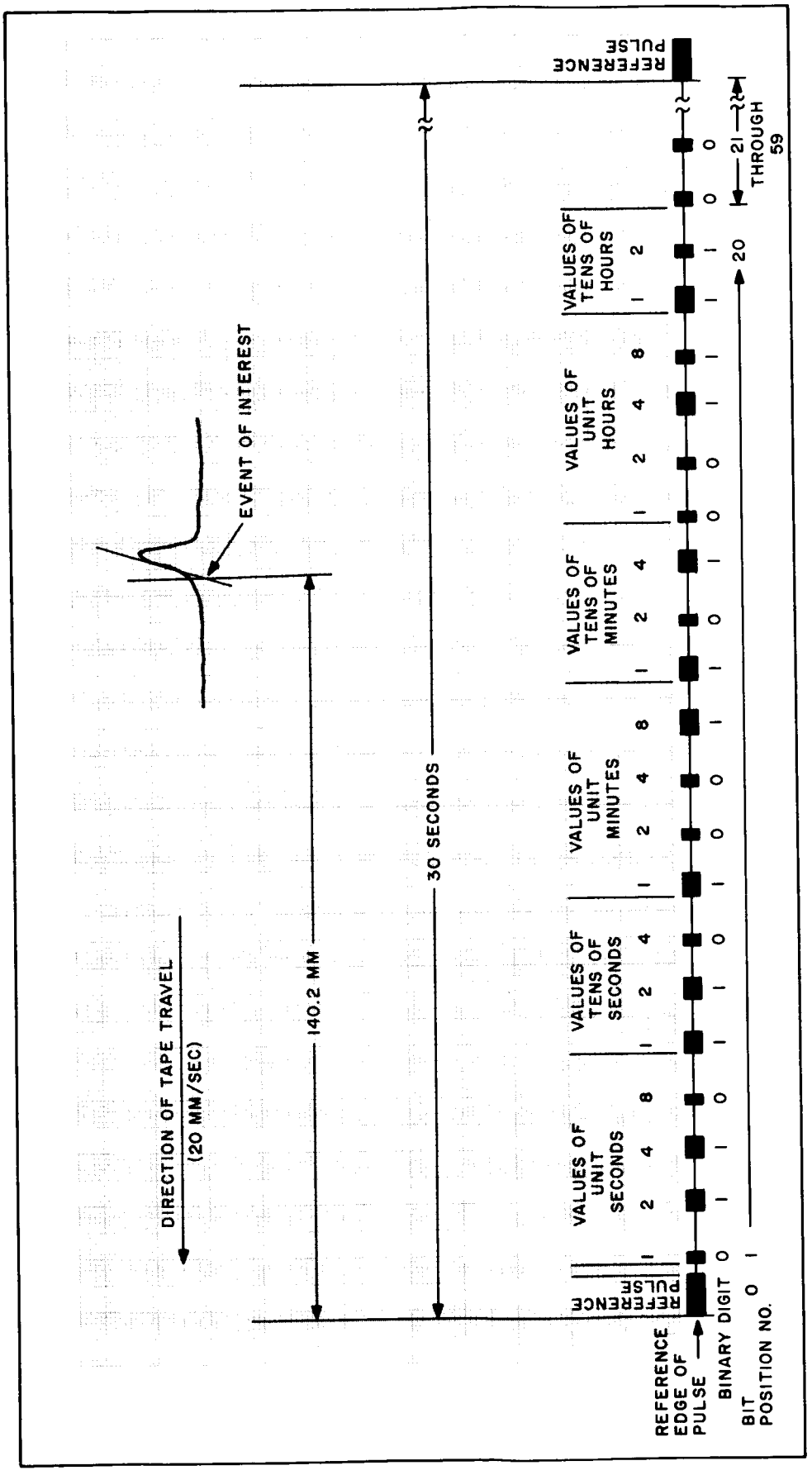

Figure B-1. Example of Time-Mark Codings

APPENDIX C

MAGNETIC ATTITUDE CONTROL ANALYSIS

APPENDIX C. MAGNETIC ATTITUDE CONTROL ANALYSIS

C-1. GENERAL

C-2. Both the QOMAC and MBC techniques for magnetic attitude control are based on the response of an axially-symmetrical spinning body to torques generated by the interaction of a satellite-borne current loop with the earth's magnetic field. The current loop which is rigidly mounted in the satellite structure has its coil axis aligned with the spin axis of the satellite. As a result, the electromagnetic torque developed will cause the spin axis to precess about the direction of the magnetic field as shown in Figure C-1.

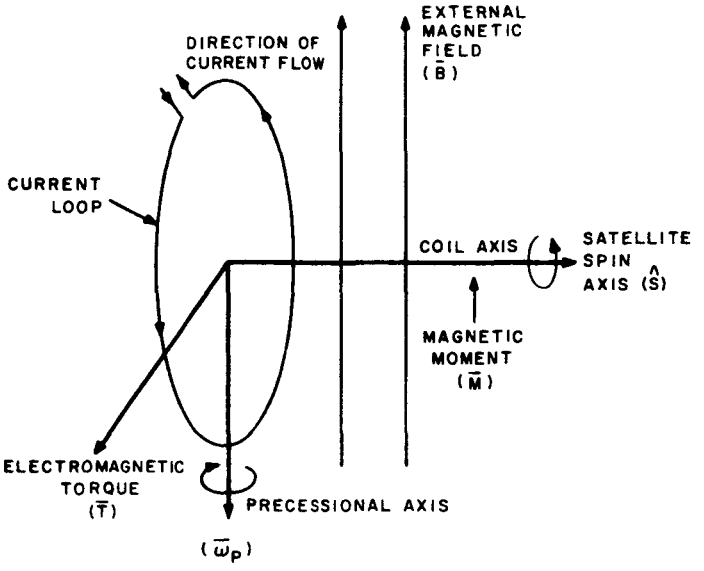

Figure C-1. Precession of a Spinning Satellite Produced by Electromagnetic Torquing

C-3. A mathematical description of the application of this technique to an orbiting satellite must include the effects of the magnetic-field variations throughout the orbital path and the variations of the satellite spin vector with respect to the orbit. Such a model has been derived, and the equations have been programmed for the IBM 7090 digital computer. The analysis presented here emphasizes the QOMAC approach since the conventional TIROS-type torquing has been widely documented.

C-4. ANALYSIS

C-5. SATELLITE DYNAMICS

C-6. The control torque developed by the magnetic interaction between the satellite coil and the earth's magnetic field is given by the vector equation:

$$\overline{T} = \overline{M} \times \overline{B} \ , \tag{C-1}$$

where:

$\overline{T}$ is the torque in newton-meters,

$\overline{B}$ is the earth's magnetic field in webers/meter^2, and

$\overline{M}$ is the torque-coil magnetic moment in ampere-turns-meter^2.

The equation of motion is then:

$$\dot{\overline{H}} = \overline{T} = \overline{M} \times \overline{B}, \tag{C-2}$$

and

$$\dot{\overline{H}} = I_s \frac{d\,(\omega_s \hat{s})}{dt} \ , \tag{C-3}$$

where:

H is the angular-momentum vector in newton-meter*-second,

I_s is the spin-axis moment of inertia in newton-meter-second^2,

ω_s is the spin rate in radians per second,

$\hat{s}$ is a unit vector along spin axis.

C-7. Terms involving transverse angular momentum have been neglected due to the low rates and forcing torques being considered. Also, the spin rate is essentially constant over long periods of time. As a result, the simplified gyroscopic equation of motion for the satellite reduces to

$$\overline{\omega}_p \times I_s \omega_s \hat{s} = \overline{M} \times \overline{B}, \tag{C-4}$$

*One newton-meter is equal to 8.851 inch-pounds.

where:

$\overline{\omega}_p$ is the precession vector.

Since the coil axis is coincident with the spin axis, the positive magnetic-moment vector is taken to be in the direction of the spin vector and is defined by

$$\overline{M} = M\hat{s}; \tag{C-5}$$

C-8. Assuming a dipole representation of the earth's magnetic field, the magnetic field vector may be written as

$$\overline{B} = \frac{V_o \overline{b}}{R^3}, \tag{C-6}$$

where:

$\frac{V_o}{R^3}$ is the strength of earth's magnetic field in the geographic equatorial plane at distance R and is equal to $0.31 \times 10^{-4} \left(\frac{R_o}{R}\right)^3$ weber/meters^2 (where R_o is the earth's radius), and

$\overline{b}$ is a normalized vector parallel to the instantaneous direction of the field.

Using this equation for $\overline{B}$, equation (C-4) becomes

$$\overline{\omega}_p \times \hat{s} = -\mu (\overline{b} \times \hat{s}), \tag{C-7}$$

where:

$$\mu = \frac{V_o M}{R^3 I_s \omega_s}.$$

C-9. From the detailed analysis of a "fast" gyroscope which is acted upon by this type of light-torque loading, it can be shown that the precession motion which satisfies equation (C-5) is

$$\overline{\omega}_p = -\mu (\overline{b}). \tag{C-8}$$

Therefore, for a positive torque-coil magnetic moment, the satellite precession motion will take place in a negative sense about the instantaneous direction of the earth's magnetic field. It will subsequently be shown that it is possible to produce an effective average direction of the earth's magnetic field that is simply related to the desired attitude correction by producing one-quarter orbit reversals of the current in the satellite coil.

C-10. SATELLITE COORDINATE SYSTEM OF REFERENCE

C-11. The satellite coordinate system used in this analysis is shown in Figure C-2, and is referred to as the ℓ-b-n system.

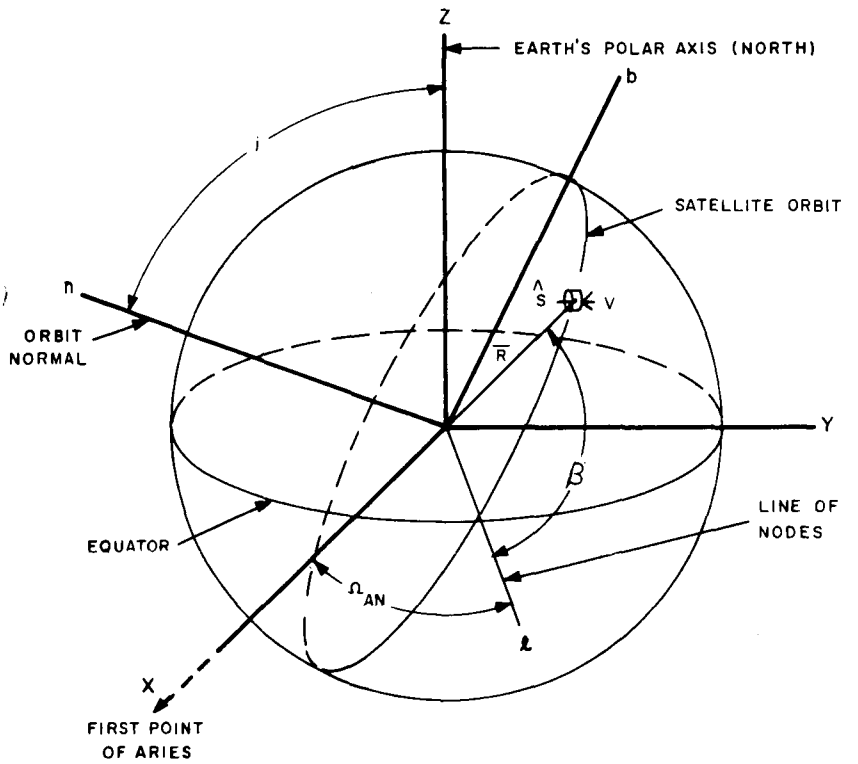

Figure C-2. Coordinate System of Reference for Magnetic Attitude Control Analysis

As shown in the figure, the $\hat{\ell}$, $\hat{b}$, and $\hat{n}$ axes are oriented such that the $\hat{\ell}$ axis is along the orbit line of nodes (toward the ascending node), the $\hat{n}$ axis is along the orbit normal, and the $\hat{b}$ axis is defined by the equation $\hat{b} = \hat{n} \times \hat{\ell}$.

Other quantities shown in Figure C-2 are defined as follows:

β is the satellite orbit angle measured counterclockwise around $\hat{n}$ from the line of nodes to the orbit radius defining the satellite's position in the orbit plane,

i is the orbit inclination angle measured counterclockwise around $\hat{\ell}$, from the earth's polar axis (Z) to $\hat{n}$,

Ω_{AN} is the right ascension of the line of nodes, and

$\overline{R}$ is the radius vector from the center of the earth to the satellite.

The ℓ-b-n coordinate system is known as an orbit-axes system, in which $\hat{\ell}$ and $\hat{b}$ always remain in the orbital plane as the orbit regresses. The X-Y-Z coordinates, are in the inertial celestial coordinate system.

C-12. DESCRIPTION OF THE EARTH'S MAGNETIC FIELD.

C-13. Prior experience in TIROS magnetic-attitude control indicates that an excellant approximation of the earth's magnetic field at satellite altitude may be generated by a simple dipole source. In this approximation, shown in Figure C-3, the magnetic dipole is inclined from the earth's polar axis by 11.4 degrees, with the dipole axis intersecting the earth at Latitude 78.6°N, Longitude 70.1°W, and at Latitude 78.6°S, Longitude 250.1°W.

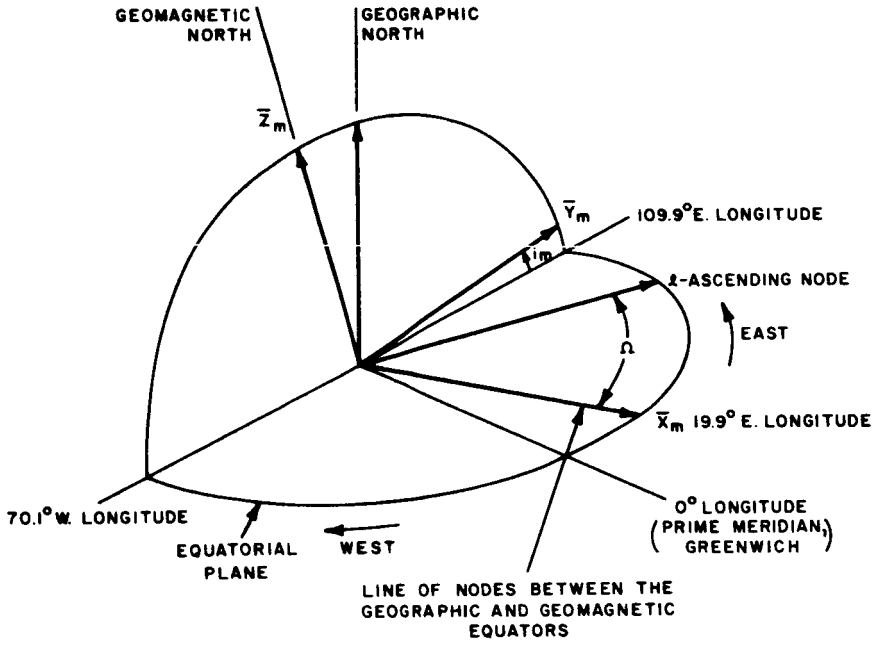

Figure C-3. Magnetic-Dipole Representation of the Earth's Magnetic Field

C-14. Based on this dipole approximation, the earth's magnetic field at an instantaneous satellite position, defined by R and β in the orbit-axes coordinate system of reference, is

$$\overline{B} = B_{\ell}\,\hat{\ell} + B_b\,\hat{b} + B_n\,\hat{n}, \tag{C-9}$$

where:

$$B_{\ell} = \frac{V_o}{R^3}\left[A_1 \sin 2\beta + \frac{1}{2}(B_1 + C_1)\sin(2\beta + \Omega) + \frac{1}{2}(B_1 - C_1)\sin(2\beta - \Omega) + \frac{C_1}{3}\sin\Omega\right],$$

$$B_b = \frac{V_o}{R^3}\left[-A_1 \cos 2\beta - \frac{1}{2}(B_1 - C_1)\cos(2\beta - \Omega) - \frac{1}{2}(B_1 + C_1)\cos(2\beta + \Omega) + \frac{B_i}{3}\cos\Omega + \frac{A_i}{3}\right],$$

$$B_n = \frac{V_o}{R^3}\left[A_3 + B_3 \cos\Omega\right],$$

$A_1 = -3/2 \sin i \cos i_m$,

$A_3 = \cos i \cos i_m$,

$B_1 = 3/2 \cos i \sin i_m$,

$B_3 = \sin i \sin i_m$,

$C_1 = 3/2 \sin i_m$,

i_m is the angle between dipole axis and earth's polar axis, and

Ω is the longitude of the ascending node minus (longitude of North Magnetic Pole + $\pi/2$).

C-15. The significant QOMAC dynamic characteristics may be derived by further simplification of the analysis using certain approximations. The resulting simple control philosophy was proved applicable to actual orbit operations by demonstrating

the predictability of spin axis motion using a computer simulation program which did not incorporate any of these approximations. These approximations are:

- The axis of the dipole approximation to the source of the earth's magnetic field is collinear with the polar axis of the earth (i.e., $i_m = 0°$, $\Omega = 0°$).

- Since orbital precession over the interval of a half-orbit, during full torque averaging for a single QOMAC cycle occurs, as calculated by the equation

$$\text{Orbit regression per half-orbit} = \frac{1.0 \text{ degree/day}}{28.8 \text{ half-orbits/day}} = 0.034 \text{ degree}$$

is quite small, the motion of the orbit can be regarded as negligible; i.e., the ℓ-b-n system may be regarded as essentially inertially fixed over a half-orbit time interval.

c. The satellite orbit is circular, having negligible ellipticity.

C-16. Using the above approximations, the components* of the earth's magnetic field as seen by the satellite simplify to:

$$B_\ell = \frac{V_o}{R^3}\left(\frac{3}{2} \sin 2\beta \sin i\right),$$

$$B_b = +\frac{V_o}{R^3}\left(\frac{3}{2} \cos 2\beta \sin i - \frac{1}{2} \sin i\right), \text{ and} \qquad \text{(C-10)}$$

$$B_n = +\frac{V_o}{R^3} \cos i,$$

C-17. PRINCIPLES OF QOMAC AND MBC SYSTEM PERFORMANCE

C-18. Applying orbit-averaging techniques to equation (A-8), using the results from equations (C-10 through C-12) and assuming conventional TIROS MBC torquing, it follows that:

*These equations for the components of the earth's magnetic-field have been used quite successfully in the digital simulation for the earlier TIROS satellite.

$$\tilde{\omega}_{p_\ell} = 0$$

$$\tilde{\omega}_{p_b} = +\frac{\mu}{2} \sin i, \text{ and}$$

$$\omega_{p_n} = -\mu \cos i.$$

where $\tilde{\omega}_p$ is the orbit-average value of $\bar{\omega}_p$.

C-19. Clearly then, given a fixed dipole in the satellite and a particular orbit, the precession axis is uniquely determined by the inclination angle. Futhermore, for the near-polar, synchronous orbit planned for the TIROS Wheel satellite, the net average precession vector is very nearly in the orbit plane, along the positive b axis. Since the injection conditions are such that the spin vector is initially approximately parallel to the b axis, out-of-plane motion by standard TIROS torquing would be almost non-existent. However, the QOMAC system provides for reversing the coil current every time the satellite traverses 90 degrees of orbit angle, and, as will be shown, a precession vector can, therefore, be generated to lie anywhere in the orbit plane. By virtue of this selectivity, the average precession vector can always be made normal to the position of the spin vector so that the net motion of this spin vector is in a plane perpendicular to the orbit plane. For the mission orientation of the TIROS-Wheel satellite, this is the shortest path for station acquisition.

C-20. Quarter-orbit reversals of current and a time delay from the ascending node are the fundamental elements of the QOMAC technique. A typical dipole-moment program for one cycle of QOMAC operation is shown in Figure C-4. Continuous repetitive cycles may be programmed to achieve greater spin axis motion.

C-21. Expressions for the average precession components as a function of an arbitrary starting phase for the quarter-orbit torque program are developed in the following paragraphs. The program will be developed for the cycle to start at delay angle β_s with respect to the ascending node. The convention is established that the torque-coil magnetic moment is always positive (in the direction of the satellite spin axis) during the first quarter-orbit of a torque cycle. Then, again using orbit-average techniques and equation (C-10), equation (C-8) becomes

$$\tilde{\omega}_{p_\ell} = -\frac{\mu}{\pi} \left\{ -\frac{3}{2} \sin i \left[\int_{\beta_s}^{\beta_s + \frac{\pi}{2}} \sin 2\beta \, d\beta - \int_{\beta_s + \frac{\pi}{2}}^{\beta_s + \pi} \sin 2\beta \, d\beta \right] \right\},$$

$$= \frac{3}{\pi} \mu \sin i \cos 2\beta_s,$$

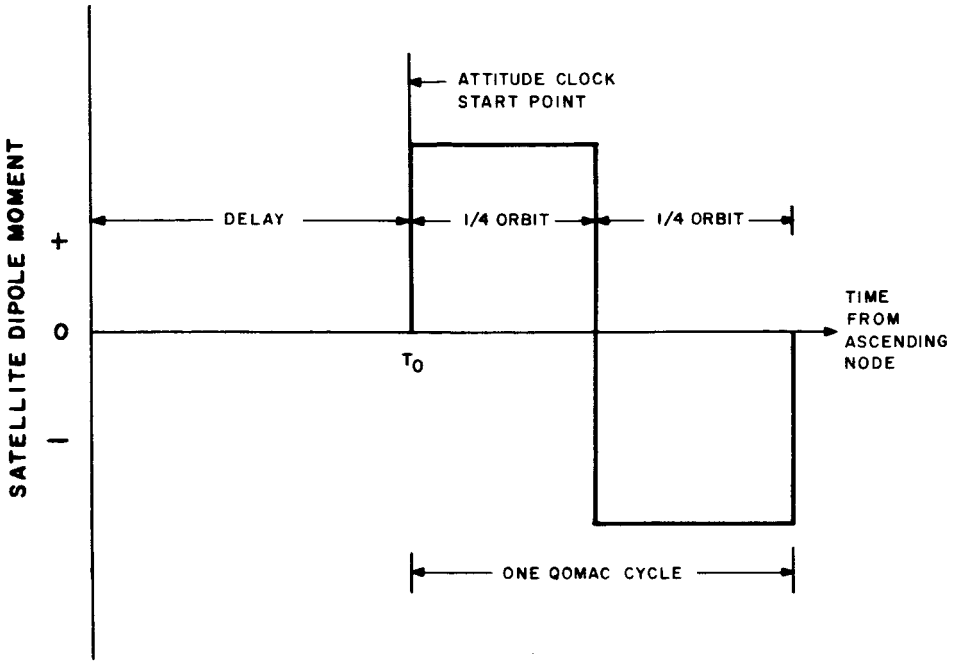

Figure C-4. QOMAC Dipole-Moment Program

$$\tilde{\omega}_{p_b} = -\frac{\mu}{\pi}\left\{\frac{3}{2}\sin i\left[\int_{\beta_s}^{\beta_s+\frac{\pi}{2}}\cos 2\beta\, d\beta - \int_{\beta_s+\frac{\pi}{2}}^{\beta_s+\pi}\cos 2\beta\, d\beta\right]\right.$$

$$\left. - \frac{1}{2}\sin i\left[\int_{\beta_s}^{\beta_s+\frac{\pi}{2}} d\beta - \int_{\beta_s+\frac{\pi}{2}}^{\beta_s+\pi} d\beta\right]\right\}, \qquad \text{(C-12)}$$

$$= \frac{3}{\pi}\mu \sin i \sin 2\beta_s, \text{ and}$$

$$\tilde{\omega}_{p_n} = 0.$$

C-22. It is interesting to note that, in the magnetic attitude-control system for the conventional TIROS, the steady-state field terms provide for torquing, while the sinusoidal field terms average to zero. The contrary is true for QOMAC. Also notice in equation (C-12) that the $\hat{n}$ component of $\tilde{\omega}_p$ is zero. Hence the precession axis is limited to remaining in the orbit plane, but by suitable choice of β_s, can be positioned anywhere in this plane. The confinement of the precession axis to the orbit plane is, for the TIROS-Wheel application, of no consequence since the mission attitude is normal to the orbit plane and this control dimension ($\tilde{\omega}_{p_n}$) is not required.

The axis about which the average precession motion occurs is then at an angle Λ measured counterclockwise around n from the ascending node to the precession axis. The angle Λ is defined by

$$\text{Tan}\,\Lambda = \frac{\tilde{\omega}_{P_b}}{\tilde{\omega}_{P_\ell}}$$

$$= \text{Tan}\; 2\beta_s ,$$

or

$$\beta_s = \frac{\Lambda}{2} , \tag{C-13}$$

or, in more general terms,

$$\beta_s = \frac{\Lambda}{2} + M\pi , \tag{C-14}$$

where

$$m = 0, 1, 2, \ldots\ldots$$

This implies that a precession axis can be selected to lie anywhere in the orbit plane, at an angle Λ with respect to the ascending node, by using equation (C-14) to select the start angle for a QOMAC cycle. Then the half-orbit average precession rate about this axis is

$$\left|\tilde{\omega}_P\right| = \frac{3}{\pi}\mu \sin i. \tag{C-15}$$

C-23. Then, by selecting Λ such that it defines the point in orbit at which the satellite attitude error is totally in yaw (spin-vector rotation about a local earth radius) and computing the appropriate initial phase angle (β_s), the spin axis will move in a plane normal to the radius vector at Λ. This will result in a nulling of the attitude error. The actual phase angle prior to starting the attitude clock will be either

$$\frac{\Lambda}{2} + m\pi ,$$

or

$$\frac{\Lambda + \pi}{2} + m\pi, \; (m = 0, 1),$$

depending on the desired direction of precession. Note that the expression for the attitude coordinates (ϕ_{max}, λ) given in Section II are such that $\lambda = \Lambda$ requires a start angle of $\frac{\Lambda}{2} + m\pi$ to acquire the orbit normal.

C-24. As shown in paragraph C-23, the derivation of the start angle as a function of Λ depending on the assumptions of an uncanted earth dipole and perfect quarter-orbit reversals of current. If the assumption of an uncanted dipole is relaxed and equation (C-9) used to represent the earth's field (i.e., canted dipole representation), orbit averaging techniques may again be applied to yield the results

$$\tilde{\omega}_{P_1} = \frac{3\mu}{\pi} (a \cos 2\beta_s - b \sin 2\beta_s),$$

$$\tilde{\omega}_{P_b} = \frac{3\mu}{\pi} (a \sin 2\beta_s + b \cos 2\beta_s), \text{ and} \qquad \text{(C-16)}$$

$$\tilde{\omega}_{P_n} = 0.$$

where:

$$a = \cos i_m \sin i_m \cos r - \sin i \cos i_m, \text{ and}$$

$$b = \sin i_m \sin r.$$

Note that when $r = i_m = 0$, these equations reduce to equation (C-12) for the uncanted case, and Λ is defined by:

$$\tan \Lambda = \frac{\tilde{\omega}_{P_b}}{\tilde{\omega}_{P_1}}, \qquad \text{(C-17)}$$

$$= \frac{a \sin 2\beta_s + b \cos 2\beta_s}{a \cos 2\beta_s - b \sin 2\beta_s}.$$

By rearranging this equation and solving for β_s, it can be shown that

$$\text{Tan } 2\beta_s = \text{Tan} \left\{ \Lambda - \text{Tan}^{-1} (b/a) \right\} ,$$

or

$$\beta_s = \frac{1}{2} \left\{ \Lambda - \text{Tan}^{-1} (b/a) \right\}^{*} . \qquad \text{(C-18)}$$

To compensate for errors in the quarter orbit clock (Dycon)**, a correction factor is added to the computation for β_s. The rationale of this correction is based on an attempt to spread the error over the whole cycle or the whole chain of cycles rather than permit the error to accumulate at the end of a cycle. This is shown in Figure C-5.

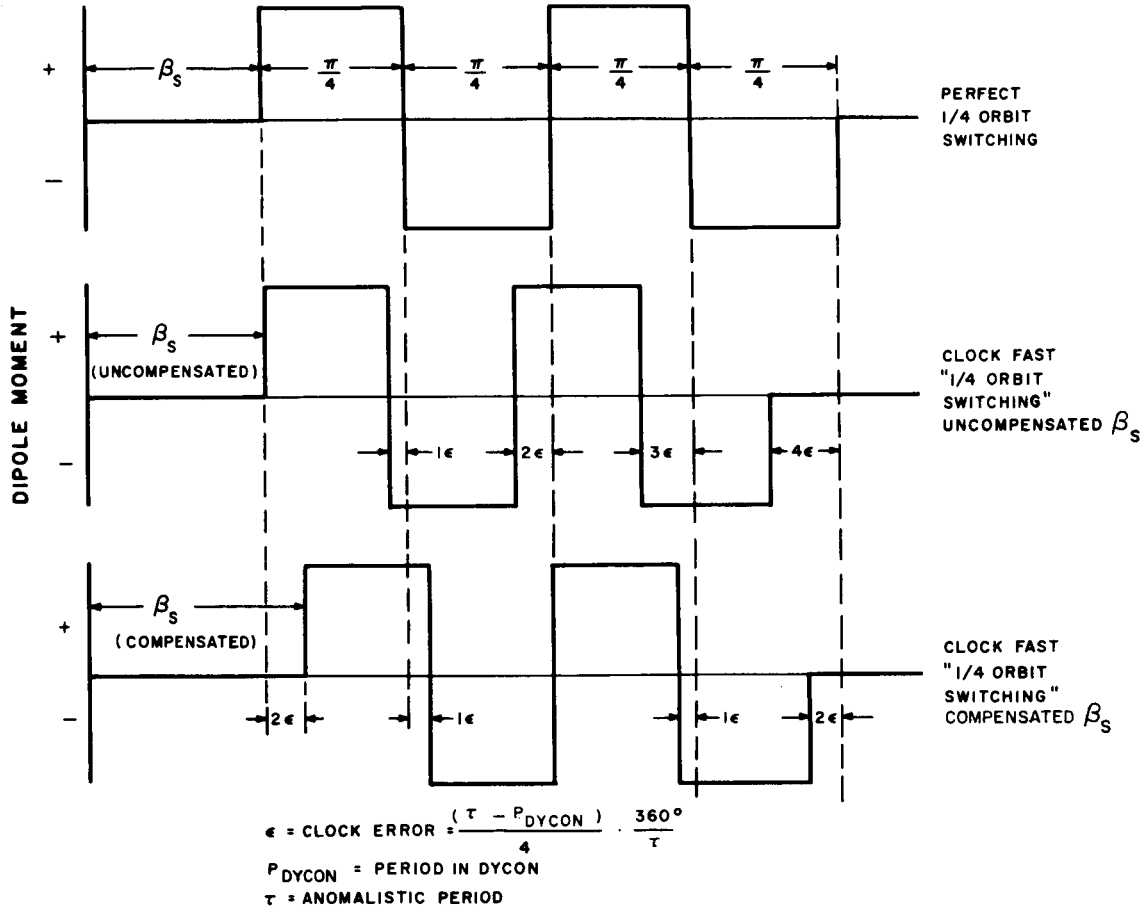

Figure C-5. Compensated and Uncompensated Dipole-Moment Programs Compared with Ideal Quarter-Orbit Switching

---

*Note that $i_m \geq \text{Tan}^{-1} (b/a) \geq -i_m$, thus eliminating quadrant problems.

**The Dycon counts quarter orbit time intervals based on an orbit period which is established before launch and cannot be changed thereafter.

β_s is then expressed by

$$\beta_s = \frac{1}{2}\left\{\Lambda - \text{Tan}^{-1}\, b/a\right\} + \left(1 - \frac{\text{Dycon}}{\tau}\right) 90^\circ\, N_Q, \qquad \text{(C-19)}$$

where N_Q is the number of consecutive QOMAC Cycles.

C-25. The MBC system serves another function in addition to nulling the residual dipole of the satellite. That is, by selecting the appropriate d-c dipole value, the residual plus the MBC value, the off-orbit-normal drift rate of the satellite can be reduced considerably. This is verified as follows:

The time derivative of the spin vector with respect to the rotating coordinate system fixed in the orbit plane is given by

$$\dot{\hat{s}} = \hat{s} \times \bar{a}, \qquad \text{(C-20)}$$

where:

$\bar{a} = \mu b + \bar{\omega}$, and

$\bar{\omega}$ = orbital precession vector.

Assuming that the orbit-normal orientation is acquired, the spin vector can be made to track the orbit normal by selecting the appropriate magnetic bias for the satellite. That is, the value of μ, which is directly proportional to the magnetic moment, must be such that $\bar{a}$ is parallel to $\hat{s}$, hence $\dot{\hat{s}}$ is equal to zero (with respect to $\hat{\ell}, \hat{b}, \hat{n}$ coordinates). Assuming that the spin vector is initially aligned with the orbit normal, i.e.,

$$\hat{s} = \hat{n};$$

noting that

$$\bar{\omega} = \omega \sin i\, \hat{b} + \omega \cos i\, \hat{n}; \text{ and using}$$

equation (C-10) and orbit averaging, it can be shown that

$$\bar{b}_{avg.} = -\frac{\sin i}{2}\hat{b} + \cos i\, \hat{n}, \text{ and}$$

$$\bar{a}_{avg.} = \left(\omega - \frac{\mu}{2}\right) \sin i\, \hat{b} + (\mu + \omega) \cos i\, \hat{n}.$$

Therefore, if the magnetic moment is selected so that

$$\omega - \frac{\mu}{2} = 0, \text{ then} \qquad \text{(C-17)}$$

$\overline{a}_{avg.}$ is parallel to $\hat{n}$, and $\hat{n}$ is equal to $\hat{s}$.

Therefore, $\hat{s}$ is parallel to $\overline{a}$, and $\dot{\hat{s}}$ is zero.

C-26. Thus, if all the assumptions leading to the relationship in equation (C-17) were valid, theoretically the drift rate could be nulled. However, due to the fact that the earth dipole is canted, that there exists a finite (not infinitesimal) granularity in the MBC values, and that the exact orbit-normal attitude acquisition is difficult to accomplish and practically impossible to verify, it is unrealistic to expect the drift rate to be zero. However, it is possible to reduce the drift rate considerably by selecting the appropriate dipole value. This was also verified using computer simulation.

APPENDIX D

MATHEMATICAL ANALYSIS OF THE BASIC SPIN-CONTROL CONCEPT

APPENDIX D

MATHEMATICAL ANALYSIS OF THE BASIC SPIN-CONTROL CONCEPT

D-1. GENERAL

D-2. The torque $\bar{T}$ generated by the interaction of the magnetic dipole moment ($\bar{M}$) of the spin-control coil and the earth's magnetic field vector ($\bar{B}$) is expressed by

$$\bar{T} = \bar{M} \times \bar{B}. \tag{D-1}$$

Previous experience with satellite magnetic-attitude control indicates that the earth's magnetic field may be approximated by a simple magnetic dipole source. The representation used in this analysis is the same as that shown in Figure C-3 and equations (C-9) of Appendix C.

D-3. ANALYSIS

D-4. Since the orthogonal horizon sensor (also required for camera triggering) is used for the commutation function and since the spin axis is normal to the orbit plane, the magnetic dipole moment $\bar{M}$ of the coil can be represented by

$$\bar{M} = M\left[\cos(\omega_s t + \nu + \beta)\,\hat{\ell} + \sin(\omega_s, t + \nu + \beta)\,b\right], \tag{D-2}$$

where ν is the angle between N_c and the local vertical when orthogonal sensor No. 1 makes the sky-earth transition, and N_c is the coil normal (dipole-moment axis).

Figure D-1 shows the coil in orbit just as the line of sight of horizon sensor No. 1 crosses from sky to earth, i.e., at a commutation point.

D-5. Substituting equations (C-9) and (D-2) into equation (D-1) and allowing for commutation every 180 degrees per spin cycle results in an average torque $\bar{T}_s$ about the spin axis as follows:

$$\bar{T}_s = \frac{3V_o\bar{M}}{\pi R^3}\left\{\sin i \cos i_m \sin\beta - \frac{1}{2}\sin i_m (\cos i + 1)\sin\beta\cos\Omega\right.$$

$$\left. + \frac{1}{2}\sin i_m (\cos i - 1)\cos\beta\sin\Omega - \frac{1}{2}\sin i_m (\cos i + 1)\sin\beta\cos\Omega\right.$$

$$-\frac{1}{2}\sin i_m(\cos i + 1)\cos\beta\sin\Omega - \frac{1}{3}\sin\Omega\sin i_m\cos\beta$$

$$-\frac{1}{3}(\cos i\sin i_m\cos\Omega - \sin i\cos i_m)\sin\beta\Big\}. \qquad \text{(D-3)}$$

The spin torque will be a maximum for $\nu = 0$ and $\nu = \pi$. Therefore, ν was chosen equal to zero in the above expression, by letting the angle between N_c and the line of sight of horizon sensor No. 2 be equal to the half-earth angle Θ_ρ, corresponding to the design altitude.

D-6. For the basic magnetic spin-control concept described above, the torque about the spin axis will vary as a function of orbit angle as shown in the non-dimensionalized plot of Figure D-2. Thus, the absolute value of spin-control torque available during every quarter-orbit is approximated by $(3V_0M/(\pi R^3)$. Using this average torque, the relation between spin-rate change and coil-current duration has been plotted and is presented in Figure D-3. A spin-rate increment of 0.1 rpm per quarter-orbit (or 25 minutes) requires a coil which has a magnetic-dipole moment of about 6 ampere-turns-meter^2.

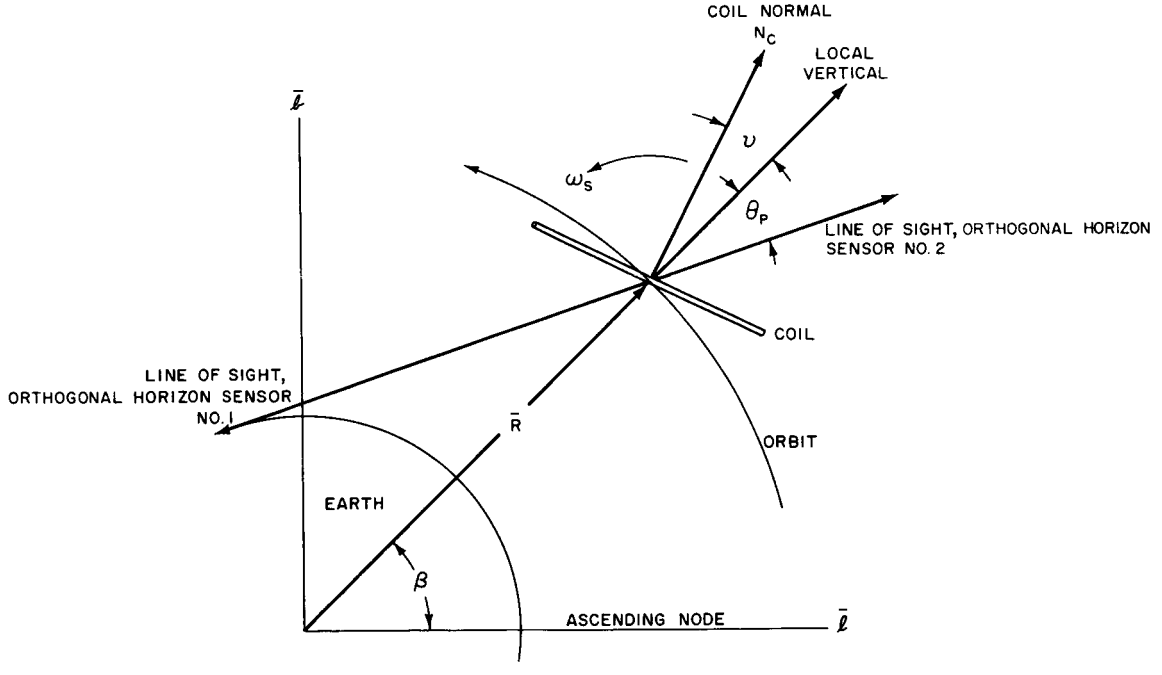

Figure D-1. Position of Spin-Control Coil at Time of Sky-to-Earth Crossing of Horizon Sensor No. 1.

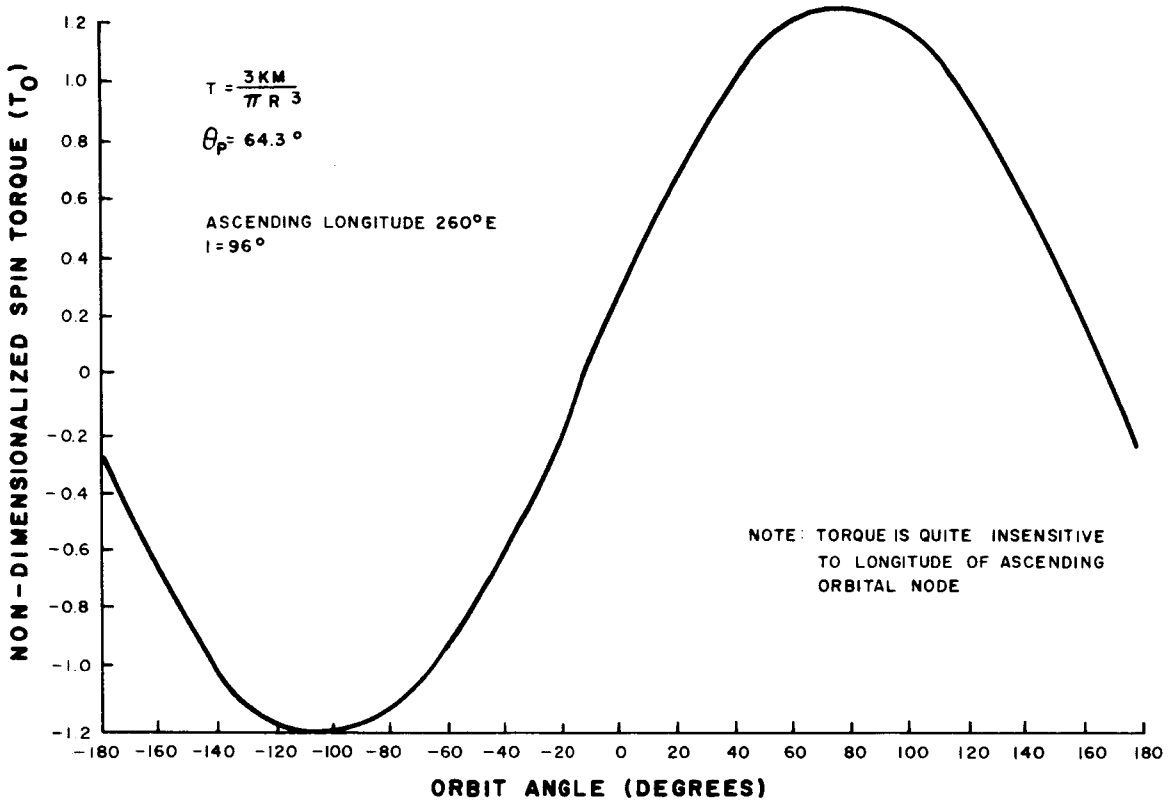

Figure D-2. Non-Dimensional Spin Torque versus Orbit Position

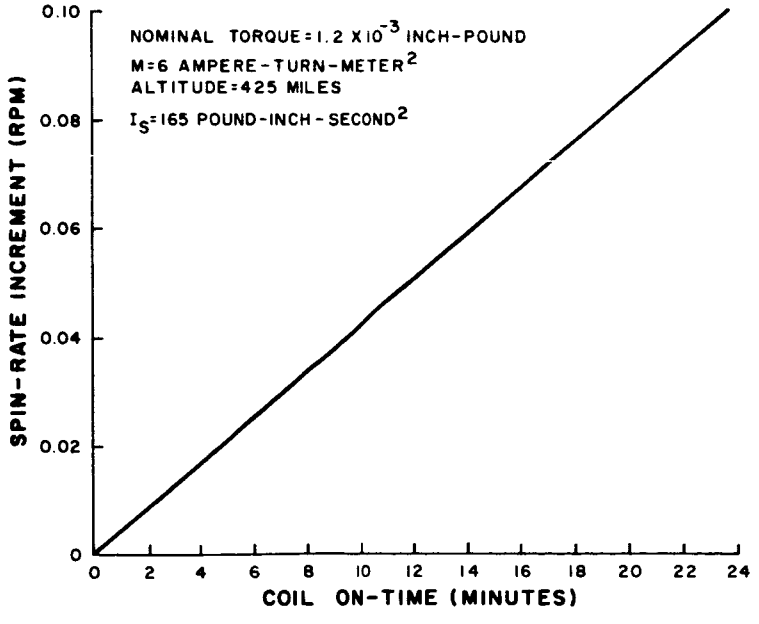

Figure D-3. Spin-Rate Increment versus Time Coil is Energized

D-7. There exists as a result of the $\hat{\ell}$ and $\hat{b}$ components of the average torque-per-spin period, a disturbance tending to precess the satellite as spin-rate control is exercised. The component of the earth's field giving rise to the precession torque is B_n. Thus, the precessional torque ($\overline{T}_{Prec}$) accompanying the operation described by equation (D-3) is

$$\overline{T}_{Prec} = \frac{2M\,B_n}{\pi}(\cos\beta\,\hat{\ell} + \sin\beta\,\hat{b}) \cdot \qquad \text{(D-4)}$$

D-8 The precessional torque is, therefore, about the local vertical. B_n varies only with angle Ω for a particular orbit altitude and inclination. Since the change in Ω is small over any one orbit, B_n and, therefore, the magnitude of precessional torque may be considered constant for any one orbit. Therefore, the amount of slow angular precession of the spin axis is defined by

$$\psi = \frac{\overline{T}_{Prec}\,\Delta^t}{I_s\omega_s} \cdot \qquad \text{(D-5)}$$

D-9. Fortunately, for high-inclination orbits such as the i = 98 degrees planned for the TIROS-Wheel satellite, the field component B_n is relatively weak, whereas the field which is instrumental in producing spin-control torque and which lies in the orbit plane is relatively strong. Therefore, the precession from the magnetic spin-control mode for the TIROS-Wheel satellite is quite small and can easily be handled by brief operation of the quarter-orbit attitude-control system. The expected precession, as a result of magnetic-spin torquing, is shown in Figure D-4.

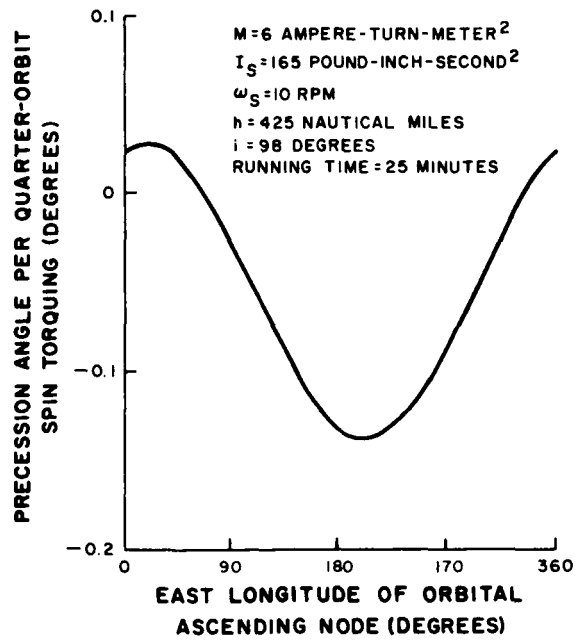

Figure D-4. Spin-Axis Precession Caused by Magnetic-Spin Torquing

APPENDIX E

RELATIONSHIPS INVOLVED IN ROLL-ANGLE NOMOGRAMS

APPENDIX E

RELATIONSHIPS INVOLVED IN ROLL-ANGLE NOMOGRAMS

E-1. The roll-angle nomograms are based upon two different equations. The one for the two-sensor case depends upon sensor cant angle and earth contact angle, and it is independent of satellite altitude. The relationship for the single-sensor case also depends on cant angle and earth contact angle; but, in addition, depends upon satellite altitude. The relationships between roll angle (ϕ) sensor cant angle (α) and earth contact angle (E) are shown in Figure E-1. In this figure the following representations are made:

a. Line BS is the positive direction of the spin axis of the spacecraft, which is at point B.

b. Point O is the center of the earth, making line OB the local vertical.

c. Plane (1) is determined by line OB and BS.

d. The local horizontal plane (2) intersects plane (1) in line BH.

e. Angle TBS (or α) is the cant angle of the horizon-sensor optics.

f. Points T and T' are points on the earth's surface at which line BT is tangent to the earth's surface and, therefore, perpendicular to a radius. These points represent the instants that the horizon sensor lines of sight just intersect the earth's disc (i.e., sky-earth and earth-sky transition points).

g. Line TL is drawn perpendicular to plane (1) from point T.

h. Line LM, which is drawn perpendicular to line BS, intersects line OB at point N, and intersects the sphere representing the earth at point J.

i. By symmetry, angle TML (or angle β) is equal to E/2.

E-2. To establish the desired relationship, the following geometrical techniques are used:

a. The projection of line BT on line OB is obtained by direct resolution.

b. To involve the angles α and β, the components of line BT in two right-angled directions in plane (1) are projected onto line OB.

c. The sum of the projections on line OB, resulting from the operation of Step b, is equated to the component obtained by direct resolution.

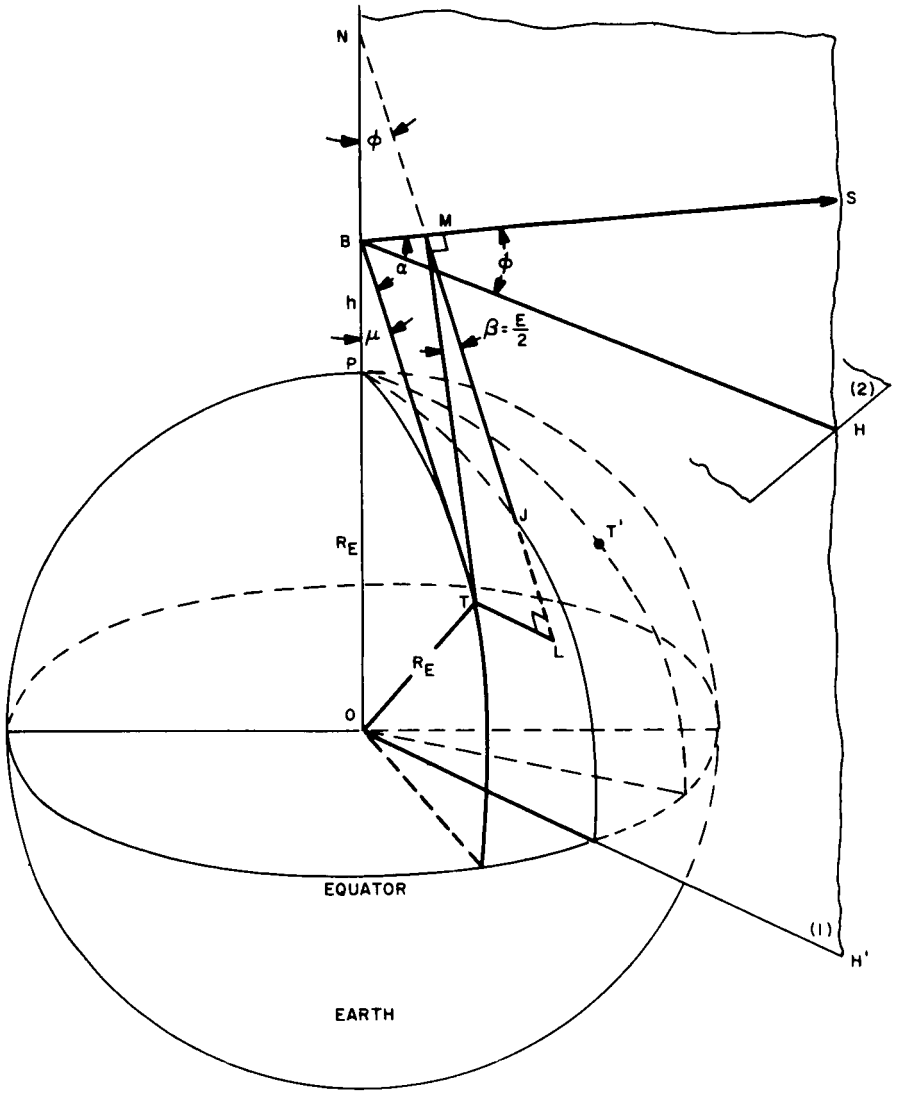

$$\cos\beta = \frac{\cos\mu}{\sin\alpha\cos\phi} + \frac{\tan\phi}{\tan\alpha} \quad ; \quad \mu = \sin^{-1}\frac{R_E}{R_E + h}$$

$$\beta = 180\ T_E / T_{SPIN} \qquad \tan\phi = \frac{\tan\alpha}{2}\left[\cos\beta_1 - \cos\beta_2\right]$$

Figure E-1. Relation of Roll Angle, ϕ, and Horizon Sensor Geometry

E-3. The detailed operations are as follows:

a. The projection of line BT on line OB, $[BT]_{OB}$, is given by

$$[BT]_{OB} = [BT]\cos\mu,$$

where:

$$\mu = \sin^{-1}\frac{r}{r+h},$$

r = earth's radius, and

h = satellite altitude.

b. The two right-angled directions in plane (1), in which components of line BT are sought along, are lines BM and LM. These components are as follows:

(1) The projection of line BT on line BM, $[BT]_{BM}$, is

$$[BT]_{BM} = [BT]\cos\alpha .$$

(2) The projection of line BT on line LM, $[BT]_{LM}$, is found using the following two steps:

(a) $[BT]_{MT} = [BT]\sin\alpha$

(b) $$[BT]'_{LM} = \left[[BT]_{MT}\right]_{LM} = \left[[BT]_{MT}\right]\cos\beta$$
$$= [BT]\sin\alpha\cos\beta$$

and because line TL is perpendicular to line LM

$$\left[[BT]_{TL}\right]_{LM} = 0.$$

(3) The projection of the components of line BT along line BM and along line LM onto line OB is given by

$$\left[[BT]_{BM}\right]_{OB} = -[BT]\cos\alpha\sin\phi, \text{ and}$$

$$\left[[BT]_{LM}\right]_{OB} = [BT]\sin\alpha\cos\beta\cos\phi .$$

c. Summation of the separate components of lines BT on line OB yields

$$[BT]\cos\mu = -[BT]\cos\alpha\sin\phi + [BT]\sin\alpha\cos\beta\cos\phi .$$

By rearrangement, this may be written as

$$\cos \beta = \frac{\cos \mu}{\sin \alpha \cos \phi} + \frac{\tan \phi}{\tan \alpha} . \qquad \text{(E-1)}$$

Further, it may be shown that

$$\beta = 180\ T_E / T_{SPIN}, \qquad \text{(E-2)}$$

where:

T_E is the horizon-sensor earth time, and

T_{SPIN} is the apparent spin period of the satellite.

Hence, for a single sensor, if β is measured from the sensor output, the instantaneous roll angle (ϕ) may be determined, provided satellite altitude is known. Equations (E-1) and E-2) can be graphically represented on a roll-angle nomogram for the range of parameters of interest.

If two sensors are used with cant angles which are supplementary (see Figure E-2), the two separate equations for α_1 and α_2 relating pertinent parameters may be combined to eliminate the altitude parameter, μ. That is,

$$\tan \phi = \frac{\tan \alpha_1}{2} \left[\cos \beta_1 - \cos \beta_2 \right], \qquad \text{(E-3)}$$

where:

α_1, β_1 pertains to horizon sensor 1 (or the uplooking sensor), and

α_2, β_2 pertains to horizon sensor 2 (or the downlooking sensor).

Equation (E-3) can also be developed into a roll-angle nomogram for the pertinent range of parameters.

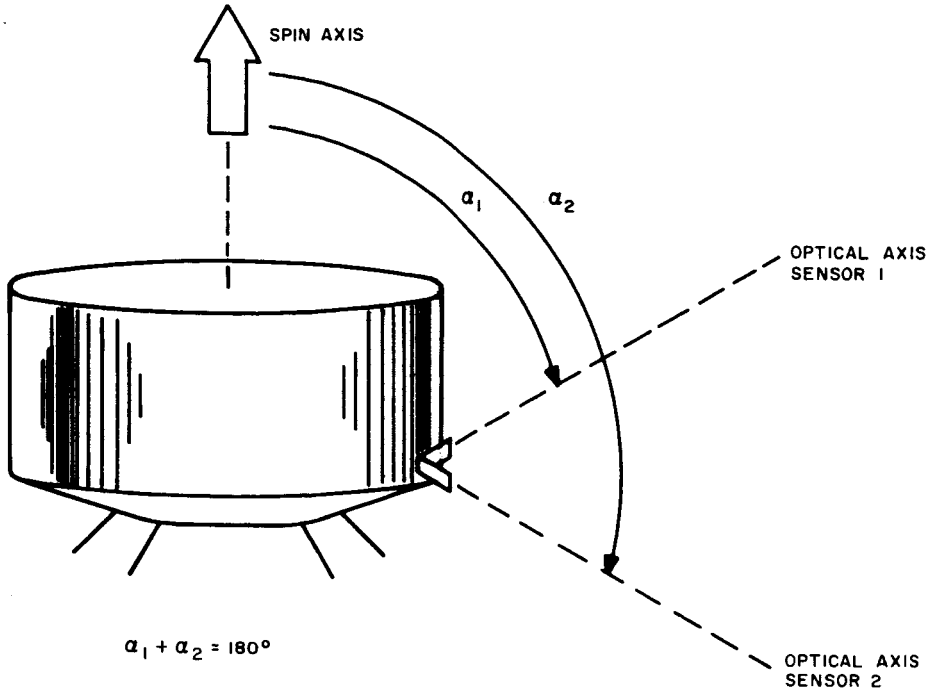

Figure E-2. Vee-Head Sensor Geometry

APPENDIX F

CURVE FITTING THE HORIZON-SENSOR DATA BY LEAST-SQUARE OPTIMIZATION

APPENDIX F

CURVE FITTING THE HORIZON-SENSOR DATA BY LEAST-SQUARE OPTIMIZATION

F-1. METHOD OF LEAST-SQUARE OPTIMIZATION

F-2. The Roll Angle method of determining attitude error is based upon the fact that as the satellite orbits around the earth the roll angle, ϕ, as measured by the attitude sensor, undergoes a cyclic variation according to the relationship

$$\text{Sin } \varphi = \text{Sin } \varphi_{max} \text{ Sin } (\omega_o t - \lambda), \qquad \text{(F-1)}$$

where t is measured from the ascending node crossing to the current location of the satellite and ω_o is the orbital rate. It is possible to improve the accuracy of attitude measurement by use of the method of least squares to obtain maximum roll angle (ϕ_{max}) and the orbit phasing parameter (λ), the components of attitude error. This method is less dependent upon personal judgment than the use of the overlay-curve-fit method described in Section II, Paragraph 2-26 of the main body of this report. However, unless the procedure is adapted for mechanical computation, the work involved is prohibitive.

F-3. Computer programs to execute the computation may be constructed with various degrees of sophistication. Inputs may be the data measured by the analyst or the output of a data reader. Subroutines which grade and select the data according to desired accuracy standards may be included. Furthermore, by due consideration of the scatter in the raw data, a measure of uncertainty or a probable error in the results may be incorporated.

F-4. The parameters, ϕ_{max} and λ, required for establishing a QOMAC program may be obtained from the horizon-sensor data by the method of least-squares through the following equations:

$$(1)\quad t_j = t'_j - t_{ANO'} \quad j = 1, 2, \ldots\ldots n,$$

$$(2)\quad k_1 = \sum_{j=1}^{n} \sin^2 \omega_o t_j,$$

$$(3)\quad k_2 = \frac{1}{2} \sum_{j=1}^{n} \sin 2\, \omega_o t_j,$$

$$(4)\quad k_3 = \sum_{j=1}^{n} \cos^2 \omega_o t_j,$$

$$(5)\quad D = k_1 k_3 - k_2^2,$$

$$(6)\quad Q_1 = \sum_{j=0}^{n} \sin \phi_j \sin \omega_o t_j,$$

$$(7)\quad Q_2 = \sum_{j=0}^{n} \sin \phi_j \cos \omega_o t_j,$$

$$(8)\quad A = \frac{k_3 Q_1 - k_2 Q_2}{D},$$

$$(9)\quad B = \frac{k_1 Q_2 - k_2 Q_1}{D},$$

$$(10)\quad \sin \phi_{max} = \sqrt{A^2 + B^2}, \text{ and}$$

$$(11)\quad \lambda = 2\pi - \tan^{-1} B/A,$$

where:

ω_o is the orbital rate,

t_j is the time parameter for the j^{th} measurement,

t'_j is the time at monitoring of the j^{th} measurement,

t_{ANO} is the time of ascending node crossing,

ϕ_j is the instantaneous roll angle at time t_j (observed),

ϕ_{max} is the satellite attitude error, and

n is the number of roll-angle measurements.

F-5. STANDARD DEVIATION OF ATTITUDE PARAMETERS, φ_{max} AND

F-6. It is possible by mathematical techniques to obtain an estimate of the accuracy with which the attitude parameters, φ_{max} and λ, have been established, based on the scatter of the monitored data. As in the case of the least square procedure, the considerable work involved in obtaining the attitude parameter by these techniques and their use is not recommended unless they can be executed by digital computer.

F-7. The procedure, as outlined below, depends upon the assumption that the error in measurement is normally and independently distributed, and does not depend upon the magnitude of the instantaneous roll angle under consideration. The parameter notation of Section F-4 has been modified by the use of the letters "m" and "e" as subscripts in order to distinguish, respectively, the measured quantities and those established by use of equation (F-1) after ϕ_{max} and λ have been determined by the least-squares method.

Thus,

φ_{mj} is the measured instantaneous roll angle at time t'_j, and

φ_{ej} is the established value of instantaneous roll angle by substitution of t'_j into equation (F-1).

The steps in the procedure are as follows:

(1) For each t_j of the monitoring period for which a φ_{mj} has been measured, obtain a value of φ_{ej} by applying t_j to equation (F-1), which contains the values of ϕ_{max} and λ obtained by the data reduction procedure.

(2) Obtain $\Delta\varphi_j = \left[\varphi_{ej} - \varphi_{mj}\right]$ for each t_j.

(3) $\overline{\Delta\varphi} = \frac{1}{n} \sum_{j=1}^{n} \Delta\varphi_j$.

(4) $$\sigma(\varphi) = \sqrt{\frac{1}{n}\sum_{j=1}^{1}(\Delta\varphi_j)^2 - (\overline{\Delta\varphi})^2}\ .$$

(5) $$\sigma(\sin\varphi) = \sigma(\varphi), \text{ for } \phi_{max} \leq 15^o.$$

(6) $$a = \sum_{j=1}^{n} \sin^2(\omega_o t_j - \lambda)\ .$$

(7) $$\beta = \sum_{j=1}^{n} \cos^2(\omega_o t_j - \lambda)\ .$$

(8) $$\gamma = \sum_{j=1}^{n} \sin 2(\omega_o t_j - \lambda)\ .$$

(9) $$\delta = a\beta - \frac{\gamma^2}{4}\ .$$

(10) $$\sigma(\varphi_{max}) = \sqrt{\frac{\beta}{\delta}}\ \frac{\sigma(\sin\varphi)}{\cos\varphi_{max}}\ .$$

(11) $$\sigma(\lambda) = \sqrt{\frac{a}{\delta}}\ \frac{\sigma(\sin\varphi)}{\sin\varphi_{max}}\ .$$

APPENDIX G

ATTITUDE DETERMINATION BY USE OF INTERSECTION METHOD

APPENDIX G. ATTITUDE DETERMINATION BY USE OF INTERSECTION METHOD

G-1. INTRODUCTION

G-2. The primary method of attitude determination, described in Section II of this manual, is to be used under normal operating conditions. The alternate method described herein is to be used in the event that it is necessary to check the satellite's attitude when the duration of the data monitoring period is too short to allow implementation of the primary or roll-angle method or during the turn-around maneuver when ϕ_{max} is poorly defined from horizon-sensor data alone.

G-3. The common objective of the primary (roll-angle) and alternate methods is to determine the maximum roll angle (ϕ_{max}), which is the attitude error of the spin vector of the satellite, and to determine the related orbital-phasing parameter (λ) required for implementation of attitude-correction commands.

G-4. REQUIRED DATA INPUTS

G-5. MONITORED ANGLE DATA

G-6. SOLAR-ASPECT SENSOR DATA

G-7. The solar-aspect sensor provides an indication of the sun angle (γ), the angle between the satellite spin vector and the line from the satellite to the sun. Because of the spin-axis stability afforded by the satellite's angular momentum, and since TIROS IX is in a sun-synchronous orbit, the sun angle can remain unchanged for several consecutive orbits and even, possibly, for days. This angle is one of the two monitored parameters required by the intersection method. The solar-aspect sensor can be put into operation by a ground command for a period of approximately 28 seconds during warm-up of either camera subsystem or during warmup before playback of the tape recorders. The output of the solar-aspect sensor is an 8-bit binary word. The first seven bits contain the sun-angle information, the last bit indicates "end-of-word." Normally, four separate binary words, one for each of the four revolutions of the 28-second operating period, are received from the satellite each time the solar-aspect sensor is commanded "on."

G-8. If the solar-aspect sensor is commanded "on" while camera subsystem No. 1 is being warmed-up, the data are transmitted on the 2300-cps subcarrier of Beacon No. 1. Conversely, if camera subsystem No. 2 is being warmed-up, the solar-aspect data are transmitted on the 1300-cps subcarrier of Beacon No. 2. If transmitted over Beacon No. 1, the solar-aspect data appears on the left channel of the telemetry chart recorder (No. 2); if transmitted over Beacon No. 2, it will appear on the right channel.

G-9. Figure G-1 shows a recording of a typical binary word from the solar-aspect sensor. If the recording is placed as shown, bit No. 1, the least significant bit, is at the left hand edge of the binary word. The "end-of-word" bit appears at the right-hand edge of the word and is always a binary "0". Each of the other bits will be either a binary "1" (upward deflection) or a binary "0" (downward deflection), depending on the value of the sun angle. The sample word shown in Figure G-1 represents the word: 0 0 1 0 1 1 1 0.

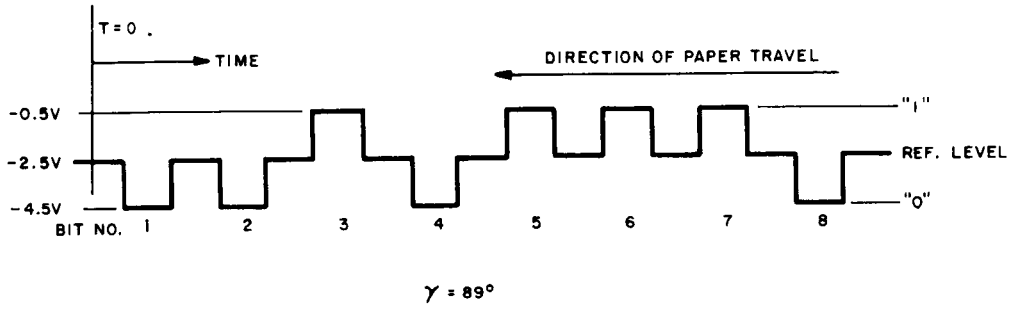

NOTES

- Bit No. 8 is always a binary "0".
- All Direct I commands shift the reference level to -3.0 V.
- During all playback sequences (except RMT on) an offset in the reference level will occur to indicate Camera Power ON.

Figure G-1. Typical Solar Aspect Data

This can be converted to sun angle from the listing in Table G-1.* From this table, it can be seen that the nominal sun angle corresponding to the binary word is 89 degrees.

*The sun-angles listed in Table G-1 are typical values for each binary word. The actual sun angle will differ slightly according to the characteristics of the individual solar-aspect sensor. The table which applies specifically to the solar-aspect sensor on TIROS IX is included in the document entitled "Operational Procedures for Telemetry Data Processing for the TIROS IX Meteorological Satellite."

TABLE G-1. TYPICAL SOLAR-ASPECT SENSOR DATA

Bit No. 1 2 3 4 5 6 7 8	α Nom. (Degrees)	α Max. (Degrees)	α Min. (Degrees)
0 0 0 0 0 0 0 0	1.0	1.65	-
1 0 0 0 0 0 0 0	2.0	2.70	1.65
1 1 0 0 0 0 0 0	3.0	3.50	2.70
0 1 0 0 0 0 0 0	4.0	4.58	3.50
0 1 1 0 0 0 0 0	5.0	5.50	4.58
1 1 1 0 0 0 0 0	6.0	6.55	5.50
1 0 1 0 0 0 0 0	7.0	7.65	6.55
0 0 1 0 0 0 0 0	8.0	8.65	7.65
0 0 1 1 0 0 0 0	9.0	9.55	8.65
1 0 1 1 0 0 0 0	10.0	10.60	9.55
1 1 1 1 0 0 0 0	11.0	11.55	10.60
0 1 1 1 0 0 0 0	12.0	12.50	11.55
0 1 0 1 0 0 0 0	13.0	13.55	12.50
1 1 0 1 0 0 0 0	14.0	14.50	13.55
1 0 0 1 0 0 0 0	15.0	15.55	14.50
0 0 0 1 0 0 0 0	16.0	16.70	15.55
0 0 0 1 1 0 0 0	17.0	17.60	16.70
1 0 0 1 1 0 0 0	18.0	18.60	17.60
1 1 0 1 1 0 0 0	19.0	19.50	18.60
0 1 0 1 1 0 0 0	20.0	20.80	19.50
0 1 1 1 1 0 0 0	21.0	21.60	20.80
1 1 1 1 1 0 0 0	22.0	22.50	21.60
1 0 1 1 1 0 0 0	23.0	23.50	22.50
0 0 1 1 1 0 0 0	24.0	24.40	23.50
0 0 1 0 1 0 0 0	25.0	25.50	24.40
1 0 1 0 1 0 0 0	26.0	26.65	25.50
1 1 1 0 1 0 0 0	27.0	27.55	26.65
0 1 1 0 1 0 0 0	28.0	28.40	27.55
0 1 0 0 1 0 0 0	29.0	29.50	28.40
1 1 0 0 1 0 0 0	30.0	30.50	29.50
1 0 0 0 1 0 0 0	31.0	31.60	30.50
0 0 0 0 1 0 0 0	32.0	32.65	31.60
0 0 0 0 1 1 0 0	33.0	33.55	32.65
1 0 0 0 1 1 0 0	34.0	34.60	33.55
1 1 0 0 1 1 0 0	35.0	35.50	34.60
0 1 0 0 1 1 0 0	36.0	36.70	35.50
0 1 1 0 1 1 0 0	37.0	37.55	36.70
1 1 1 0 1 1 0 0	38.0	38.50	37.55

TABLE G-1. TYPICAL SOLAR-ASPECT SENSOR DATA (Continued)

Bit No. 1 2 3 4 5 6 7 8	α Nom. (Degrees)	α Max. (Degrees)	α Min. (Degrees)
1 0 1 0 1 1 0 0	39.0	39.50	38.50
0 0 1 0 1 1 0 0	40.0	40.65	39.50
0 0 1 1 1 1 0 0	41.0	41.55	40.65
1 0 1 1 1 1 0 0	42.0	42.55	41.55
1 1 1 1 1 1 0 0	43.0	43.50	42.55
0 1 1 1 1 1 0 0	44.0	44.35	43.50
0 1 0 1 1 1 0 0	45.0	45.55	44.35
1 1 0 1 1 1 0 0	46.0	46.50	45.55
1 0 0 1 1 1 0 0	47.0	47.55	46.50
0 0 0 1 1 1 0 0	48.0	48.40	47.55
0 0 0 1 0 1 0 0	49.0	49.50	48.40
1 0 0 1 0 1 0 0	50.0	50.50	49.50
1 1 0 1 0 1 0 0	51.0	51.50	50.50
0 1 0 1 0 1 0 0	52.0	52.65	51.50
0 1 1 1 0 1 0 0	53.0	53.50	52.65
1 1 1 1 0 1 0 0	54.0	54.40	53.50
1 0 1 1 0 1 0 0	55.0	55.50	54.40
0 0 1 1 0 1 0 0	56.0	56.35	55.50
0 0 1 0 0 1 0 0	57.0	57.55	56.35
1 0 1 0 0 1 0 0	58.0	58.55	57.55
1 1 1 0 0 1 0 0	59.0	59.50	58.55
0 1 1 0 0 1 0 0	60.0	60.40	59.50
0 1 0 0 0 1 0 0	61.0	61.50	60.40
1 1 0 0 0 1 0 0	62.0	62.50	61.50
1 0 0 0 0 1 0 0	63.0	63.50	62.50
0 0 0 0 0 1 0 0	64.0	64.50	63.50
0 0 0 0 0 1 1 0	65.0	65.50	64.50
1 0 0 0 0 1 1 0	66.0	66.45	65.50
1 1 0 0 0 1 1 0	67.0	67.50	66.45
0 1 0 0 0 1 1 0	68.0	68.40	67.50
0 1 1 0 0 1 1 0	69.0	69.50	68.40
1 1 1 0 0 1 1 0	70.0	70.60	69.50
1 0 1 0 0 1 1 0	71.0	71.50	70.60
0 0 1 0 0 1 1 0	72.0	72.40	71.50
0 0 1 1 0 1 1 0	73.0	73.50	72.40
1 0 1 1 0 1 1 0	74.0	74.45	73.50
1 1 1 1 0 1 1 0	75.0	75.50	74.45
0 1 1 1 0 1 1 0	76.0	76.60	75.50
0 1 0 1 0 1 1 0	77.0	77.50	76.60

TABLE G-1. TYPICAL SOLAR-ASPECT SENSOR DATA (Continued)

Bit No. 1 2 3 4 5 6 7 8	α Nom. (Degrees)	α Max. (Degrees)	α Min. (Degrees)
1 1 0 1 0 1 1 0	78.0	78.55	77.50
1 0 0 1 0 1 1 0	79.0	79.50	78.55
0 0 0 1 0 1 1 0	80.0	80.45	79.50
0 0 0 1 1 1 1 0	81.0	81.50	80.45
1 0 0 1 1 1 1 0	82.0	82.50	81.50
1 1 0 1 1 1 1 0	83.0	83.55	82.50
0 1 0 1 1 1 1 0	84.0	84.45	83.55
0 1 1 1 1 1 1 0	85.0	85.50	84.45
1 1 1 1 1 1 1 0	86.0	86.60	85.50
1 0 1 1 1 1 1 0	87.0	87.50	86.60
0 0 1 1 1 1 1 0	88.0	88.65	87.50
0 0 1 0 1 1 1 0	89.0	89.60	88.65
1 0 1 0 1 1 1 0	90.0	90.50	89.60
1 1 1 0 1 1 1 0	91.0	91.50	90.50
0 1 1 0 1 1 1 0	92.0	92.70	91.50
0 1 0 0 1 1 1 0	93.0	93.50	92.70
1 1 0 0 1 1 1 0	94.0	94.65	93.50
1 0 0 0 1 1 1 0	95.0	95.55	94.65
0 0 0 0 1 1 1 0	96.0	96.60	95.55
0 0 0 0 1 0 1 0	97.0	97.55	96.60
1 0 0 0 1 0 1 0	98.0	98.55	97.55
1 1 0 0 1 0 1 0	99.0	99.55	98.55
0 1 0 0 1 0 1 0	100.0	100.40	99.55
0 1 1 0 1 0 1 0	101.0	101.50	100.40
1 1 1 0 1 0 1 0	102.0	102.60	101.50
1 0 1 0 1 0 1 0	103.0	103.55	102.60
0 0 1 0 1 0 1 0	104.0	104.50	103.55
0 0 1 1 1 0 1 0	105.0	105.60	104.50
1 0 1 1 1 0 1 0	106.0	106.40	105.60
1 1 1 1 1 0 1 0	107.0	107.55	106.40
0 1 1 1 1 0 1 0	108.0	108.75	107.55
0 1 0 1 1 0 1 0	109.0	109.55	108.75
1 1 0 1 1 0 1 0	110.0	110.60	109.55
1 0 0 1 1 0 1 0	111.0	111.55	110.60
0 0 0 1 1 0 1 0	112.0	112.70	111.55
0 0 0 1 0 0 1 0	113.0	113.60	112.70
1 0 0 1 0 0 1 0	114.0	114.50	113.60
1 1 0 1 0 0 1 0	115.0	115.60	114.50
0 1 0 1 0 0 1 0	116.0	116.30	115.60

TABLE G-1. TYPICAL SOLAR-ASPECT SENSOR DATA (Continued)

Bit No. 1 2 3 4 5 6 7 8	α Nom. (Degrees)	α Max. (Degrees)	α Min. (Degrees)
0 1 1 1 0 0 1 0	117.0	117.50	116.30
1 1 1 1 0 0 1 0	118.0	118.65	117.50
1 0 1 1 0 0 1 0	119.0	119.60	118.65
0 0 1 1 0 0 1 0	120.0	120.75	119.60
0 0 1 0 0 0 1 0	121.0	121.50	120.75
1 0 1 0 0 0 1 0	122.0	122.50	121.50
1 1 1 0 0 0 1 0	123.0	123.60	122.50
0 1 1 0 0 0 1 0	124.0	124.70	123.60
0 1 0 0 0 0 1 0	125.0	125.50	124.70
1 1 0 0 0 0 1 0	126.0	126.75	125.50
1 0 0 0 0 0 1 0	127.0	127.70	126.75
0 0 0 0 0 0 0 0	128.0	-	127.70

G-10. HORIZON-SENSOR DATA

G-11. A minimum of one channel of horizon-sensor data which preferably covers or overlaps the same time period as the obtained solar-aspect sensor data must be available for reduction. For accuracy the obtained data span should include data from 5 to 10 consecutive rotations of the satellite. This data is used to determine the nadir angle (η), which is the complement of the roll angle. This parameter is the other of the two monitored quantities required by the intersection method of attitude determination.

G-12. EPHEMERIS DATA

G-13. The intersection method of attitude determination requires the following ephemeris data:

(1) δ_{ω}, the declination of the satellite,

(2) α_{ω}, the right ascension of the satellite,

(3) δ_{H}, the declination of the sun, and

(4) α_{H}, the right ascension of the sun.

The information necessary to ascertain δ_ω and α_ω is found in the WMSAD, which is published by NASA. By entering the WMSAD via the nearest minute of GMT (Greenwich Mean Time) corresponding to the real time of the monitored data, the longitude and latitude of the satellite are read out. The value of declination, δ_W, of the satellite is the same as its latitude; its algebraic sign is positive if latitude is north and negative if south. The right ascension, α_W, of the satellite is found from the relationship.

$$\alpha_W = \text{E. long. of satellite} + \text{G. H. A.}$$

where

G.H. A. is the Greenwich Hour Angle of the First Point of Aries at the GMT of the monitored data.

If the longitude of the satellite is listed as west, obtain the form desired from the equation

E. Long. of satellite = 360 - W. long. of spacecraft.

The ephemeris data of the sun as well as the G.H.A. are found in the "American Ephemeris and Nautical Almanac" for 1965.

G-15. BASIC CONCEPTS OF INTERSECTION METHOD

The Intersection Method, whether it is executed by a computational procedure or by a graphical one, attains its end by indicating the coordinates of the points of intersection of two cycles located on the surface of the celestial sphere*. The circles are determined by sun angle and nadir angle respectively. The spherical coordinates of one of the points of intersection fix the attitude of the satellite in space; those of the other are a byproduct of the mathematics and are to be set aside.

G-15. DETAILED PROCEDURES

G-16. DETERMINATION OF RIGHT ASCENSION AND DECLINATION OF SPIN VECTOR

G-17. The right ascension and declination of the satellite's spin vector can be determined by (1) manual solution of a series of trigonometric equations, (2) computerized solution of a series of trigonometric equations, (3) graphical solution using

*The celestial sphere is a sphere of infinite radius whose center is located at the center of the earth. Points of interest are located on it by projection from the center outward.

the 36-inch globe equipped with circle-scribing attachments which is available at TTCC or AED. Of these, the graphical method provides for the most convenient and rapid determination of α_S and δ_S, and the computerized method provides the greatest accuracy.

G-18. The basic geometric relationships required to ascertain attitude in terms of right ascension and declination are depicted on the celestial sphere in Figure G-2. W is the point at which the satellite's radius vector intersects the celestial sphere, and H is the point at which the sun's radius vector intersects the sphere. Two circles are drawn on the sphere; one with its center at W and the other at H. The radii of these circles are equal to the nadir angle and sun angle, respectively. The celestial coordinates (right ascension and declination) of one of the points of intersection of these circles represents the attitude of the satellite spin vector; the other point of intersection is a spurious result. The two can be readily distinguished because the location of the spurious point will vary with the nadir angle, while the point representing the true attitude of the satellite spin vector will remain essentially constant throughout the investigated data span, despite variations in nadir angle.

G-19. The three methods of determining the right ascension and declination of the spin vector of the satellite are described in the following paragraphs.

G-20. METHOD I: MANUAL COMPUTATION SOLUTION. Proceed as follows:

a. Calculate angle c, the angle between the sun's radius vector and the satellite's radius vector using the equation

$$\cos c = \sin \delta_W \sin \delta_H + \cos \delta_W \cos \delta_H \cos (\alpha_H - \alpha_W),$$

where the subscripts of the right ascension α and declination δ are as follows:

W designates the satellite, and

H designates the sun.

b. Using the values of parameters of Step a and the following relationships, calculate the values of auxiliary angles ν and ρ:

$$\cos \nu = \frac{\cos \eta - \cos c \cos \gamma}{\sin c \sin \gamma}, \text{ and}$$

$$\cos \rho = \frac{\sin \delta_W - \cos c \sin \delta_H}{\sin c \cos \delta_H},$$

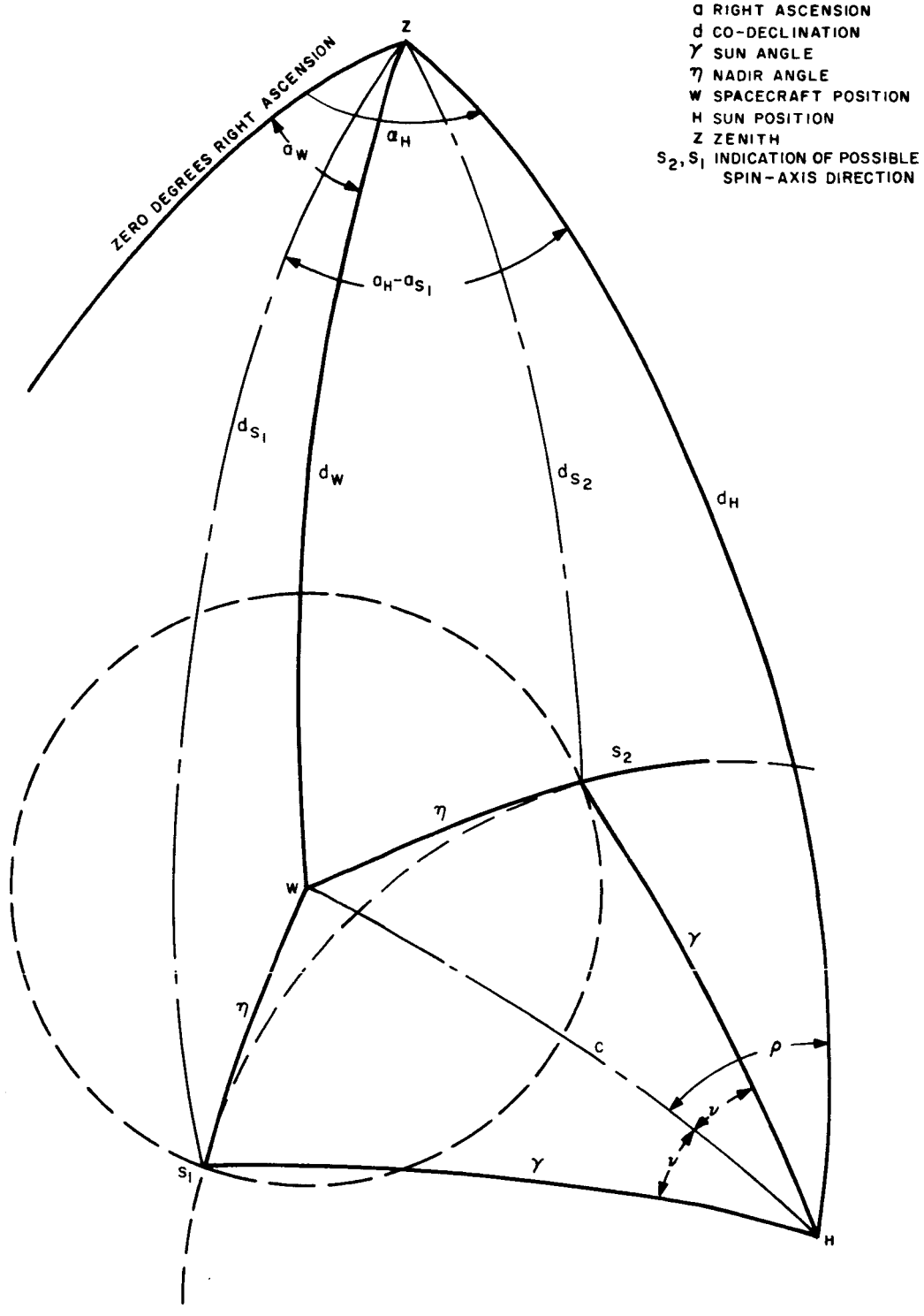

Figure G-2. Attitude Geometry Drawn on the Celestial Sphere

where:

η is the nadir angle, expressed by:

$$\eta = 90 - \phi_i;$$

ϕ_i is the instantaneous roll angle obtained by reduction of the horizon-sensor data described in Paragraph F-1 (the reduction procedure is presented in Section II of this manual);

and

γ is the sun angle extracted from the solar-aspect sensor data as described in Paragraph G-9.

c. Calculate the two possible values of declination of the spin vector, using the values of auxiliary angles ν and ρ determined in Step b and the following equations:

$$\sin \delta_{S_1} = \cos \gamma \sin \delta_H + \sin \gamma \cos \delta_H \cos (\rho + \nu), \text{ and}$$

$$\sin \delta_{S_2} = \cos \gamma \sin \delta_H + \sin \gamma \cos \delta_H \cos (\rho - \nu).$$

d. Calculate the two possible values of right ascension of the spin vector using the following equations:

$$\sin (\alpha_H - \alpha_{S_1}) = \frac{\sin \gamma \sin (\rho + \nu)}{\cos \delta_{S_1}}, \text{ and}$$

$$\sin (\alpha_H - \alpha_{S_2}) = \frac{\sin \gamma \sin (\rho - \nu)}{\cos \delta_{S_2}}.$$

e. Determine which pair of coordinates is the true declination and right ascension of the spin vector (i.e., δ_{S_1} and α_{S_1} and δ_{S_2} and α_{S_2}) by either of the following methods:

(1) Compare the two solutions with the attitude history. The correct solution should be obvious, since it will be in line with the curve of attitude history. The spurious result will not be in line with this curve.

(2) Recompute the right ascension and declination using the data from a different period within the investigated span of data. Compare the results of the two sets of computations. The true values of declination and right ascension will be essentially the same in both computations. The spurious results will vary as a function of the nadir angle.

G-21. METHOD II: GRAPHICAL SOLUTION . Proceed as follows:

a. Refer to paragraph G-13 to obtain the right ascension (α_W) and declination (δ_W) of the satellite for the time of interest (i.e., the time at which solar-aspect and horizon-sensor data under investigation were received from the satellite). Mark the point W defined by these parameters onto the surface of the special 36-inch globe. This point represents the location of the satellite. Obtain the right ascension (α_H) and declination (δ_H) of the sun for the time of interest, from the American Ephemeris and Nautical Almanac.* Mark the point H defined by these parameters onto the surface of the special 36-inch globe.

b. Using the scribe, which is calibrated in degrees, construct a circle on the surface of the globe with its center at point W and its radius equal to the nadir angle (complement of the roll angle extracted from horizon-sensor data as described in Section II).

c. In the same manner, construct a second circle with its center at point H and its radius equal to the sun angle (extracted from the solar-aspect sensor data as described in Paragraph G-7).

d. Determine from the grid on the globe the right ascension and declination of the two points where the two constructed circles intersect. One of these two points represents the right ascension and declination of the satellite's spin vector; the other is a spurious result. Determine which is the true result as described in Step e of Paragraph G-20.

G-22. METHOD III: COMPUTERIZED SOLUTION: The computerized solution is essentially the same as the manual solution. However, the equations have been developed especially for processing by a digital computer and, therefore, differ in form from those used in Method I. These equations are listed in Table G-2.

*Alternatively, the location, H, of the sun may be found by recourse to the calender date as marked on the ecliptic circle drawn on the globe.

TABLE G-2. ATTITUDE COMPUTATION EQUATIONS RECOMMENDED FOR PROCESSING BY DIGITAL COMPUTER

$\cos c = \sin\delta_W \sin\delta_H + \cos\delta_W \cos\delta_H \cos(\alpha_H - \alpha_W)$	(1)
$\tan\frac{\nu}{2} = \frac{r}{\sin(p-\eta)}$ where $p = \frac{1}{2}(\eta + \gamma + c)$ and $r = \sqrt{\sin(p-\eta)\sin(p-\gamma)\sin(p-c)/\sin p}$	(2)
$\tan\frac{\rho}{2} = \frac{r'}{\sin(p'+\delta_W)}$ where $p' = \frac{1}{2}(\pi + c - \delta_W - \delta_H)$ and $r' = \sqrt{\sin(p'+\delta_W)\sin(p'+\delta_H)\sin(p'-c)/\sin p'}$	(3)
$\sin\delta_{S_1} = \cos\gamma \sin\delta_H + \sin\gamma \cos\delta_H \cos(\rho+\nu)$	(4a)
$\sin\delta_{S_2} = \cos\gamma \sin\delta_H + \sin\gamma \cos\delta_H \cos(\rho-\nu)$	(4b)
$\tan\left(\frac{\alpha_H - \alpha_{S_1}}{2}\right) = \frac{r''}{\sin(p''-\gamma)}$ where $p'' = \frac{1}{2}\left(\pi + \gamma - \delta_H - \delta_{S_1}\right)$ and $r'' = \sqrt{\sin(p''-\gamma)\sin(p''+\delta_H)\sin(p''+\delta_{S_1})/\sin p''}$	(5a)
$\tan\left(\frac{\alpha_H - \alpha_{S_2}}{2}\right) = \frac{r'''}{\sin(p'''-\gamma)}$ where $p''' = \frac{1}{2}\left(\pi + \gamma - \delta_H - \delta_{S_2}\right)$ and $r''' = \sqrt{\sin(p'''-\gamma)\sin(p'''+\delta_H)\sin(p'''+\delta_{S_2})/\sin p'''}$	(5b)

G-23. DETERMINATION OF RIGHT ASCENSION AND DECLINATION OF ORBIT-NORMAL VECTOR

G-24. Calculate the right ascension α_n, and declination δ_n, of the orbit-normal vector using the following relations

$$\alpha_n = \alpha_{ANO} - 90°,$$

$$\delta_n = 90° - i, \text{ and}$$

$$\alpha_{ANO} = \text{E. long ANO} + \text{G.H.A.},$$

where (see Figure F-2):

α_{ANO} is the right ascension of the ascending-node crossing for the orbit under consideration,

G.H.A. is the Greenwich Hour Angle of the 1st point of Aries at the time of the ascending node,

i is the orbital inclination angle, and

E. long ANO is the east longitude of the ascending node and is found for the orbit of interest in the WMSAD.

G-25. DETERMINATION OF MAXIMUM ROLL ANGLE (ϕ_{MAX}) AND ORBITAL-PHASING PARAMETER (λ)

G-30. Manually, or using the computer, calculate the maximum roll angle (ϕ_{max}) and the orbital-phasing parameter (λ) using the following relationships:

$$\cos \phi_{max} = \sin \delta_n \sin \delta_S + \cos \delta_n \cos \delta_S \cos (\alpha_S - \alpha_n), \text{ and}$$

$$\tan \lambda = \frac{- \cos \delta_S \cos (\alpha_S - \alpha_{ANO})}{\sin \delta_S \sin i + \cos i \cos \delta_S \sin (\alpha_S - \alpha_{ANO})},$$

where:

δ_n and α_n are the declination and right ascension of the orbit-normal vector (calculated in Paragraph G-24),

δ_S and α_S are the declination and right ascension of the satellite's spin vector (calculated in Paragraph F-10, G-21 or G-22), and

α_{ANO} is the right ascension of the ascending-node crossing obtained from the NASA WMSAD for the orbit under consideration by the procedure given in Paragraph G-24.